5-Hydroxymethylfurfural Oxidation on Supported Metal Catalysts

---

A Dissertation

Presented to

the faculty of the School of Engineering and Applied Science

University of Virginia

---

in partial fulfillment

of the requirements for the degree

Doctor of Philosophy

by

Sara Ellen Davis

December

2012

APPROVAL SHEET

The dissertation

is submitted in partial fulfillment of the requirements

for the degree of

Doctor of Philosophy

AUTHOR

The dissertation has been read and approved by the examining committee:

Robert J. Davis

Advisor

Matthew Neurock

John Hudson

Gary Koenig

Petra Reinke

Accepted for the School of Engineering and Applied Science:

Dean, School of Engineering and Applied Science

December

2012

Abstract

One molecule often cited as a key building block chemical in the development of a biorenewables-based chemicals industry is 5-hydroxymethylfurfural (HMF). Derived from fructose and glucose, HMF can be oxidized to 2,5-furandicarboxylic acid (FDCA), a potential replacement for the non-renewable polyethylene terephthalate monomer comprising PET plastics. The oxidation of HMF with dioxygen over Pt and Au catalysts in aqueous solution offers an environmentally benign process for the production of renewables-based plastics.

The oxidation of HMF to FDCA over Pt and Au catalysts at ambient temperatures required addition of base, such as NaOH, as well as the use of dioxygen. The rate of oxidation of HMF was an order of magnitude faster over Au than over Pt catalysts; however, at standard conditions (NaOH:HMF = 2:1, 295 K, 690 kPa O_2) the major oxidation product over Au was the monoacid hydroxymethylfurancarboxylic acid (HFCA), whereas Pt produced a majority FDCA. Increasing the amount of NaOH (NaOH:HMF = 20:1) resulted in a majority product FDCA over Au.

Isotopically labeled $H_2{}^{18}O$ and $^{18}O_2$ were used to determine the source of oxygen inserted in the acid products and showed that oxygen insertion proceeds through water rather than dioxygen. A mechanism was proposed in which molecular oxygen is reduced to peroxide and hydroxide, scavenging electrons from the metal surface, closing the catalytic cycle and regenerating hydroxide. Base-free HMF oxidation in water to FDCA was achieved through the use of higher temperatures (348 K) over Pt/C catalysts. Isotopic labeling studies confirm this oxidation reaction proceeds through the same mechanism as the one at high pH.

The reaction kinetics of HMF oxidation in aqueous solution with O_2 to HFCA and FDCA were evaluated over a 3 wt% Pt/Activated Carbon catalyst in a semibatch reactor. In addition, the reaction kinetics of intermediate HFCA oxidation to FDCA over supported Pt were also investigated. The reactions were found to be zero order in substrate concentration, indicating high coverage of the Pt surface in substrate. The oxidation of HMF was found to be first order in initial NaOH concentration, though the oxidation of HFCA was found to be zero order in initial NaOH concentration above a 2:1 NaOH:HFCA ratio. Arrhenius plots of both HMF and HFCA oxidation revealed similar apparent activation energies, 29.0 kJ mol^{-1} and 29.6 kJ mol^{-1}, respectively.

Solid bases as catalyst support may offer enhanced reaction rates for the oxidation of HMF to FDCA. Although attempts have been made at using hydrotalcites (HT) for this purpose, experiments demonstrate considerable leaching of these materials into solution was observed. Carbon nanofibers (CNF) treated with ammonia at high temperatures (1173 K) created supports with basic pyridine and pyrrole groups (CNF-N), on which Au and Pt particles were anchored. Likewise, CNF materials functionalized with acidic O-containing groups (CNF-ox) were used to support metal nanoparticles. Interesting synergy between Au and basic CNF-N materials was noted, wherein the diacid FDCA was produced in majority over this catalyst in just 2:1 NaOH:HMF at 295 K. Under the same conditions, Au particles supported on carbon black produced a majority of the monoacid HFCA, as did a physical mixture of basic CNF-N (no metal) and Au/C_{black}.

Acknowledgements

I thank my advisor, Robert J. Davis, for his guidance and patience during my graduate studies. In addition, I would like to thank all of the Davis group members, past and present, with whom I have interacted throughout the years, in particular Joe Kozlowski and Dr. Bhushan Zope. Many thanks are extended to my classmates for their support and camaraderie over the past few years, in particular Dr. Ernie Perez, Adrian Gospoderek, Dr. Rosemary Cox-Galhotra, Dr. David Hibbitts, and Joe Costanzo. I express my gratitude also to the staff of the Chemical Engineering Department, especially Ricky Buchanan, Vickie Faulconer, and Teresa Morris. I would like to recognize the kind help and friendship of the members of the Department of Inorganic Chemistry and Catalysis at Utrecht University.

To my family and my fiancé Todd, thank you for your overwhelming love and encouragement that has helped me reach this point.

I gratefully acknowledge funding support from the National Science Foundation under grant Nos. OISE 0730277 and EEC-0813570.

Table of Contents

List of Figures

List of Tables

Chapter 1

Introduction

Portions of this introduction are based on a critical review paper: Davis, S.E., Ide, M.S., and Davis, R.J. "Selective oxidation of alcohols and aldehydes over supported metal nanoparticles." Green Chemistry. *In press. DOI: 10.1039/C2GC36441G*

The diminishing supply of oil has heightened interest in the development of more sustainable alternatives to petroleum-derived fuels and chemicals. Although much attention is paid to the transportation and energy sectors of the economy, 5% of current consumption of crude oil is used for the production of chemicals (1). Renewable resources such as solar and wind power can meet some of the world's energy demands. Advances in battery technology may shift some of the energy consumed in the transportation sector away from liquid fuels. Still, replacements for common petroleum-derived chemicals require a source of carbon atoms. A potential renewable source of carbon atoms is biomass.

The U.S. National Renewable Energy Laboratory (NREL) has described a theoretical facility to convert biomass to produce fuels, power, and chemicals, analogous to the way a contemporary petroleum refinery does (2). A major challenge to the development of a biorefinery, and thus the biorenewable chemicals industry, is identifying key intermediates and platform chemicals. While today's petroleum refinery benefits from years of optimization and a well-defined set of platform chemicals for the production of value-added chemicals, the implementation of the biorefinery is still under development.

The methods for conversion of biomass to value-added fuels and chemicals are likewise under development. Homogeneous, heterogeneous, and bio-catalysts are all potential vehicles for

the conversion of biomass. Currently, the Center for BioRenewable Chemicals (CBiRC), a National Science Foundation Engineering Research Center, is investigating the integration of biocatalysis and heterogeneous catalysis for the development of a biorenewable chemicals industry to replace today's petroleum-based chemicals industry. CBiRC's approach is to use biocatalysis to transform carbohydrates to platform chemicals, and heterogeneous catalysts to convert platform chemicals to final value-added chemicals. The potential for easy separation of products and recovery and recyclability of catalyst makes heterogeneous catalysts advantageous when compared to homogeneous and bio-catalysts.

In 2004, the US Department of Energy (DOE) sought to identify the molecules with the greatest potential for use as value-added chemicals from biomass (3, 4). One of these molecules is 2,5-furandicarboxylic acid (FDCA). This molecule is of interest because of its potential for use as a monomer in the production of biomass-derived polymers. Terephthalic acid is the monomer used in the production of polyethylene terephthalate (PET plastics) and polybutylene terephthalate (PBT plastics), and the structural similarity between FDCA and terephthalic acid is highlighted in Figure 1-1.

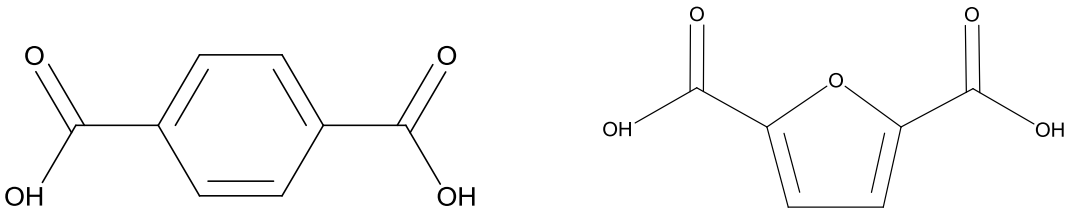

Terephthalic Acid FDCA

Figure 1.1 Structures of terephthalic acid and 2,5-furandicarboxylic acid

The physical properties of polymers made from FDCA have been investigated extensively. The physical and chemical properties of plastics made from FDCA polymers (polyethylene furanoate, PEF) have been shown to be similar to PET plastics (5, 6). The findings are so promising, in fact, that Avantium has recently announced a 30 million Euro investment in the development of a commercial facility for the large scale production of PEF and other FDCA-based polymers (6). Very recently, the synthesis of poly(butylene 2,5-furandicarboxylate, PBF) was reported, as a potential renewable alternative to petroleum-derived thermoplastic PBT (7).

The synthesis of FDCA can be achieved through selective oxidation of 5-hydroxymethylfurfural (HMF), a molecule often proposed to be an important platform chemical in the conceptual biorefinery (2, 4). 5-Hydroxymethylfurfural is readily produced by dehydration of glucose and fructose (8-13). The Dumesic group has demonstrated an economically viable method for HMF synthesis in a biphasic fructose dehydration with a high yield of HMF (80% selectivity to HMF at 90% conversion of fructose, with substrate of 10 – 50 wt% fructose) (12). Other groups have demonstrated catalytic conversion of sugars to HMF in ionic liquids (14). Limited success has been realized in producing FDCA from fructose/glucose in a one-pot synthesis method (15-17).

Oxidation of HMF is an interesting and complicated reaction because the substrate is not stable in water at high pH (18-21), subject to conversion via the Cannizzaro reaction and other degradation pathways. However, under most conditions, a high pH is necessary for its oxidation. There has been a push to find a base-free oxidation route, for both economic and environmental benefits, despite the extremely low solubility of the common target product, FDCA, in neutral water (22, 23). The base-free oxidation of HMF utilizing Au on hydrotalcite (HT) as a solid base support was reported recently (24, 25); however, other work demonstrated the likely leaching of

this solid base material into solution as a stoichiometric replacement for homogenous base (25, 26). This is a good demonstration of the complexity and technical barriers to base-free HMF oxidation at present.

The oxidation of HMF to FDCA encompasses two steps: aldehyde oxidation and alcohol oxidation. It is generally believed that the alcohol oxidation is the slow step in this oxidation (20, 21, 27). The main intermediates in HMF oxidation are seen in Figure 1.2. The di-aldehyde intermediate, 2,5-diformylfuran (DFF), is rarely seen in solution at high pH, probably because of the high reactivity of the aldehyde in aqueous media. The most commonly seen intermediate is the acid-alcohol product, 5-hydroxymethyl-2-furancarboxylic acid (HFCA), which results from oxidation of the aldehyde moiety to acid.

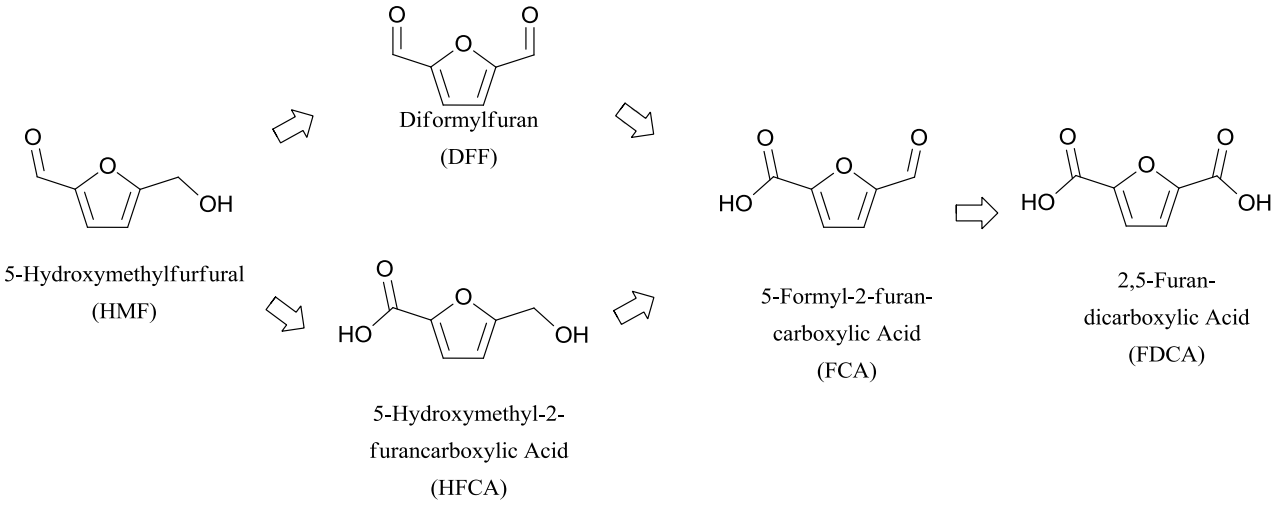

Figure 1.2 Intermediates in HMF oxidation

HMF oxidation in methanol

Although water is a solvent commonly used during HMF oxidation, some studies investigated the reaction in methanol, which forms the ester products corresponding to the acids shown in Figure 1.2 (28). A major advantage of converting HMF in methanol compared to water is the solubility of the final product. The solubility of the diacid product, FDCA, is low in water at neutral pH (22, 23), whereas the ester of the diacid is readily soluble in many common solvents. An early study of HMF oxidation in methanol was reported by Taarning et al. using Au/TiO_2 as the catalyst (28). The oxidation reaction was optimized at 403 K and 400 kPa of O_2 in the presence of 8% sodium methoxide as a base to enhance the reaction rate. These optimized conditions produced a 98% yield of diester in 3 h, with the main intermediate being 5-hydroxymethylmethylfuroate (HMMF). Lowering the temperature to 295 K resulted in approximately 95% yield of HMMF after 3 h, since the oxidation reaction apparently stopped after formation of the intermediate. A rate of HMF oxidation can be calculated at 10% conversion based on their work, and it is given in Table 1.1.

Table 1.1. Turnover frequencies and reaction conditions for 5-hydroxymethylfurfural oxidation[a]

Catalyst	Particle Size (nm)	T (K)	Pressure (kPa)	Solvent	TOF (s^{-1})	Reference
Au/TiO_2	2.6[b]	295	100	Methanol + 8% Sodium Methoxide	0.14	(28)
Au/CeO_2	3.5	403	1000	Methanol	0.31	(29)
Au/Fe_2O_3	3.5	403	1000	Methanol	0.12	(29)
Au/TiO_2	3.5	403	1000	Methanol	0.30	(29)
Au/C	3.5	403	1000	Methanol	0.47	(29)
Au-Cu/TiO_2	4.4	368	1000	Water + 4:1 NaOH : HMF	0.18	(30)
Au/TiO_2	2.6	295	690	Water + 2:1 NaOH : HMF	1.6	(22)
Au/C	10.5	295	690	Water + 2:1 NaOH : HMF	5.0	(22)
Au/C	3.0	295	690	Water + 2:1 NaOH : HMF	2.3	(22)
Pt/C	2.5	295	690	Water + 2:1 NaOH : HMF	0.08	(22)
Pd/C	3.3	295	690	Water + 2:1 NaOH : HMF	0.15	(22)
Au/TiO_2	2.6	295	2000	Water + 2:1 NaOH : HMF	1.2	(22)
Au/TiO_2	2.6	295	3000	Water + 2:1 NaOH : HMF	1.4	(22)

[a]All reactions were performed in batch mode.
[b]Not given; estimated from data from World Gold Council standard catalyst.

Casanova et al. (31) explored the reaction over Au/CeO_2 at a similar temperature (403 K) but at higher pressure (1000 kPa) and without addition of base, in an attempt to improve the recyclability of catalysts for this reaction. The primary intermediate in that case was the ester of HFCA, and the final product diester was formed in 99% yield after 5 h. They proposed that the

rate limiting step in the sequence is the oxidation of the alcohol side chain to an aldehyde, which is analogous to the presumed rate limiting step during HMF oxidation in aqueous solution.

The effect of support on reaction rate and product selectivity was also investigated. The TOFs were calculated from initial rates (at 0.25 h) of both HMF disappearance and of diester formation. However, the TOFs were based on total metal rather than on surface metal, so the values have been recalculated and presented in Table 1.1. It should be noted that production of diester is the result of subsequent oxidation steps that are presumably slower than the initial oxidation of HMF. According to Table 1.1, Au/C had the highest rate of HMF oxidation but, relative to the other catalysts in the study, demonstrated low final yield of the diester product. On the other hand, Au/CeO_2 had the highest activity of the group for the formation of diester product (99% yield in 5 h). An experiment with Au/CeO_2 in the absence of O_2 yielded large amounts of the acetal product and 3.8% of the monoester product, which suggests that CeO_2 acts as an oxygen donor. When non-nanometric ceria was used as support, the activity of the catalyst was significantly reduced, in agreement with results from CeO_2-based catalysts for benzyl alcohol oxidation (32).

The effect of temperature was also investigated in the range 353 K – 403 K over the Au/CeO_2 and yielded an overall activation energy of 34 kJ mol^{-1}. Although other alcohols, such as ethanol and butanol, were also tested for the oxidation-esterification, methanol was the most suitable (31). The effect of water was probed, and a negative effect on the initial reaction rate was noted. In fact, when 20% water was loaded, the reaction did not even reach completion. Interestingly, no trace of carboxylic acid was noted, possibly because of the presence of a Lewis acid site on the catalyst support aiding in the rapid reaction of any formed carboxylic acid to methyl ester.

HMF oxidation in aqueous solutions

In aqueous solutions, HMF oxidation has been thoroughly investigated over Pt, Pd, and Au catalysts and some recent work has also looked at Au-Cu bimetallics and Ru(OH) catalysts (18-21, 23, 23, 24, 26-28, 33-35). The effects of added base concentration, temperature, dioxygen pressure, and catalyst composition have been studied. In general, the oxidation of HMF at moderate temperatures (295 - 368 K) over Au and Pt catalysts requires the addition of a homogeneous base, though a consensus has not been reached in the literature about the amount of homogenous base that should be employed. The degradation of HMF in presence of base is of concern, and most researchers seek to find a balance between high enough concentration of base to allow the oxidation to proceed at a reasonable rate but low enough to limit degradation. The work of Davis et al. showed that the intermediate HFCA is much more stable in NaOH than is HMF, so rapid oxidation of HMF to HFCA, through the use of a high catalyst loading, can allow for higher concentrations of NaOH to be employed to facilitate the subsequent oxidation of HFCA to FDCA (18).

The work of Davis et al. also showed that the activity of Au catalysts for HMF oxidation was an order of magnitude higher than either Pt or Pd catalysts. The selectivity to the desired diacid, however, was much higher over the Pt and Pd catalysts. At their standard conditions of 295 K and 690 kPa O_2 and 2 equivalents NaOH, the major product over Pt and Pd catalysts was FDCA (selectivity of 79% and 71%, respectively) while the major product over the Au catalysts was HFCA (selectivity of 92% over Au/TiO_2 catalyst). Gorbanev et al., however, demonstrated high selectivity to FDCA over Au catalysts in water by increasing the amount of catalyst and NaOH (20 equivalents) (21).

Over a Au/TiO_2 catalyst, Gorbanev et al. investigated the effect of NaOH concentration and demonstrated that at 303 K and 2000 kPa O_2, the selectivity to diacid did not change in the range 5 – 20 equivalents NaOH (21). Below 5 equivalents, the selectivity shifted more toward the mono-acid HFCA. In the absence of base at the same conditions, only 13% conversion of HMF was seen, with the majority product HFCA (yield 12%) and little FDCA (selectivity 1%).

Casanova et al. (20) and Pasini et al. (19) also varied the amount of NaOH to determine the effect of base on product selectivity. Casanova et al. found that using 4 equivalents of NaOH in the presence of Au/CeO_2 produced a 96% yield of diacid in 5 h, while 2 equivalents afforded 96% yield in 20 h (20). Using just 1 equivalent of NaOH resulted in only 20% yield in 14 h (76% yield of HFCA) and the oxidation did not proceed further. Pasini et al. found that, in the presence of $Au\text{-}Cu/TiO_2$ or Au/TiO_2, the product selectivity was influenced by amount of NaOH in the range of 1 – 4 equivalents (19). Increasing the NaOH concentration in the range 4 - 10 equivalents did not change product selectivity. The work also showed that using 20 equivalents of NaOH in the absence of catalyst resulted in complete degradation of HMF after 2.5 h.

The role of O_2 pressure in HMF oxidation over Au/TiO_2 catalysts was investigated by Gorbanev et al. (21) and Davis et al. (18). Over the range 690 kPa to 3000 kPa, no appreciable difference in the rate of HMF oxidation was noted. In contrast, Vinke et al., reported that reaction rate over Pt/Al_2O_3 was first order with respect to O_2 pressure; however, this assertion is made without showing any data (35).

The effect of O_2 pressure on product selectivity was investigated by Pasini et al. (19), Davis et al. (18) and Gorbanev et al. (21) over Au catalysts. A positive correlation between O_2 pressure and selectivity to diacid was noted. A control experiment conducted by Gorbanev, et al. in the absence of O_2 but in the presence of catalyst and 20 equivalents of NaOH found full

conversion of HMF after 18 h, with 51% yield of HFCA and the balance comprised of decomposition products. This demonstrates the necessity of dioxygen in this reaction to prevent undesirable side reactions in the highly basic solution (21).

Lilga et al., used a flow reactor to investigate the acid/base nature of the medium on HMF oxidation over Pt/Al_2O_3, Pt/ZrO_2, and Pt/SiO_2 catalysts (23). Under basic conditions (Na_2CO_3) at 373 K and 1035 kPa air, complete conversion of HMF to FDCA was observed. However, however, the selectivity shifted to FCA after 2 h of operating at 100% conversion of HMF, which might be attributed to adsorption of products onto the catalyst. Successive experiments in batch reactors report the same phenomenon, yet the original activity could be returned by washing the catalyst with hot water (23). In neutral conditions, the reaction was substantially slower but the downstream separations were easier (23). Product inhibition was apparently much higher than that in the basic conditions, likely because of the low solubility of the reaction products in neutral solution. It was noted that inorganic supports adsorbed less of the products, which also correlated with the surface area of the supports.

Acidic conditions were achieved through addition of acetic acid (23). While the solubility of FDCA is limited in neutral feeds, the solubility in 40% acetic acid and 60% water is twice that in 100% water. At 373 K and with air as the oxidant, the dialdehyde (DFF) is the major product, though at higher temperatures and with O_2 as the oxidant, 100% conversion and 85% selectivity to FDCA was realized.

Verdeguer et al. investigated PtPb/C catalysts and found that hydroxyl bases were more effective than carbonate bases at promoting the reaction (27). Vinke et al. found the rate of HMF oxidation over Pt/Al_2O_3 to be independent of pH between 8 – 11, but at lower pH values, the rate was lower (35).

It is quite clear that the oxidation of HMF in basic aqueous solution is facile over metal catalysts at room temperature (18, 19, 23, 28, 33, 35). Increasing the temperature, however, can reduce the reaction time or change the product selectivity. For example, Pasini et al. showed that at 333 K over Au-Cu/TiO_2 catalysts, the major product was the monoacid HFCA (19). Raising the temperature by just 20 K shifted the selectivity toward the diacid FDCA, and raising the temperature an additional 15 K produced 99% yield of FDCA. This is consistent with a rapid oxidation of HMF to HFCA and a slow oxidation of HFCA to FDCA. Vinke et al. found the observed activation energy to be 37.2 kJ mol^{-1} over Pt catalysts (35), which is similar to the value found over Au catalysts in MeOH solvent (34 kJ mol^{-1}) (31).

Casanova et al. varied the temperature between 298 and 403 K and found a positive effect on conversion over their Au/TiO_2 catalysts, as expected. However, higher temperatures caused the formation of some undesired byproducts (degradation products) (20). Attempted reuse of the catalyst revealed significant deactivation, which was attributed to the buildup of 2.5 wt% C during the reaction. Extensive washing of the spent catalyst did not improve activity. The researchers claimed that the used catalyst was still able to oxidize the alcohol group, but its ability to oxidize the aldehyde group was diminished. This was confirmed by carrying out a reaction with HFCA and a used catalyst; the reaction was completed in 4 h, yielding 93% FDCA. Since the catalyst can be used to oxidize the aldehyde at 298 K without loss of activity, a new reaction protocol was established wherein the first oxidation step of HMF to HFCA was conducted at 298 K, and then the temperature was raised to 403 K to allow for complete and efficient oxidation to the diacid product while limiting catalyst deactivation. With this method, the spent catalyst could be successfully reused 3 times.

A possible promotional role of the support (Fe_2O_3, C, CeO_2 and TiO_2) on Au nanoparticles was examined by Casanova et al. (20). The Au/CeO_2 and Au/TiO_2 supported catalysts showed the best activity (over Au/TiO_2, 84% selectivity to diacid after 8 h; over Au/CeO_2, 96% selectivity to diacid after 5 h), while Au/Fe_2O_3 and Au/C produced lower yields of FDCA. Highlighting the important collaborative effect of CeO_2 and Au, the Au on nanoparticulate CeO_2 reached high yields of FDCA in half the time of the Au on non-nanoparticulate CeO_2. The reductive pretreatment of the catalyst was shown to increase the activity, likely because it increases amount of Ce^{3+}, which has been shown previously to be important in catalyst activity (32).

Monometallic Au and Cu catalysts, as well as bimetallic Au-Cu/TiO_2 catalysts, were synthesized by Pasini et al. (19). Interestingly, the reaction with Cu/TiO_2 produced no FDCA whereas the bimetallic Au-Cu yielded twice the FDCA yield of the monometallic Au catalysts, demonstrating a synergistic effect of alloying the two metals. The optimum metal loading was found to be 1.5 wt% and the preparation method played a role in catalyst activity. Catalysts synthesized from preformed Au-Cu sols supported on TiO_2 were more active than those synthesized by post-deposition of a Au sol onto a monometallic Cu/TiO_2 catalyst. This may be indicative of the promotional activity of Cu, or because Cu aids the dispersion of Au. The bimetallic catalyst was able to be recycled 5 times without losing activity, whereas the Au monometallic catalyst lost activity after just 1 recycle, highlighting the beneficial effect of alloying Cu with Au.

Pasini et al. also found an effect of pretreatment on catalyst performance (19). The calcined catalyst produced a higher yield of HFCA and a lower yield of FDCA (92% and 8%, respectively) than did the uncalcined catalyst (69% yield HFCA and 31% yield FDCA). In

addition, the particle size of the calcined catalyst was larger than the uncalcined (6 nm compared to 4.4 nanometers, respectively). From this information, the group hypothesizes that the HFCA oxidation may be more sensitive to size of metal nanoparticles than is the HMF oxidation.

The hypothesis of Pasini et al., together with the difference in product selectivity between Pt and Au catalysts, highlight the need for an understanding of the two steps in HMF oxidation to FDCA: aldehyde oxidation and alcohol oxidation. Thus, a brief introduction to the mechanisms of primary alcohol and aldehyde oxidation reactions follows.

Alcohol oxidation mechanism

The oxidation of a primary alcohol proceeds first to an aldehyde and subsequently to a carboxylic acid, as outlined in Figure 1.3. The oxidation of an alcohol to an aldehyde over a heterogeneous catalyst likely occurs in three steps: first, the alcohol adsorbs on the metal surface, producing an adsorbed metal alkoxide. Second, β-hydride elimination occurs to produce a carbonyl species and a metal hydride. Last, the metal-hydride is oxidized by dioxygen to regenerate the metal surface. The oxidation of an aldehyde to carboxylic acid is believed to proceed through a geminal diol intermediate.

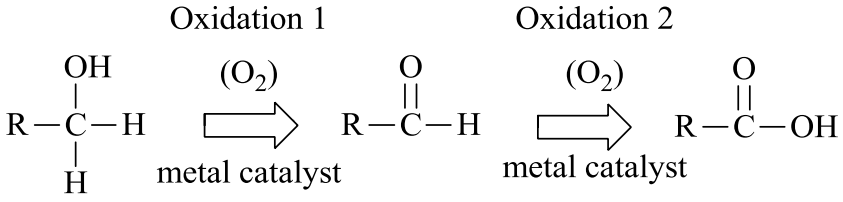

Figure 1.3. General oxidation scheme for primary alcohol oxidation to acid

Metal-alkoxide formation

As mentioned above, the mechanism of primary alcohol oxidation to aldehyde over a supported metal catalyst likely begins with the formation of a metal alkoxide (36-41); however, the nature of the metal or the nature of substrates adsorbed on the metal may influence its formation. In the case of benzyl alcohol and Ru/Al_2O_3 or $Ru(OH)_x/Fe_3O_4$ catalysts, a Ru-alkoxide has been hypothesized to form via ligand exchange between Ru-OH and the alcohol, producing a Ru-alkoxide and a water molecule (42). In other work with Ru and Pd catalysts, activation of the O-H bond in benzyl alcohol on the metal surface is proposed, yielding a metal-alkoxide and a metal-hydride (37, 38, 41, 43).

The selective oxidation of primary alcohols over secondary alcohols was demonstrated for benzyl alcohol and phenylethanol oxidation over Ru catalysts (38, 40). These results are consistent with formation of a metal alkoxide intermediate, as the formation of this species is well known for the selective oxidation of primary alcohols (38, 42, 44, 45). In a seeming contradiction, Mori et al. report similar reaction rates for benzyl alcohol and 1-phenylethanol oxidation over a Pd catalyst, yet propose the same metal alkoxide intermediate (37). Further support for metal alkoxide formation was derived from 2-propanol oxidation with O_2 over Ru/Al_2O_3. Production of H_2O and acetone were monitored during the reaction and revealed a 1:1 molar ratio (38, 42). Similarly, the uptake of O_2 was monitored during benzyl alcohol oxidation, and a 1:2 molar ratio of O_2 to aldehyde was observed (37, 40-42). These studies demonstrate that simple dehydrogenation of alcohol to aldehyde does not take place.

β-hydride elimination

A β-hydride elimination is widely accepted as the second step of alcohol oxidation over metal catalysts, producing a carbonyl group and a metal-hydride (37, 38, 40-42, 44, 45).

The Hammett methodology has been employed by a few groups to probe the mechanism of benzyl alcohol oxidation and to confirm the β-hydride elimination step (38). Comparing the rates of para-substituted benzyl alcohols over Ru catalysts yielded a Hammett ρ value of -0.461, which indicates the formation of a carbocation-type intermediate due to hydride abstraction from the Ru-alkoxide (38). Similarly, a Hammett ρ value of -1.10 was found over a Au catalyst, indicating that a similar mechanism operates despite the higher oxygen coverage on Ru than on Au (39).

The hydride abstraction step was also confirmed through the incorporation of deuterium in the α-position of the alcohol. The deuterated alcohol should react significantly slower than the non-deuterated alcohol and the kinetic isotope effect was found to be 1.82. Transfer hydrogenation was noted in a mixture of acetophenone and 2-propanol with a Ru catalyst, further supporting the formation of a Ru-H species (38). Interestingly, the β-hydride elimination step has been proposed as the likely rate-determining step in alcohol oxidation (37, 38, 40, 41).

Oxidation of Metal-Hydride and Regeneration of Catalyst Surface

The third step in alcohol oxidation to aldehyde is the oxidation of the metal-hydride species generated from the β-hydride elimination step to regenerate either the metal-hydroxide (38, 40) or metal surface (37, 41). The oxidation of the metal-hydride likely proceeds through a peroxide intermediate to yield a water molecule and one half of an O_2 molecule (37).

Oxidation of Aldehyde to Carboxylic Acid

It is well known in organic chemistry that aldehydes in H_2O undergo reversible hydration to geminal diols and that the rate of hydration is accelerated at elevated pH. The geminal diol will likely adsorb to a metal surface to form a metal alkoxide, which will undergo β-hydride elimination to form a carboxylic acid (46).

Focus of this work

While extensive investigations of HMF oxidation have been undertaken, the body of literature would benefit from a greater understanding of the roles of reaction conditions, metal selection, and catalyst support. In light of the previous discussion, we set out to address the following topics:

1. The mechanism of Au- and Pt-catalyzed oxidation of HMF in liquid water at high pH, and the mechanism of Pt-catalyzed oxidation in absence of added base,

2. The kinetics of HMF (aldehyde) and HFCA (alcohol) oxidation,

3. The influence of carbon support structure on HMF oxidation rate,

and

4. The influence of catalyst support acidity and basicity on HMF oxidation.

Chapter 2 reviews previous work comparing the performance of Au, Pt, and Pd catalysts for HMF oxidation, to provide context for the proceeding chapters. Chapter 3 addresses the mechanism of HMF oxidation at high pH and Chapter 4 discusses the kinetics of both HMF and HFCA oxidation to contribute to the understanding of aldehyde/alcohol oxidation. A discussion of HMF oxidation in the absence of added base is included in Chapter 5. Chapter 6 provides a look at the impact of carbon support structure on catalyst performance and the influence of the

acidic or basic characteristics of catalyst supports. Finally, Chapter 7 will offer conclusions and suggestions for further investigations.

In this work, the products of kinetic and mechanistic experiments were analyzed using high performance liquid chromatography (HPLC) and mass spectrometry (MS). Guidance for MS analysis was provided by Dr. Bhushan Zope. Catalyst characterization was performed using H_2 chemisorption, N_2 physisorption, transmission electron microscopy (TEM), and titration of acidic and basic sites. Microscopy was graciously provided by Angelica Sanchez of the University of New Mexico, under the advisement of Dr. Abhaya Datye. The synthesis of carbon nanofibers was conducted at Utrecht University with the assistance of Robert W. Gosselink, under the advisement of Dr. Johannes (Harry) Bitter and Dr. Krijn de Jong.

Chapter 2

Oxidation of 5-hydroxymethylfurfural over supported Pt, Pd and Au catalysts

This chapter was previously published as: Davis, S.E., Houk, L.R., Tamargo, E.C., Datye, A.K., and Davis, R.J. "Oxidation of 5-hydroxymethylfurfural over supported Pt, Pd, and Au catalysts." Catalysis Today *160 (2011) 55-60. It was also the basis for my Masters Thesis. It is printed here to provide context for the proceeding chapters.*

Introduction

Although there has been much work investigating the oxidation of HMF over the past two decades, the direct comparison of different metal catalysts for this reaction has not been made. To the best of our knowledge, the reactivity of Pt, Pd and Au catalysts had never been directly compared under identical conditions prior to this work. Moreover, the influence of reaction conditions on the turnover frequency of Au-catalyzed HMF oxidation had not been reported previously. Thus, we investigated the oxidation of HMF in water over several supported Pt, Pd and Au metal catalysts. Water was chosen as a green solvent to minimize environmental impact. Sodium hydroxide was used to facilitate the reaction because an earlier report indicated that hydroxide was more effective than carbonate (35). The influence of support on product selectivity and reaction rate was investigated for Au catalysts. The influence of hydroxide base concentration on the rate of oxidation and the effect of O_2 pressure on rate and product selectivity over supported Au were also explored.

Experimental Methods

Catalyst preparation

A gold on carbon catalyst was prepared through the formation of a gold sol and the subsequent deposition of the gold sol onto a carbon support (47). The sol was prepared by adding 0.075 g of $HAuCl_4 \cdot 4H_2O$ (~50 wt% Au, Aldrich) to 1500 cm^3 of deionized water along with 0.00375 g polyvinyl alcohol (Acros). The colloid was reduced by adding 0.1 M $NaBH_4$ (Aldrich) dropwise in a 4:1 molar ratio of $NaBH_4$:Au. Following reduction, the sol was ruby red in color. Five grams of carbon lampblack (Fisher Scientific) was suspended in 100 cm^3 of deionized H_2O and sonicated for 1 h and subsequently added to the sol. The sol-carbon slurry was stirred for 1 hour prior to filtration. The filtrate was clear in color, indicating the Au sol had deposited on the support. The catalyst was washed with several liters of water to remove any residual chlorine and dried overnight at 403 K in air. The catalyst was subsequently reduced in flowing N_2 and H_2 gases in a 9:1 ratio at 150 cm^3/min for 6 h at 573 K. The Au catalyst was stored in a refrigerator and used without any additional pretreatment. Metal weight loading was determined by ICP analysis performed by Galbraith Laboratories, Knoxville, TN.

Gold standard catalysts were obtained from the World Gold Council. A 1.6 wt % Au on TiO_2 catalyst (Type A, Lot. No. Au-TiO_2 #02-8), as well as a 0.8 wt % Au on C (Type C, Sample 40D) catalyst were used in this study. The platinum and palladium catalyst used here were both 3 wt % metal on activated carbon, supplied by Aldrich. Both the Pd and Pt catalysts were reduced in H_2 (UHP, Messer Gas) flowing at 150 $cm^3\,min^{-1}$ for 6 h at 573 K and cooled under flowing H_2. The catalysts were refrigerated and used without further pretreatment.

Oxidation reactions

The aqueous phase oxidation of 5-hydroxymethylfurfural (HMF) (Acros, ≥98% purity) was carried out in a 50 cm^3 Parr Instrument Company 4592 batch reactor equipped with a glass liner. Dioxygen was UHP, supplied by Messer Gas.

In all reactions, 7.0 cm^3 of the reactant solution (0.15 M HMF and 0.3 M NaOH) was added to the reactor along with the appropriate amount of catalyst. The reactor was purged with flowing O_2 and then pressurized to the desired value. A constant pressure was maintained by a continuous O_2 feed. Samples of the product solution were acquired by removing the top of the reactor, taking the sample, flushing the reactor with O_2 and repressurizing. The maximum O_2 transport rate from the gas to the liquid was determined by oxidation of sodium sulfite (48), and the HMF oxidation rate was kept significantly below this limit when quantitative rates were measured. The oxidation of sodium sulfite at the standard agitation speed and 690 kPa O_2 resulted in a maximum gas-liquid transfer rate of 4×10^{-7} mol O_2 s^{-1}.

The samples from the oxidation reactions were filtered using PTFE 0.2 μm filters and diluted with deionized H_2O in a 1:3 sample to water ratio. The analysis was conducted using a Waters e2695 high performance liquid chromatograph (HPLC) at 308 K equipped with refractive index and UV/Vis detectors. The HPLC utilized either a Waters Atlantis C_{18} column and deionized H_2O flowing at 1 cm^3 min^{-1} or a Bio-Rad Aminex HPX-87H column and 5 mM H_2SO_4 flowing at 0.5 cm^3 min^{-1} to perform the separation. The retention times and calibrations for observed products were determined by injecting known concentrations.

Chemisorption of H_2

The dispersion of Pt and Pd was determined using a Micromeritics ASAP 2020 automated adsorption system. The Pt/C catalyst was heated to 648 K at 4 K min^{-1} under flowing H_2 (UHP, Messer Gas) and reduced at that temperature for 1.5 h. The sample was subsequently evacuated for 2 h at 648 K and then cooled to 308 K for analysis. The Pd/C catalyst was heated to 473 K at 4 K min^{-1} under flowing H_2. The sample was evacuated and held for 2 h at 473 K before being cooled down to 373 K for analysis. The analysis was carried out at 373 K in the pressure range of 0.06-0.6 atm to avoid formation of the ß-phase hydride (49).

Scanning Transmission Electron Microscopy

High-angle annular dark field (HAADF) imaging was performed using a JEOL 2010F FASTEM field emission gun scanning transmission electron microscope operated at 200 kV. The Au/C catalyst sample was suspended in ethanol by grinding in an agate mortar and pestle, and deposited on a holey carbon support film on Cu TEM grids. The images were recorded and analyzed using Digital Micrograph software.

Results and discussion

Catalyst characterization

The Au metal loadings and particle sizes for the catalysts are listed in Table 2.1. A typical STEM image of the Au/C (sol) and the particle size distribution (Figure 2.1) sample indicated that the majority of particles are about 3 nm in diameter, with a small number of particles larger than 4.0 nm. The mean particle size determined by evaluating 792 particles over five different regions of the sample was 3.0 nm. The surface average diameter for the Au/C (sol) sample was

8.8 nm, which corresponds to an estimated dispersion (fraction of metal at the surface) of 0.14 (determined as the inverse of the surface average diameter) (50). Although a mean particle size of 10.5 nm was provided by the WGC for their Au/C, the Au/C (WGC) catalyst has been previously imaged by Ketchie et al. (51). The particle size distribution was reported; that work resulted in a mean particle diameter of 12.2 nm, which compares well to that provided by the WGC. However, the surface average diameter for Au/C (WGC) was 18.8 nm, corresponding to a dispersion of about 0.05. Because the Au/TiO_2 catalyst was not imaged independently, the mean particle size of 2.6 nm provided by the WGC was used to estimate a dispersion of 0.38. Chemisorption of H_2 was used to determine the dispersion for the Pt/C and Pd/C catalysts as 0.40 and 0.32, respectively.

Table 2.1. Catalyst characterization results

Catalyst	Metal Loading (wt%)	Mean Metal Particle Size (nm)	Surface Average Diameter (nm)[a]	Dispersion
Pt/C	3.04[b]	2.5[c]	-	0.40
Pd/C	2.9[b]	3.3[c]	-	0.32
Au/C (WGC)	0.8[d]	10.5[e]	18.8[f]	0.05[g]
Au/C (sol)	0.77[b]	3.0[h]	8.8[h]	0.11[g]
Au/TiO_2	1.6[d]	2.6[e]	-	0.38[i]

[a] surface average diameter = $(\sum d^3/\sum d^2)$
[b] from ICP analysis (Galbraith Labs, Knoxville, TN)
[c] inverse of dispersion (determined via H_2 chemisorption)
[d] from ICP analysis provided by the World Gold Council
[e] from TEM analysis provided by the World Gold Council
[f] from TEM analysis(51)
[g] inverse of surface average diameter, used to normalize rates for exposed Au atoms for Au/C (WGC) and Au/C (sol)
[h] from TEM analysis, this work
[i] inverse of mean particle diameter (nm), used to normalize rates for exposed Au atoms for Au/TiO_2

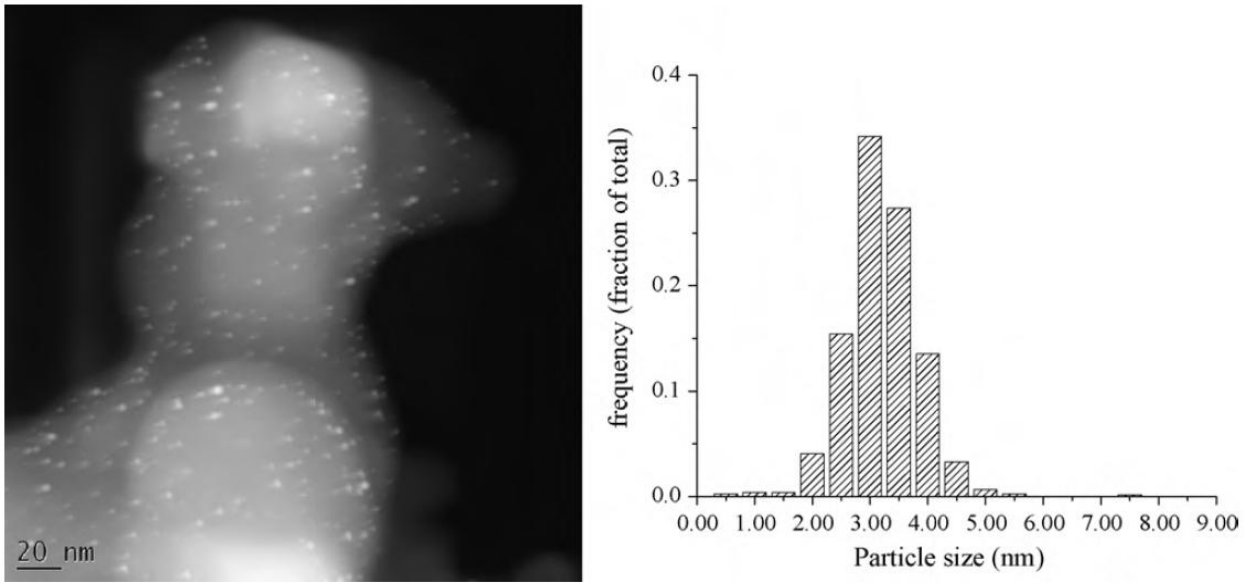

Figure 2.1. STEM image of Au/C (sol) catalyst. The accompanying particle size distribution indicates a mean particle size of 3.0 nm.

Oxidation reactions

The oxidation of HMF in an aqueous solution under 690 kPa O_2 at 295 K did not occur in 6 h over Pt/C or Au/C (WGC) without the presence of base. Thus, NaOH was added to the reaction medium to provide the basic environment. It should be noted that HMF in the presence of NaOH in water reacted to form undesirable decomposition products such as formic acid and bis(hydroxymethyl)furan. Therefore, the concentration of base was optimized so that side reactions were minimized while oxidation proceeded. A concentration of 0.3 M NaOH (NaOH:HMF 2:1) was chosen. The background conversion of HMF in NaOH solution without catalyst was 10% over 0.5 h.

The oxidation products of HMF are depicted in Figure 2.2. The product 2,5-bis(hydroxymethyl)furan (BHMF) was formed in the Cannizzaro reaction, which is a disproportionation reaction induced by high concentration of base. A typical reaction profile for HMF oxidation over supported Pt is reported in Figure 2.3. The oxidation of HMF proceeded

through HFCA and FCA to FDCA. The oxidation of HMF over Pd and Au catalysts apparently proceeded through HFCA because FCA was not observed in the course. In general, the product distributions reported here are consistent with those discussed earlier (20, 21, 27, 35).

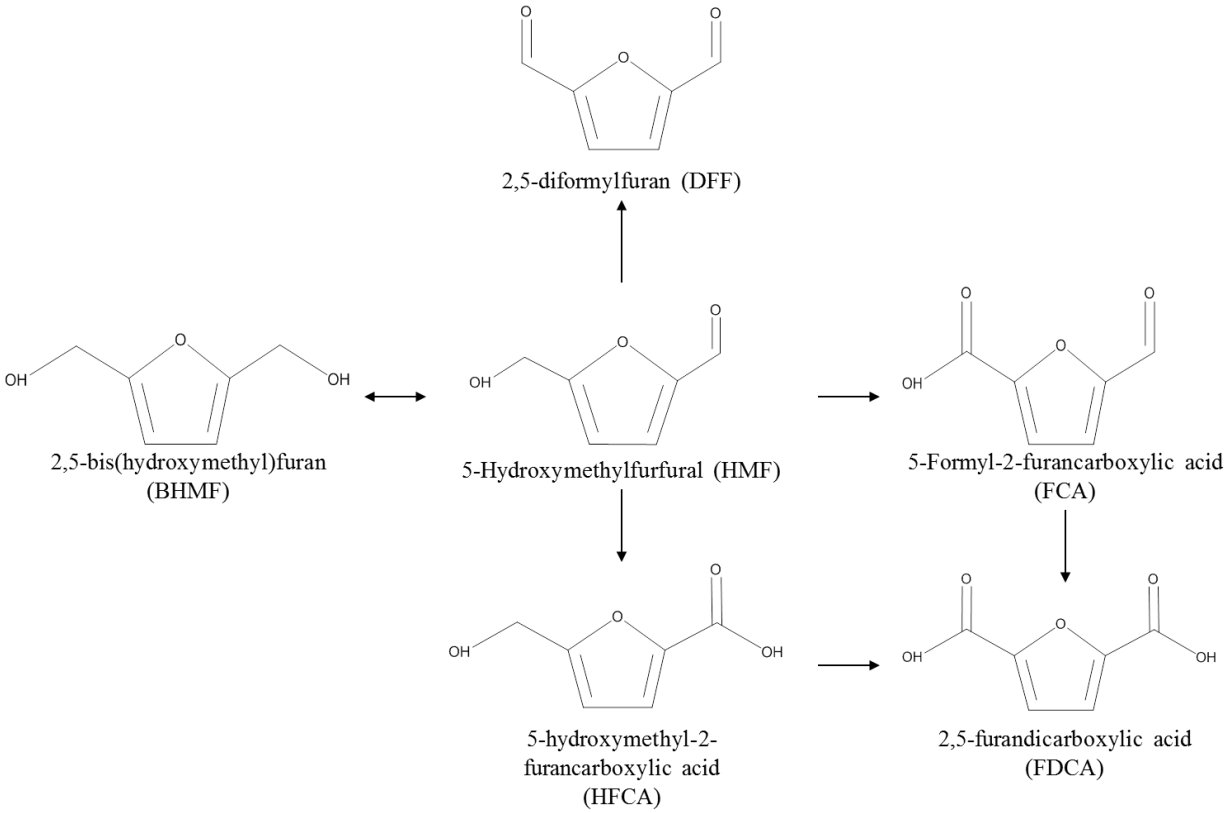

Figure 2.2. Products of HMF Oxidation

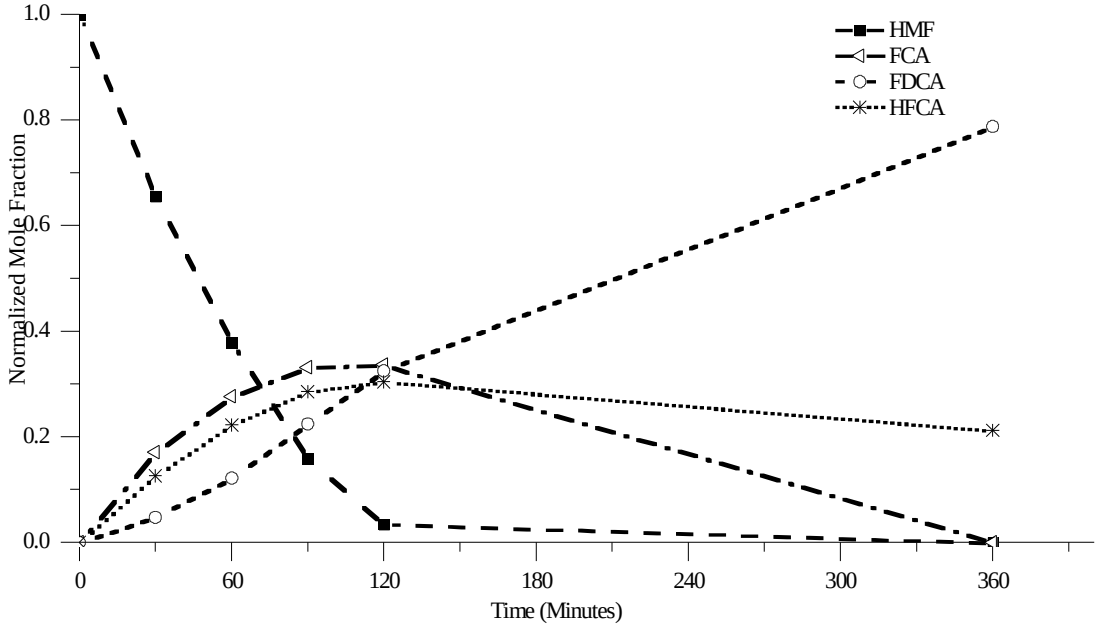

Figure 2.3. Sample reaction profile for oxidation of HMF over Pt/C. Reaction conditions: 0.15 M HMF, 0.3 M NaOH, 295 K, 690 kPa O_2

All catalysts were investigated for the oxidation of 0.15 M HMF in 0.3 M NaOH at 690 kPa O_2 and 295 K and a catalyst loading equivalent to metal : substrate = 6.7×10^{-3}. The results of these runs after 6 h (high HMF conversion) can be seen in Table 2.2. Although the conversion of HMF was 100% after 1 h over all three Au catalysts, the major product was HFCA, even after 6 h. In contrast to Pt and Pd, Au did not readily oxidize the alcohol sidechain under these reaction conditions. Despite the complete conversion of HMF after 1 h, the relative concentrations of FDCA and HFCA were virtually unchanged between 1 h and 6 h. After 6 h, additional feed solution (0.15 M HMF, 0.3 M NaOH) was added to the reactant mixture to yield a new HMF concentration in the reactor of 0.05 M, which was readily oxidized to HFCA in less than 1 h. These results conclusively demonstrated that the Au catalyst did not deactivate significantly during HMF oxidation. Because the product selectivity was nearly the same for all

of the Au catalysts tested, the reaction path was not affected by the carbon or titania support.

Table 2.2. Oxidation of HMF over Supported Pt, Pd and Au Catalysts[a]

Catalyst	Conversion (%)	S_{FDCA} (%)	S_{HFCA} (%)
Pt/C	100	79	21
Pd/C	100	71	29
Au/C (WGC)	100	8	92
Au/C (sol)	100	7	93
Au/TiO_2	100	8	92

[a]Reaction conditions: 0.15 M HMF solution in 0.3 M NaOH, Metal:HMF = 6.67×10^{-3} mol/mol, T = 295 K, P = 690 kPa O_2. S refers to selectivity after 6 h.

While the time to reach complete conversion of HMF over Pt was much longer than for Au or Pd, the desired product (FDCA) was obtained in majority (S_{FDCA} = 79%). Oxidation of HMF over Pd also yielded a majority of FDCA (S_{FDCA} = 71%).

The catalyst loadings for the runs in Table 2.2 were selected to give high conversions in relatively short reaction times. However, the flux of O_2 through the gas-liquid film was very near the mass transfer limit. Therefore, the amount of catalyst loaded into the reactor was lowered in order to obtain rate data unaffected by gas-liquid transport effects. The results of those reactions are summarized in Table 2.3. It should be noted that the amount of catalyst used for the results in Table 2.3 were substantially lower for the Pd and Au catalysts relative to the amount used for Table 2.2.

Table 2.3. Turnover Frequencies and Product Selectivities during HMF Oxidation over Supported Pt, Pd and Au Catalysts[a]

Catalyst	Metal:HMF	TOF[b] (s^{-1})	Conversion (%)	S_{FDCA} (%)	S_{HFCA} (%)	S_{BHMF} (%)	S_{FCA} (%)
Pt/C	6.67×10^{-3}	0.08	50	16	33	1	50
Pd/C	2.00×10^{-3}	0.15	50	18	80	2	-
Au/C (WGC)	8.70×10^{-4}	5.0	50	-	95	5	-
Au/C (sol)	5.48×10^{-4}	2.3	50	21	77	2	-
Au/TiO_2	3.57×10^{-4}	1.6	50	3	84	13	-

[a]Reaction conditions: 0.15 M HMF solution in 0.3 M NaOH, T = 295 K, P = 690 kPa O_2.
[b]TOF is calculated from the moles of HMF consumed in 30 minutes, normalized by the surface metal atoms in the reactor. Conversion of HMF was typically less than 20% after 30 minutes.

Although the metal loadings were much lower for the Au catalysts, the major product was still HFCA. Nevertheless, Au catalysts were substantially more active at converting HMF than either Pt or Pd. The turnover frequency on Au ranged from 2 to 5 s^{-1} whereas the TOF on Pd and Pt was 0.15 and 0.08, respectively. The Pd catalyst was slightly more active than the Pt catalyst for HMF oxidation, which is consistent with the findings reported by Vinke et al (35). The high activity of Au catalysts relative to Pt and Pd has also been observed for the oxidation of octanol (52). Moreover, Ketchie et al. reported Au to be significantly more active than Pd for glycerol oxidation in basic solution (53). Interestingly, the Au/C (sol) catalyst did produce some FDCA under these conditions (sel = 21% at 50% HMF conversion).

The effect of O_2 pressure on reaction rate and product selectivity over the Au/TiO_2 catalyst was investigated and the results are summarized in Table 2.4. The turnover frequency was independent of the O_2 pressure in the range investigated. However, as the pressure of O_2 increased from 690 kPa to 2000 kPa to 3000 kPA, the selectivity for FDCA increased from 3% to 28% to 36% at 50% conversion, which agrees with the trend noted by Casanova et al. between

100 kPa and 1000 kPa over their Au/CeO_2 (20). In contrast, Gorbanev et al. reported the selectivity for the diacid increased as the O_2 pressure increased from 1000 kPa to 2000 kPa but then remained constant to 3000 kPa (21). Their selectivity to the diacid over a Au catalyst at 2000 kPa O_2 was 78%, which was much higher than that observed here.

Table 2.4. The influence of O_2 pressure on reaction and selectivity of HMF oxidation over Au/TiO_2 catalyst[a]

P (kPa)	TOF[b] (s^{-1})	Conversion (%)	S_{FDCA} (%)	S_{HFCA} (%)	S_{BHMF} (%)
690	1.6	50	3	84	13
2000	1.2	50	28	69	3
3000	1.4	50	36	64	-

[a]Reaction conditions: 0.15 M HMF and 0.3 M NaOH, T = 295 K, Metal : HMF = 3.57×10^{-4}
[b]TOF is calculated from the moles of HMF consumed in 30 minutes, normalized by the surface metal atoms in the reactor. Conversion of HMF was typically less than 20% after 30 minutes.

It should be noted that the amount of catalyst and concentration of base used in Table 2.4 was much less than those in Ref. (21). Therefore, we reproduced the conditions used in Ref. (21) and compare our results in to those published previously in Table 2.5. The product selectivity on both the $AuTiO_2$ and the Au/C catalyst were similar to that reported by Gorbanev et al. (21). The selectivity to diacid (FDCA) was enhanced by substantially increasing the base concentration. Evidently, the aldehyde side chain is readily oxidized over Au at lower concentrations of base, but higher concentrations (20 equivalents) were needed to oxidize the alcohol side chain. Likewise, Casanova et al. report higher selectivity to FDCA when a 4:1 ratio of NaOH : HMF was used, instead of a 2:1 ratio (20). This finding is consistent with previous work on glycerol

oxidation over supported Au catalysts in which high base concentration is thought to deprotonate the alcohol and facilitate its conversion to aldehyde (51). Casanova et al. also observe the need for high base concentration to produce FDCA from HMF. Moreover, they report that the sequential reaction of intermediate HFCA to FDCA is greatly accelerated by increasing the reaction temperature to values greater than 373 K and emphasize that the slow reaction of HFCA to FDCA limits the overall rate (20).

Table 2.5. Selectivity of HMF Oxidation on Au Catalysts at High Base Concentration[a]

	Reaction time = 6 h[b]		Reaction time = 22 h[b]	
Catalyst	**S_{FDCA}**	**S_{HFCA}**	**S_{FDCA}**	**S_{HFCA}**
Au/C (sol)	31	69	72	28
Au/TiO_2	32	68	80	20
Au/TiO_2[c]	50	50	78	19

[a]Reaction conditions: 0.1 M HMF in 2.0 M NaOH, Metal : HMF = 8.0×10^{-3}, P = 2000 kPa O_2
[b]Conversion of HMF was 100%
[c]data from Gorbanev et al (21)

While high pH is necessary to oxidize the alcohol side group of HMF or HFCA, high pH can also lead to degradation products. A reaction utilizing a lower metal : HMF ratio (used for runs in Table 2.4) and a high NaOH concentration (used for runs in Table 2.5) was conducted over Au/TiO_2 to elucidate the role of base concentration on product distribution. Although the selectivity to diacid in this experiment (56% conversion of HMF, 8% selectivity to FDCA) was lower than that reported in Table 2.4, the major product was BHMF at high base concentration. Continued reaction to ~100% conversion resulted in the formation of formic acid and other degradation products. Evidently, high base concentrations can be detrimental to selectivity

because of undesirable side reactions, even at 295 K. To avoid degradation of HMF in concentrated base solution, a high Au catalyst loading (such as that used for the experiments reported in Table 2.5) is needed to rapidly oxidize HMF to HFCA, an intermediate product that is stable in base.

It should be noted that no evidence for leaching of Au into solution was observed. A sample of the reaction mixture at the end of the reaction catalyzed by Au/C (sol) was filtered with a PTFE 0.2 μm filter to remove solid catalyst, and tested for trace Au by ICP analysis performed by Galbraith Laboratories, Knoxville TN. The ICP analysis determined the Au concentration in the liquid to be <0.2 ppm.

Conclusions

This work presents a comparison of the rate and product distribution for HMF oxidation over supported metal catalysts, Pt/C, Pd/C, Au/C and Au/TiO_2. The rate of oxidation of HMF over Au catalysts was an order of magnitude greater under the standard conditions of 295 K, 690 kPa O_2, 0.15 M HMF and 0.3 M NaOH. However, the rapid conversion of HMF over the Au catalysts was to the intermediate product HFCA, formed by oxidation of the aldehyde side chain of HMF. Under identical conditions, Pt and Pd were able to effectively oxidize the HFCA to FDCA, which indicates Pt and Pd can activate the alcohol side chain of HFCA whereas Au cannot. For Au to catalyze the formation of FDCA from HFCA, high pressures of O_2 and high concentrations of base were required, although the effect of base appeared to be more important than the O_2 pressure. Indeed, the rate of oxidation on Au/TiO_2 was independent of O_2 pressure. From our previous work on Au-catalyzed glycerol oxidation (51), we speculate that OH^- is required to activate the alcohol and form an aldehyde intermediate, which can subsequently

oxidize to the carboxylate in the presence of OH^-, Au catalyst and O_2. Evidently, Pt and Pd provide an alternative catalytic route to dehydrogenate the alcohol side chain that is unavailable on Au.

Acknowledgements

This material is based upon work supported by the National Science Foundation under Grant Nos. OISE 0730277 and EEC-0813570. Microscopy was performed by Levi Houk at the University of New Mexico, under the advisement of Dr. Abhaya Datye. The assistance of Erin C. Tamargo in the preparation of the Au/C (sol) catalyst is gratefully acknowledged.

Chapter 3

On the mechanism of selective oxidation of 5-hydroxymethylfurfural to 2,5-furandicarboxylic acid over supported Pt and Au catalysts

This chapter was previously published as Davis, S.E., Zope, B.N., and Davis, R.J. "On the mechanism of 5-hydroxymethylfurfural to 2,5-furandicarboxylic acid over supported Pt and Au catalysts." Green Chemistry, *14 (2012) 143-147.*

Introduction

The previous chapter has shown that supported Au is more active than supported Pt for HMF oxidation, although Au is less selective to the desired product (FDCA) under conditions of 0.15 M HMF, 0.3 M NaOH, 690 kPa O_2, and 295 K. For gold-catalyzed oxidation of HMF, increasing the NaOH:HMF ratio and the dioxygen pressure increased the selectivity to FDCA (18, 20, 21). Thus, an understanding of the precise roles of added base and molecular oxygen is important to developing an environmentally-friendly method for FDCA production. Moreover, additional studies on the activation of molecular oxygen in HMF oxidation on Au nanoparticles will provide new methods to control the reactivity of oxygen in organic transformations, thereby allowing the development of sustainable alternatives to traditional processes utilizing harmful inorganic oxidants.

Zope et al. reported a combined experimental and computational investigation of the selective oxidation of ethanol and glycerol over Au and Pt catalysts in liquid water (54). That study provided a detailed description of the reaction path for alcohol oxidation. In addition, Casanova et al. propose a reaction scheme for the key steps in HMF oxidation (20). In the

current work, we extend the studies of Zope et al.(54) and Casanova et al.(20) to include the oxidation of HMF over supported Au and Pt catalysts with labeled reagents $^{18}O_2$ and $H_2{}^{18}O$.

Experimental Methods

Catalyst Preparation

A supported gold catalyst (1.6 wt% Au/TiO_2; Sample 137A) was obtained from the World Gold Council (WGC). A supported Pt catalyst (3 wt% Pt/activated carbon) was obtained from Aldrich Chemical Co. The Pt catalyst was reduced in H_2 (UHP, Messer Gas) flowing at 150 cm^3 min^{-1} for 6 h at 573 K, cooled under flowing H_2 and gently exposed to air prior to use, whereas the Au catalyst was used as received. The catalysts were refrigerated and used without further pretreatment.

Oxidation of HMF

The aqueous phase oxidation of HMF (Acros, $\geq$98% purity) was carried out in a 50 cm^3 Parr Instrument Company 4592 batch reactor equipped with a glass liner. Dioxygen was either UHP (Messer Gas) or 97% $^{18}O_2$ (chemical purity >99.8%, Cambridge Isotope Laboratories).

In all reactions, 5.0 cm^3 of the reactant solution (aqueous HMF and NaOH) were added to the reactor along with the appropriate amount of catalyst. In reactions utilizing $H_2{}^{18}O$, the reactant solution was made using 97% $H_2{}^{18}O$ (99.8% pure, Cambridge Isotope Laboratories). The reactor was purged with flowing O_2 or $^{18}O_2$ and then pressurized to the desired value. A constant pressure was maintained by continuously feeding O_2 or $^{18}O_2$.

Because the product formation over Pt and Au as a function of reaction conditions were well described in our previous work (18), those conditions were replicated in the present study, with one exception. The dioxygen pressure in the experiments utilizing $^{18}O_2$ was lower here (345 kPa) than in previous work due to the pressure limit of the $^{18}O_2$ lecture bottle. Control experiments without any labeled compound were conducted prior to each experiment utilizing

^{18}O species under conditions identical to the labeling experiments. The control experiments confirmed that the small decrease in dioxygen pressure relative to our previous study had no significant effect on product selectivity. Our previous work showed that activity and product distribution during HMF oxidation were different over Au catalysts compared to Pt catalysts, even as the average metal particle sizes were nearly identical (2.6 nm and 2.5 nm, respectively) (18). This work also ruled out the effect of support on product selectivity (18). In addition, suitable choice of NaOH:HMF ratio, O_2 pressure and HMF:Au ratio resulted in a favorable product distribution to the diacid FDCA. Therefore, we investigated different scenarios to elucidate the similarities and/or differences between the Au and Pt catalysts for oxidation. Three different scenarios were used: HMF oxidation to a majority of FDCA over Pt/C using standard conditions (0.15 M HMF, 0.3 M NaOH, 690 kPa O_2, 295 K), HMF oxidation to a majority of HFCA over Au/TiO_2 using standard conditions, and HMF oxidation to a majority of FDCA over Au/TiO_2 in high base conditions (0.1 M HMF, 2.0 M NaOH, 2000 kPa O_2, 295 K).

The samples from the oxidation reactions were filtered using 0.2 μm PTFE filters. The product analysis was conducted using a Waters e2695 high performance liquid chromatograph (HPLC) at 308 K equipped with refractive index and UV/Vis detectors. The HPLC utilized a Bio-Rad Aminex HPX-87H column and 5 mM H_2SO_4 flowing at 0.5 cm^3 min^{-1} to perform the separation.

Mass spectrometry was performed using a Waters Micromass ZQ quadrupole mass spectrometer (in electronegative mode) using a direct injection of the product mixture. Prior work in our lab indicated that exchange of oxygen between the water and the product can occur during HPLC analysis (55). This exchange process was avoided by direct injection of the product into the mass spectrometer. Known compounds, in aqueous solution with NaOH, were directly

infused into the mass spectrometer to obtain reference spectra. The parent peak for HFCA appeared at a mass-to-charge ratio (m/z) of 141 (mass of HFCA 142 minus 1, since H^+ was removed during ionization). A sodium adduct of HFCA also appeared at m/z of 163 (mass of HFCA with one Na atom in place of one H atom, minus one proton removed during ionization). In the case of FDCA, a prominent peak appeared at m/z of 177, which corresponds to the mass of FDCA with a Na atom in place of one H atom, minus one proton removed during ionization.

To confirm that the products of HMF oxidation did not exchange O appreciably with liquid water, unlabeled HFCA and FDCA were dissolved separately in $H_2{}^{18}O$ in the presence of NaOH and Au/TiO_2 for the duration of a reaction experiment (6 h in the case of 0.3 M NaOH and 22 h in the case of 2.0 M NaOH). Separate control experiments were conducted in both 0.3 M and 2.0 M concentrations of NaOH to replicate experimental conditions used for the reactions. The mass spectra of HFCA and FDCA in control solutions confirmed that negligible amounts of ^{18}O from labeled water ($H_2{}^{18}O$) were incorporated into the products at standard and high base conditions.

The presence of hydrogen peroxide formed in a sample reaction mixture was evaluated by a colorimetric method (56). First, a 1 cm^3 sample of the filtered reaction product was immediately acidified with 1 cm^3 of 0.5 M H_2SO_4, to which 0.1 cm^3 of $TiO(SO_4)$ (15 wt% in dilute H_2SO_4, Aldrich) was added. Absorbance was subsequently measured at 405 nm on a Varian Cary 3E UV-vis spectrometer. A calibration curve of absorption versus H_2O_2 concentration was prepared by diluting a standard mixture of 30 wt% H_2O_2 (57). The lower limit of H_2O_2 detection was ~0.005 mM.

Results and Discussion

The oxidation of HMF catalyzed by Au/TiO_2 under standard conditions resulted in majority of HFCA ($\geq$98% selectivity) being produced after 6 h, as the oxidation of HMF to HFCA is rapid over Au (18). Previous studies showed no increase in selectivity to the diacid even if the reaction time was extended to 24 h (18). To understand the role of O_2 during oxidation, an oxidation experiment over Au/TiO_2 was carried out using $^{18}O_2$. The major product of oxidation, HFCA, under $^{18}O_2$ pressure in $H_2{}^{16}O$ showed no incorporation of ^{18}O atoms (Figure 3.1a). A control experiment without O_2 was carried out for HMF oxidation over Au/TiO_2 under standard reaction conditions. The major product, HFCA, was still obtained in significant selectivity (65%) with the rest of the product mixture being composed of 2,5-bishydroxymethylfuran (BHMF). This finding suggests that molecular oxygen does not play a direct role in the oxidation path. Similarly, Gorbanev, *et al.* found 100% conversion of HMF and 51% selectivity to HFCA (selectivity to BHMF = 38%, selectivity to levulinic acid = 11%) over 18 h under like conditions (21). Other work has shown that HMF rapidly degrades to BHMF and other products (levulinic acid, formic acid) in the presence of NaOH in solution, but that HFCA is stable in the presence of NaOH (18, 21). Recent work investigating the role of molecular oxygen in glycerol oxidation proposes an indirect but essential role in which oxygen scavenges electrons from the metal catalyst surface to close the catalytic cycle (55). Thus, molecular oxygen is believed to allow selective oxidation of aldehydes on the metal surface by aiding in sustaining a high turnover frequency and suppressing the oxidation route in solution-phase. As a result, in the presence of O_2, the HMF oxidation rate was significantly higher and almost complete selectivity to the monoacid HFCA product was observed. To understand the role of water, HMF oxidation was carried out in labeled water, $H_2{}^{18}O$. The analysis of the products from reactions under $^{16}O_2$ and

$H_2{}^{18}O$ showed peaks at m/z 145 and 167, corresponding to HFCA and the Na-adduct of HFCA with incorporation of two ^{18}O atoms (Figure 3.1a).

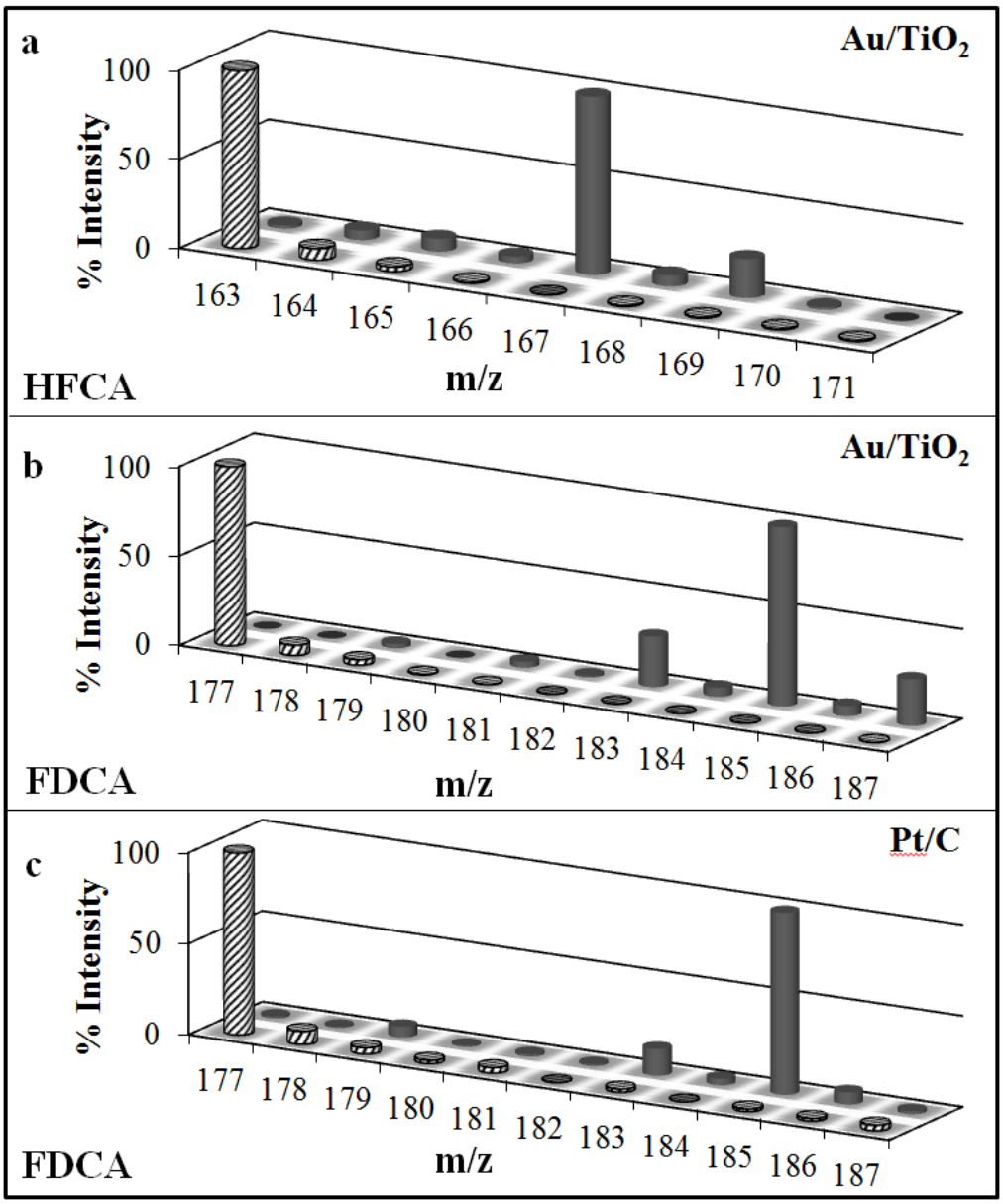

Figure 3.1. Mass spectra of major products from the oxidation of HMF (ionized in electronegative mode). Striped bars indicate experiments conducted in $^{18}O_2$ and $H_2{}^{16}O$; solid bars indicate experiments conducted in $^{16}O_2$ and $H_2{}^{18}O$. In all cases, HMF conversion = 100% and T = 295 K. m/z of major products without ^{18}O: HFCA = 141; Na Adduct of HFCA = 163; Na Adduct of FDCA = 177. (a) Catalyst: Au/TiO_2; majority product after 6 h: HFCA. Experimental conditions (both cases) HMF:Au = 150; NaOH:HMF = 2. In $^{16}O_2$, P = 690 kPa; in $^{18}O_2$, P = 345 kPa. (b) Catalyst: Au/TiO_2; majority product after 22 h: FDCA. Experimental conditions (both cases) HMF : Au = 100; NaOH : HMF = 20. In 16O2, P = 2000 kPa; in $^{18}O_2$, P = 345 kPa. (c) Catalyst: Pt/C; majority product after 6 h: FDCA. Experimental conditions (both cases) HMF:Pt = 150; NaOH:HMF = 2. In $^{16}O_2$, P = 690 kPa; in $^{18}O_2$, P = 345 kPa.

Interestingly, incorporation of multiple ^{18}O atoms in the acid product was observed during reaction with $H_2{}^{18}O$. Because the reaction products HFCA and FDCA did not exchange O with water on the time scale of the reaction, the appearance of ^{18}O in the products during reactions performed in $H_2{}^{18}O$ suggests that aqueous-phase oxidation proceeds through a geminal diol formed by the reaction of the aldehyde with the solvent. It is well known that aldehydes in water and base (OH^-) rapidly undergo reversible hydration in two steps: nucleophilic addition of a hydroxide ion to the carbonyl group, followed by proton transfer from water to the alkoxide ion intermediate (46). The reversibility of geminal diol formation accounts for two ^{18}O atoms found in the HFCA product formed during HMF oxidation (see Figure 3.2, Step 1). Incorporation of multiple ^{18}O atoms in reactions performed with $H_2{}^{18}O$ is consistent with the findings of similar studies of ethanol and glycerol oxidation (55).

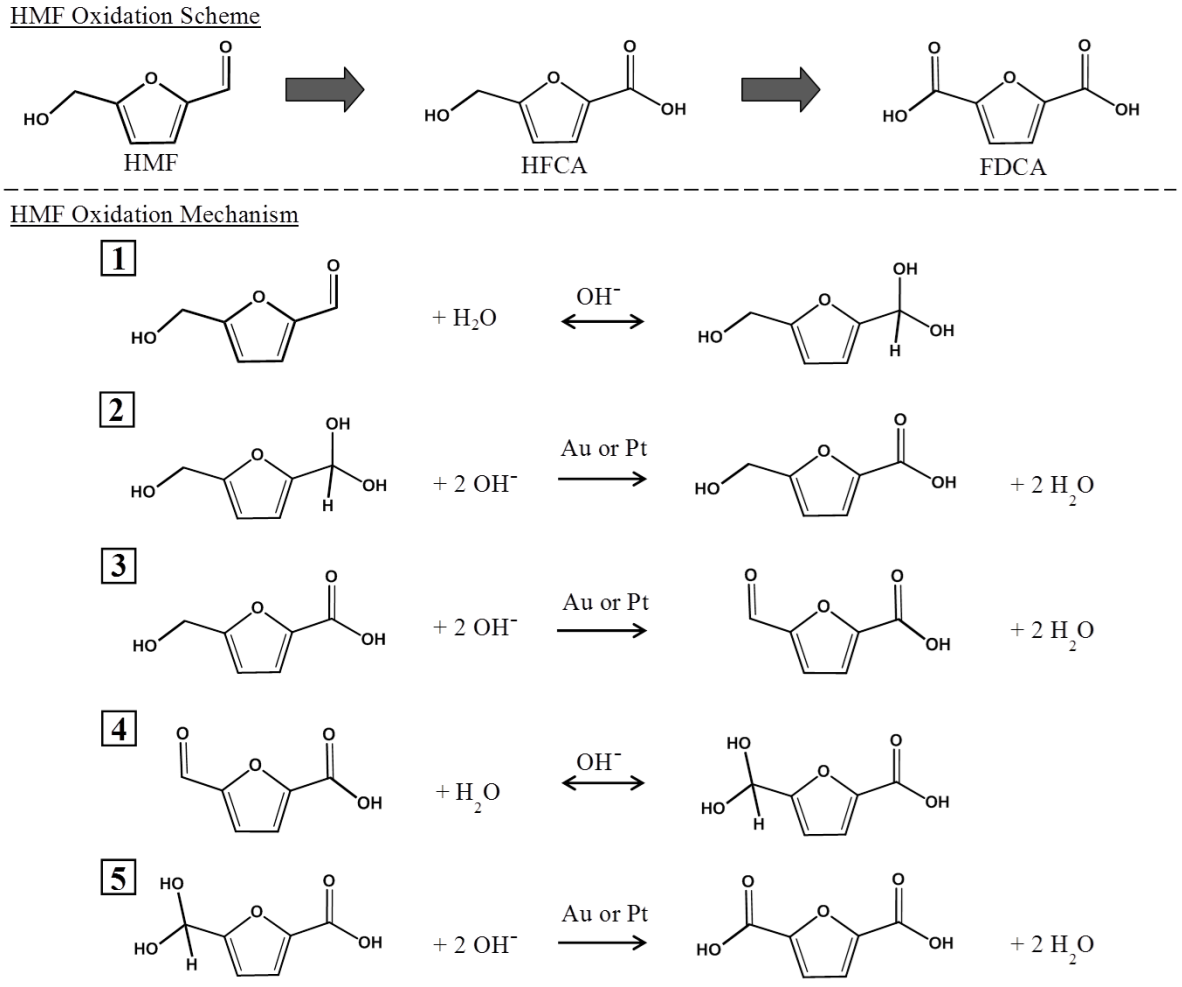

Figure 3.2. Overall reaction scheme and proposed mechanism for the oxidation of HMF in aqueous solution in the presence of excess base (OH^-) and either Pt or Au. Dioxygen (not shown) serves as a scavenger of electrons that are deposited into the metal particles during the catalytic cycle.

To obtain high yields of the desired product (FDCA), higher NaOH concentration, catalyst loading, and dioxygen pressure were required (18). Thus, reaction conditions (0.1 M HMF, 2.0 M NaOH, 2000 kPa O_2, 295 K) were utilized for the next set of experiments, except in the case of $^{18}O_2$ (P = 345 kPa, due to the pressure limit of the lecture bottle). The product selectivity was not significantly affected by the lower dioxygen pressure (Table 3.1). The

reaction time was increased to 22 h to accommodate the slow conversion of HFCA to FDCA. The major product under these conditions was FDCA (selectivity ≥69%). Again, the analysis of the product FDCA (Figure 3.1b) showed incorporation of ^{18}O into the product during the experiment with $^{16}O_2$ and $H_2{}^{18}O$ but not with labeled gaseous oxygen, $^{18}O_2$ and $H_2{}^{16}O$. The FDCA peak appeared at m/z equal to 185, indicating four ^{18}O atoms were incorporated into the Na-adduct of the product. Although the reaction conditions significantly affected the product distribution during HMF oxidation, the mode of oxygen incorporation was unchanged.

Table 3.1. Results from HMF Oxidation over Supported Au and Pt Catalysts at 295 K[a]

Catalyst	^{18}O Label	Molar ratio HMF:Metal	Molar ratio NaOH:HMF	O_2 P (kPa)	Time (h)	S_{HFCA}[b] (%)	S_{FDCA}[c] (%)
Au/TiO_2	none	150	2	345	6	97	3
Au/TiO_2	$^{18}O_2$	150	2	345	6	98	2
Au/TiO_2	$H_2{}^{18}O$	150	2	690	6	99	1
Au/TiO_2	none	100	20	345	22	35	65
Au/TiO_2	$^{18}O_2$	100	20	345	22	30	69
Au/TiO_2	$H_2{}^{18}O$	100	20	2000	22	21	79
Pt/C	none	150	2	345	6	33	67
Pt/C	$^{18}O_2$	150	2	345	6	32	68
Pt/C	$H_2{}^{18}O$	150	2	690	6	37	63

[a]Conversion of HMF is 100% in all cases.
[b]Selectivity to HFCA
[c]Selectivity to FDCA

A control experiment conducted in the absence of O_2 but under otherwise the same high base conditions (2.0 M NaOH) and over Au resulted in 100% conversion of HMF with 85% yield of HFCA. Moreover, simply dissolving HMF in 2.0 M NaOH solution (no O_2 or metal

catalyst) gave 97% conversion of HMF and 28% yield of HFCA, with the remainder of species being decomposition products such as levulinic acid and BHMF. Apparently, the presence of O_2 was necessary to produce FDCA from HFCA in high base conditions over Au/TiO_2 catalysts. Molecular oxygen was not needed to convert HMF to HFCA.

Platinum is known to deprotonate an alcohol to an alkoxy intermediate under neutral or mildly alkaline conditions (58). Thus, HMF oxidation was also studied over a Pt/C catalyst at standard conditions and was $\geq$60% selective to FDCA after 6 h (Table 3.1). The mass spectra corresponding to FDCA from labeling experiments with ^{18}O are reported in Figure 3.1c. Mass spectrometry analysis of the products of HMF oxidation under $^{18}O_2$ pressure in $H_2{}^{16}O$ contained peaks at m/z values of 141, 163, and 177, corresponding to HFCA, the Na-adduct of HFCA and the Na adduct of FDCA, respectively, with no incorporation of ^{18}O atoms. However, analysis of products from reactions under $^{16}O_2$ pressure in $H_2{}^{18}O$ revealed peaks at 145, 167, and 185, corresponding to HFCA with the incorporation of two ^{18}O atoms, the Na-adduct of HFCA with the incorporation of two ^{18}O atoms, and the Na adduct of FDCA with the incorporation of four ^{18}O atoms. Higher selectivity to the desired product, FDCA, observed here with Pt/C at standard conditions of low base and low catalyst loading confirms the noble nature of Au compared to Pt. The results also suggest that the water solvent also plays an important role during Pt-catalyzed oxidation, despite the recognized ability of Pt to dissociate O_2.

A proposed mechanism for the oxidation of HMF is depicted in Figure 3.2. As discussed above, molecular oxygen was not essential for oxidation of the aldehyde side-chain of HMF to produce HFCA. However, control experiments indicated that base and a metal catalyst were required to produce FDCA at the reaction temperature used here. The aldehyde side-chain is believed to undergo rapid reversible hydration to a geminal diol via nucleophilic addition of a

hydroxide ion to the carbonyl and subsequent proton transfer from water to the alkoxy ion intermediate (Figure 3.2, Step 1). This step accounts for the incorporation of two ^{18}O atoms in HFCA when the reaction is performed in $H_2{}^{18}O$. The second step is the dehydrogenation of the geminal diol intermediate, facilitated by the hydroxide ions adsorbed on the metal surface, to produce the carboxylic acid (Figure 3.2, Step 2).

An oxidation experiment performed in the absence of base over both Au and Pt catalysts resulted in no conversion of HMF, indicating the important role of OH^- during oxidation at 295 K. Production of the desired product, FDCA, requires further oxidation of the alcohol side-chain of HFCA. Base is believed to deprotonate the alcohol side-chain to form an alkoxy intermediate, a step that may occur primarily in the solution (55). Hydroxide ions on the catalyst surface then facilitate the activation of the C-H bond in the alcohol side-chain to form the aldehyde intermediate, 5-formyl-2-furancarboxylic acid (FCA) (Figure 3.2, Step 3). The next two steps (Figure 3.2, Steps 4 and 5) oxidize the aldehyde side-chain of FCA to form FDCA. These two steps are expected to proceed analogously to Steps 1 and 2 for oxidation of HMF to HFCA. The reversible hydration of the aldehyde group in Step 4 to a geminal diol accounts for two more ^{18}O atoms incorporated in FDCA when the oxidation is performed in $H_2{}^{18}O$. Thus, the sequence in Figure 3.2 explains the incorporation of all 4 ^{18}O atoms in FDCA when the reaction is performed in labeled water.

Platinum is known to activate the geminal hydrogen atoms associated with alcohols (58). Also, supported Pt catalyzes alcohol oxidation in the absence of base, albeit at a very slow rate (55). These facts explain the high selectivity to FDCA during HMF oxidation over Pt compared to Au under identical conditions. Significantly increasing the concentration of hydroxide ions available, by increasing the concentration of NaOH in the reaction medium, facilitates hydrogen

abstraction reactions (both C-H and O-H) on Au surfaces, therefore increasing the rate of FDCA formation over Au catalysts.

Although the role of molecular oxygen in the oxidation mechanism is not obvious, O_2 is essential to produce FDCA in significant amounts during HMF oxidation over supported metal catalysts. The precise role of O_2 has been debated in literature, including direct participation of atomic oxygen during dehydrogenation or oxidation steps (59) or, more recently, as an electron scavenger undergoing reduction to peroxide species and hydroxide ions (55). Our results from isotopic labeling studies indicate that molecular oxygen is not directly incorporated into the products of HMF oxidation but instead hydroxide ions from water act as a source of oxygen. Also, a test for the presence of peroxide in the product mixture of a typical reaction over Au/TiO_2 under standard conditions revealed 0.3 mM of H_2O_2 in solution after 1 h. The presence of peroxide during oxidation reactions over Au indicates that O_2 is reduced during these reactions.(53) Activation of O_2 occurs through formation of peroxide intermediates (60). In the next step, the peroxide intermediates likely undergo further reduction to form hydroxide species (55). Therefore, O_2 is suggested to undergo reduction by removing the electrons deposited into the metal particles during the adsorption and reaction of hydroxide ions thereby completing the catalytic redox cycle. Although the reduction of O_2 to form hydroxide species would indicate that ^{18}O species should be present in the acid products of reactions run with $^{18}O_2$ and $H_2{}^{16}O$ after many turnovers, no such labeling is seen in Figure 3.1. This explained by a quick calculation of the molar ratio of ^{18}O:^{16}O species in solution at 50% conversion of HMF, showing a very low amount of ^{18}O species relative to ^{16}O species. For every mole of HMF converted to FDCA, 6 moles of OH^- are consumed (Figure 3.2) and thus, under ideal cases, 6 moles of OH^- would be

regenerated from O_2. Hydroxide ions are regenerated from the reduction of O_2, which occurs through the formation and dissociation of peroxide and hydrogen peroxide intermediates:

$$O_2 + H_2O \rightarrow OOH^* + HO^* \quad (1)$$

$$OOH^* + H_2O \rightarrow H_2O_2^* + HO^* \quad (2)$$

$$HO^* + e^- \leftrightarrow HO^- + * \quad (3)$$

where * represents a site on the metal catalyst (60).

Under our conditions and assuming conditions of 50% conversion of HMF with 100% selectivity to FDCA (to calculate the highest possible amount of $^{18}OH^-$ species in solution), 0.0023 moles of $^{18}OH^-$ would be produced. The amount of ^{16}O species present from to the H_2O is 0.28 moles; thus, the molar ratio of ^{18}O:^{16}O species is 0.008. The ratio of ^{18}O:^{16}O species incorporated into the acid products would be even lower, as ^{18}O would not be preferentially incorporated. Detection of such a low amount of ^{18}O is difficult using the techniques at our disposal.

Conclusions

The oxidation of HMF to FDCA in aqueous solution at high pH is a sequential reaction in which the aldehyde site chain is first rapidly oxidized by the solvent. In a subsequent reaction, hydroxide ions from water in the presence of Au or Pt metal catalysts promote O-H and C-H bond activation of the alcohol side chain of HMF and then add directly to aldehyde intermediates to eventually form acid products. Molecular oxygen is required to scavenge the electrons

deposited into the metal catalyst particles during the reaction mechanism, thus closing the catalytic cycle.

Acknowledgements

This material is based upon work supported by the National Science Foundation under Grant Nos. OISE 0730277 and EEC-0813570, and by the United States Department of Energy under Grant No. DE-FG02-95ER14549. The guidance provided by Dr. Bhushan Zope for mass spectroscopy analysis is gratefully recognized. Helpful discussions with David Hibbitts and Professor Matthew Neurock are also acknowledged.

Chapter 4

The kinetics of HMF and HFCA oxidation over Pt

The work in this chapter was the basis for a portion of the publication: Davis, S.E., Sanchez, A., Gosselink, R.W., Bitter, J.H., de Jong, K.J., Datye, A.K., and Davis, R.J. "The influence of carbon support and reaction conditions on the selective oxidation of 5-hydroxymethylfurfural over Pt and Au nanoparticles," in preparation.

Introduction

The oxidation of HMF to FDCA involves the oxidation of both an aldehyde group and an alcohol group. The aldehyde group, which is highly reactive in high concentrations of aqueous NaOH, is rapidly oxidized to acid in the presence of a metal catalyst (18). Although Au alone is unable to activate the alcohol group, Au in conjunction with high concentrations of OH^- can activate the alcohol group and oxidize it to an aldehyde, which can be rapidly oxidized to acid (18). In contrast, supported Pt and Pd catalysts, even in presence of relatively low OH^- concentrations (2:1 NaOH:HMF), produced a majority of the diacid product, FDCA, at a relatively low concentration of NaOH (2:1 NaOH:HMF), which is likely the result of higher alcohol reactivity on those metals compared to Au (18). However, the turnover frequency, or TOF, of HMF oxidation over Pt and Pd catalysts is reportedly lower than that over Au catalysts.

Understanding the roles of substrate concentration, NaOH concentration, O_2 pressure, and temperature on the reaction rate for HMF and HFCA oxidation may yield insight into oxidative transformations of other biomass-derived molecules. Other studies have investigated the effects of temperature, O_2 pressure, and NaOH concentration on product yield during HMF

oxidation, but to the best of our knowledge, a systematic study on the influence of these parameters on reaction rate has not been reported.

Experimental Methods

Catalyst Preparation

A 3 wt% Pt on activated carbon (Aldrich) was also used in this study. It was reduced in H_2 (UHP, Messer Gas) flowing at 150 cm^3 min^{-1} for 6 h at 573 K and cooled under flowing H_2. After exposure to air, the catalyst was refrigerated and used without further pretreatment.

Catalyst Characterization - Chemisorption of H_2

The dispersion of Pt was determined using a Micromeritics ASAP 2020 automated adsorption system. The Pt catalyst was heated to 473 K at 4 K min^{-1} under flowing H_2 (UHP, Messer Gas) and reduced for 1.5 h. The samples was evacuated for 2 h at 473 K and then cooled to 308 K for analysis.

Oxidation reactions

The aqueous phase oxidation of HMF (Acros, ≥98% purity) or HFCA (ChemBridge, 95% purity) was carried out in a 50 cm^3 Parr Instrument Company 4592 batch reactor equipped with a glass liner. In all reactions, 7.0 cm^3 of the reactant solution was added to the reactor along with the appropriate amount of catalyst. The reactor was purged with flowing O_2 (UHP, Messer Gas) and then pressurized to the desired value. A constant pressure was maintained by a continuous O_2 feed. Samples of the product solution were acquired by removing the top of the reactor, taking the sample, flushing the reactor with O_2 and repressurizing. The maximum O_2 transport rate from the gas to the liquid was determined by oxidation of sodium sulfite (48), and the reactant oxidation rate was kept significantly below this limit when quantitative rates were measured. The samples from the oxidation reactions were filtered using PTFE 0.2 μm filters and

diluted with deionized H_2O in a 1:3 sample:water ratio. The analysis was conducted using a Waters e2695 high performance liquid chromatograph (HPLC) at 303 K equipped with refractive index and UV/vis detectors. The HPLC utilized a Bio-Rad Aminex HPX-87H column and 5mM H_2SO_4 flowing at 0.5 cm^3 min^{-1} to perform the separation. The retention times and calibrations for observed products were determined by injecting known concentrations.

Results and Discussion

Reaction kinetics of HMF and HFCA oxidation over commercial Pt/C

Though the influence of temperature, substrate concentration, O_2 pressure, and base concentration on the product distribution during HMF oxidation has been widely investigated and reported in the literature, there are few reports on the effects of these parameters on reaction rates. To the best of our knowledge there have been no reports on the influence of these parameters on the Pt-catalyzed oxidation rate of HFCA, the main intermediate of HMF oxidation to FDCA. Generally, the first step of HMF oxidation is oxidation of the aldehyde moiety to carboxylic acid, HFCA. The first step in oxidation of HFCA is oxidation of the alcohol moiety to aldehyde. We chose a commercially-available 3 wt% Pt/C catalyst (Aldrich) for these investigations. The dispersion of Pt was determined by H_2 chemisorption to be 98%.

The effect of substrate concentration was investigated over the range of 0.05 M to 0.15 M. All other reaction parameters (295 K, 690 kPa O_2, 0.30 M NaOH concentration, 0.01 or 0.02 g 3 wt% Pt/C depending on substrate) were held constant for each experiment. Initial reactant concentrations were chosen based on standard conditions in previous work (0.15 M substrate, 0.30 M NaOH) (18). To ensure an excess of NaOH was available throughout the reaction, the range of initial substrate concentrations was kept below 0.15 M. Because the rate of HMF

conversion was greater than that of HFCA, the catalyst loading in the HMF oxidation experiments was 0.01 g whereas 0.02 g was used in the HFCA experiments. Turnover frequencies derived from initial rates and metal dispersions of fresh catalysts are plotted versus initial substrate concentration for both HMF and HFCA oxidation in Figure 4.1.

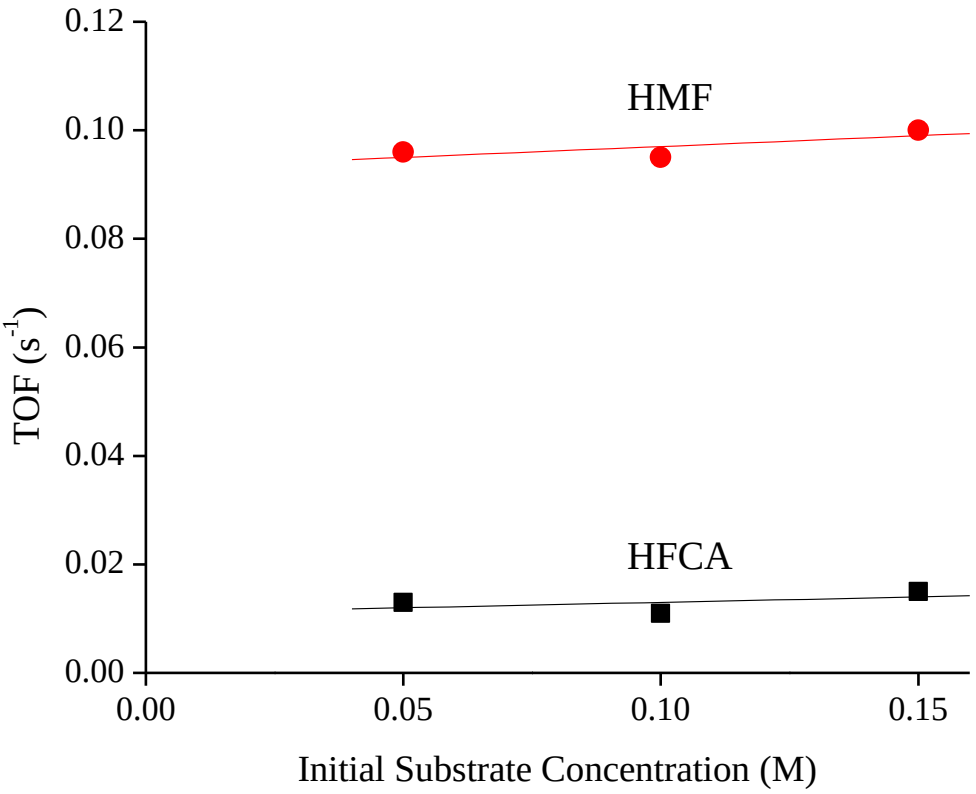

Figure 4.1 Turnover frequencies of HMF and HFCA oxidation as a function of initial substrate concentration confirm zero order behavior. Reaction conditions: 0.30 M NaOH, 295 K, 690 kPA O_2, 0.01 g 3 wt% Pt/C (HMF) or 0.02 g 3 wt% Pt/C (HFCA)

As Figure 4.1 shows, the oxidation rates of both HMF and HFCA were zero order in substrate concentration over the range investigated. This finding is in agreement with Vinke et

al., who investigated HMF oxidation over Pt/Al_2O_3 (35). In general, zero order behavior is consistent with the Pt catalyst surface being highly covered with reactant.

The influence of initial NaOH concentration was also probed. The initial substrate concentration 0.15 M was chosen for both HMF and HFCA, and the rest of the conditions were held constant, as described earlier (295 K, 690 kPa O_2, 0.01 or 0.02 g Pt/C depending on substrate). Turnover frequencies are plotted as a function of NaOH concentration in Figure 4.2.

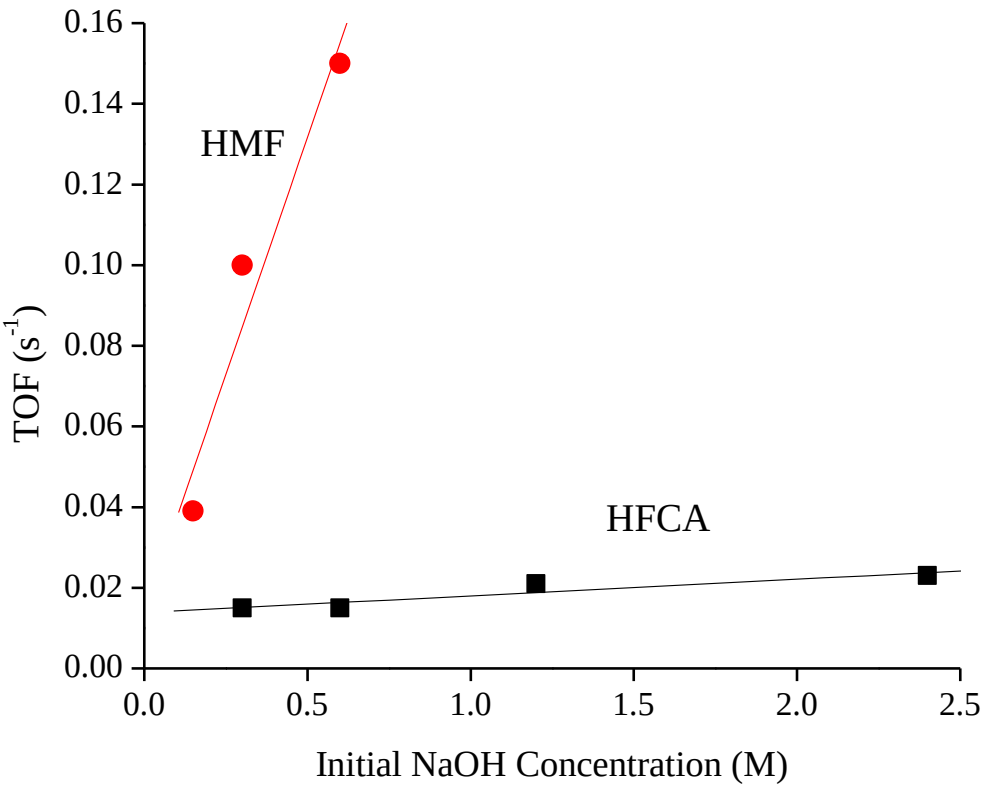

Figure 4.2 Turnover frequencies of HMF and HFCA oxidation as functions of initial NaOH concentration. Reaction conditions: 0.15 M HMF or HFCA, 295 K, 690 kPA O_2, 0.01 g 3 wt% Pt/C (HMF) or 0.02 g 3 wt% Pt/C (HFCA)

The rate of HMF oxidation was first order with respect to NaOH concentration in the range 0.15 M – 0.60 M NaOH. It should be noted that the low end of the concentration range, 0.15 M, represents a 1:1 ratio of NaOH:HMF, and thus production of acid product will lower the pH during the reaction. Moreover, the oxidation of HMF proceeds through the main intermediate HFCA. Thus, the initial oxidation rate, calculated based on the consumption of HMF, is attributed to the rate of oxidation of the aldehyde moiety to acid, i.e. HMF to HFCA.

The influence of NaOH concentration on the rate of HFCA oxidation over Pt was not the same as its influence on HMF oxidation. A run utilizing 0.15 M NaOH resulted in very little conversion of HFCA (5% conversion in 3 h), presumably because the 1:1 stoichiometry of NaOH:HFCA of this experiment suggests that all of the NaOH was consumed in neutralizing the acid groups of HFCA. At higher NaOH concentrations (above 0.30 M NaOH, 2:1 NaOH:HFCA), the reaction rate was nearly zero order in NaOH concentration.

The results here indicate that the oxidation of the aldehyde moiety of HMF depends on NaOH concentration, whereas the oxidation of the alcohol moiety of HFCA does not, above 2:1 NaOH:HFCA. Aldehydes in aqueous solution are recognized to undergo rapid, reversible hydration to geminal diols and the reaction is accelerated at high pH (46). Previous work indicated that the oxidation of HMF proceeds through hydration of aldehyde in solution and subsequent dehydrogenation of the geminal diol on the catalyst surface to produce carboxylic acid (33). This work demonstrates that this step of HMF oxidation follows a first order dependence on NaOH concentration. The higher concentration of OH^- in solution likely facilitates the hydration to geminal diol while the increased density of hydroxide on the metal surface likely increases the rate of dehydrogenation of the geminal diol to carboxylic acid. Above a critical concentration (2:1 NaOH:HFCA, or 0.30 M NaOH in this case), however, there

is no dependence of HFCA oxidation rate (the second oxidation step in HMF oxidation to FDCA) on NaOH concentration.

The effect of O_2 pressure in the range 690 – 3000 kPa on HMF oxidation rate was previously investigated over a Au/TiO_2 catalyst and reported to be zero order. The relationship between HMF oxidation rate and O_2 pressure, and between HFCA oxidation rate and O_2 pressure over Pt, however, has not been probed. Thus, the O_2 pressure was varied between 690 kPa and 2070 kPa and the initial turnover frequencies were evaluated (Figure 4.3).

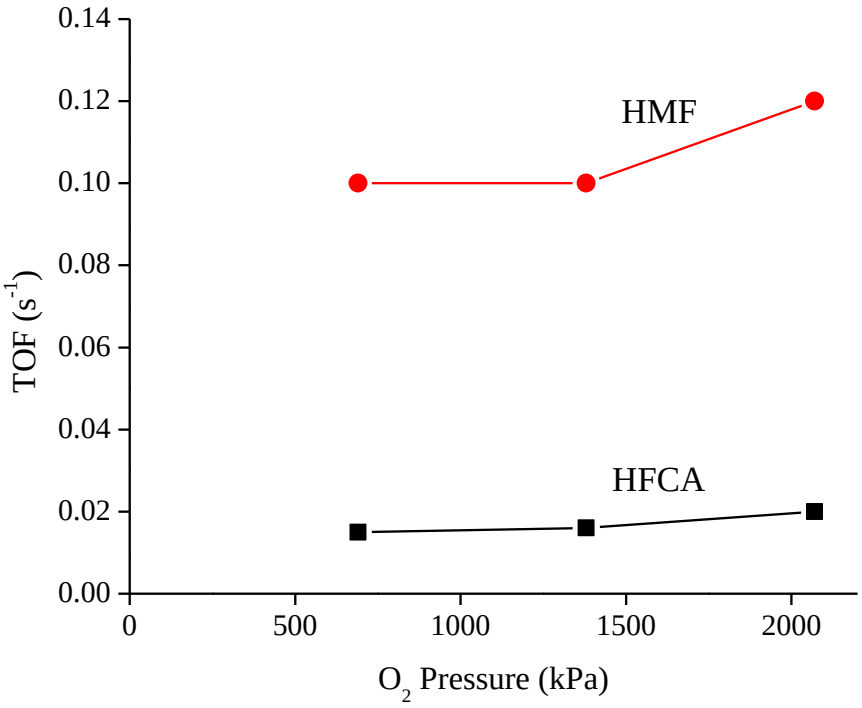

Figure 4.3 Turnover frequencies of HMF and HFCA oxidation as function of O_2 pressure. Reaction conditions: 0.15 M HMF or HFCA, 0.30 M NaOH, 295 K, 0.01 g 3 wt% Pt/C (HMF) or 0.02 g 3 wt% Pt/C (HFCA)

In both cases, the O_2 pressure was increased by 300%, but the rate of oxidation increased by only 20% for HMF oxidation and 10% for HFCA oxidation. Thus, the rates of HMF and HFCA oxidation were nearly zero order in O_2 over the range of 690 to 2070 kPa. This result is not surprising, given the proposed mechanism for HMF oxidation, in which the role of O_2 is simply to scavenge electrons from the catalyst surface.

The temperature dependence of both HMF and HFCA oxidation was established and overall activation energies for both HMF and HFCA oxidation were calculated. The oxidation of HMF was investigated at temperatures between 273 K and 308 K to keep the oxidation rate below the known external mass transfer limit in our system. Likewise, oxidation of HFCA was investigated between 295 K and 323 K. Arrhenius-type plots from HMF and HFCA oxidation are shown in Figure 4.4.

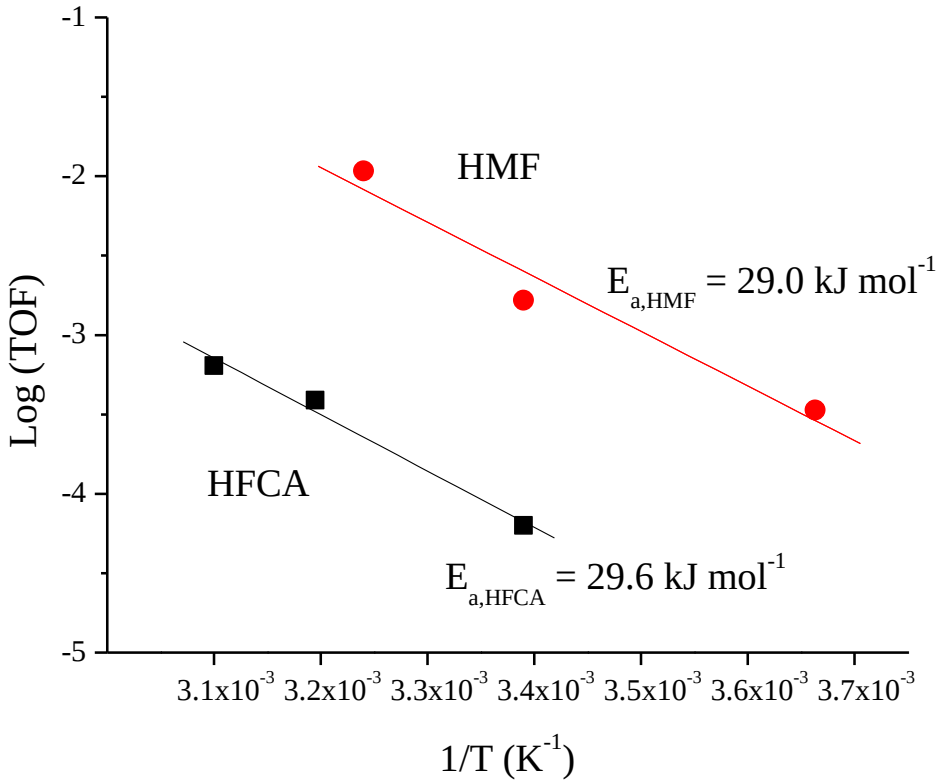

Figure 4.4. Arrhenius plots of HMF and HFCA oxidation. Reaction conditions: 0.15 M HMF or HFCA, 0.30 M NaOH, 690 kPa O_2, 0.01 g 3 wt% Pt/C (HMF) or 0.02 g 3 wt% Pt/C (HFCA)

The overall activation energy of HMF oxidation was calculated to be 29.0 kJ mol^{-1} in this study, which is lower than 37.2 kJ mol^{-1} reported by Vinke et al. over Pt/Al_2O_3 (reaction conditions: constant pH = 9.0, p(O_2) = 0.2 atm (p(total) 1.0 atm), 1.0 g 5 wt% Pt/Al_2O_3, 0.1 M HMF) (35).

The overall activation energy of HFCA oxidation was 29.6 kJ mol^{-1}, which is surprisingly similar to that of HMF oxidation. The important role of base in the conversion of both molecules

likely affects the overall activation energies. Moreover, the contributions from solution chemistry (reversible hydration of aldehydes, deprotonation of alcohols) during the aqueous oxidation of HMF and HFCA are significant, and this likely influences the overall activation barrier to oxidation.

Conclusions

The kinetic studies in this work showed that the oxidation of HMF over Pt catalyst was zero order with respect to substrate concentration, first order with respect to NaOH concentration, and had an activation energy of 29.0 kJ mol^{-1}. In addition, the oxidation of reaction intermediate HFCA over Pt was found to be zero order in substrate concentration and O_2 pressure. The HFCA reaction rate was zero order in NaOH concentration above 2:1 NaOH:HFCA, but was influenced by NaOH concentration below this threshold. The observed activation energy of HFCA (alcohol oxidation) was found to be 29.6 kJ mol^{-1}, which was surprisingly similar to the observed HMF activation energy.

Acknowledgements

Support from the National Science Foundation (Grant Nos. OISE 0730277 and EEC-0813570) is gratefully acknowledged.

Chapter 5

Base-free oxidation of HMF

The work in this chapter was the basis for portions of the publications: Zope, B.N., Davis, S.E., and Davis,R.J. "Influence of Reaction Conditions on Diacid Formation During Au-Catalyzed Oxidation of Glycerol and Hydroxymethylfurfural," Topics in Catalysis, *55 (2012) 24-32. and Davis, S.E., Sanchez, A., Gosselink, R.W., Bitter, J.H., de Jong, K.J., Datye, A.K., and Davis, R.J. "The influence of carbon support and reaction conditions on the selective oxidation of 5-hydroxymethylfurfural over Pt and Au nanoparticles," in preparation.*

Introduction

The previous sections have discussed extensively the positive influence of added base on the rate of metal-catalyzed alcohol oxidations. The addition of homogeneous base, however, presents negative environmental and economic impacts since the high pH of the medium is corrosive and the product salts need to be neutralized to release free acid. Thus, there has been a recent push to find alternatives to the use of homogeneous bases.

Lilga et al. reported on the base-free oxidation of HMF to FDCA over a Pt/ZrO_2 catalyst in a flow reactor (23, 61). Apparently, the oxidation proceeds over Pt in the absence of homogeneous base at a relatively higher temperature (373 K) than that commonly used in previous studies. The group utilized low concentrations of HMF (0.5 – 3 wt%) to keep the product FDCA within its solubility limit, ultimately realizing 98% yield of FDCA (373 K, 1035 kPa O_2). The mechanism of base-free oxidation of HMF was not reported.

The mechanism for HMF oxidation over Au and Pt catalysts was recently investigated through the use of isotopically-labeled dioxygen and water and was found to be the same over both Au and Pt (33), as reported in Chapter 3. Similar techniques were used in this work to probe the mechanism of base-free HMF oxidation.

The use of a solid base support for the metal catalyst also has potential to negate the need for addition of homogeneous base to the reaction. For example, some investigators explored hydrotalcites as solid base supports for Au catalysts in the aqueous oxidation of HMF to FDCA (24, 26). However, if a solid base material is to be used to replace homogeneous base, the interaction between the basic sites on the catalyst and the product acid FDCA must be considered. Reportedly, hydrotalcite materials are not highly stable in presence of acid and may selectively leach Mg (62). In addition, the very low solubility of the product acids HFCA and FDCA in neutral water must also be addressed, as products may precipitate and/or inhibit access to the metal catalyst (22, 23). Thus, the leaching of hydrotalcites during HMF oxidation was tested in this work.

Experimental Methods

Catalyst Preparation

A 3 wt% Pt on activated carbon (Aldrich) was also used in this study. It was reduced in H_2 (UHP, Messer Gas) flowing at 150 cm^3 min^{-1} for 6 h at 573 K and cooled under flowing H_2. After exposure to air, the catalyst was refrigerated and used without further pretreatment.

Chemisorption of H_2

The dispersion of Pt was determined using a Micromeritics ASAP 2020 automated adsorption system. The Pt catalyst was heated to 473 K at 4 K min^{-1} under flowing H_2 (UHP, Messer Gas) and reduced for 1.5 h. The sample was evacuated for 2 h at 473 K and then cooled to 308 K for analysis.

Oxidation reactions

The aqueous phase oxidation of HMF (Acros, ≥98% purity) was carried out in a 50 cm^3 Parr Instrument Company 4592 batch reactor equipped with a glass liner. In all reactions, 7.0 cm^3 of the reactant solution was added to the reactor (which was preheated to the desired temperature using heating tape and a temperature controller) along with the appropriate amount of catalyst. The reactor was purged with flowing O_2 (UHP, Messer Gas) and then pressurized to the desired value. A constant pressure was maintained by a continuous O_2 feed. At the end of the desired reaction time, a portion of the product mixture was filtered using PTFE 0.2 μm filters and used as-is for mass spectroscopy.

The remaining slurry (known volume) was washed with a known volume of a 0.30 M NaOH solution to dissolve any acid products that may have precipitated. This slurry was filtered

as above and samples were diluted 1:3 product:water v:v for product quantification via a Waters e2695 high performance liquid chromatograph (HPLC) at 303 K equipped with refractive index and UV/vis detectors. The HPLC utilized a Bio-Rad Aminex HPX-87H column and 5mM H_2SO_4 flowing at 0.5 cm^3 min^{-1} to perform the separation. The retention times and calibrations for observed products were determined by injecting known concentrations.

Leaching of Mg and Al from hydrotalcite catalysts

To investigate the leaching of Mg and Al from hydrotalcite catalysts, aqueous HMF (1 mmol HMF in 6 cm^3 H_2O) was added to the batch reactor, which was flushed with helium and pressurized to 340 kPa. The reactor was heated to 363 K over 30 minutes, at which point the Au/TiO_2 and HT were added. The reactor was flushed with O_2 and pressurized to 340 kPa. The Au/TiO_2 and hydrotalcite (HT), described above, were used without further pretreatment. The reaction product mixture was filtered using a PTFE 0.2 μm filter, and the resulting mixture was analyzed via HPLC. The product mixture was also analyzed by ICP (Galbraith Laboratories, Knoxville, TN) for Mg and Al content.

Mass Spectrometry

Mass spectrometry was performed using a Waters Micromass ZQ quadrupole mass spectrometer (in both electronegative and electropositive modes, depending on the molecule being ionized) using a direct injection of the product mixture. Prior work in our lab indicated that exchange of oxygen between the water and the product can occur during HPLC analysis (54). This exchange process was avoided by direct injection of the product into the mass spectrometer. Known compounds in aqueous solution were directly infused into the mass spectrometer to

obtain reference spectra. The electronegative mode was best to ionize HFCA, FCA, and FDCA. The parent peak for HFCA appeared at a mass-to-charge ratio (m/z) of 141 (mass of HFCA, 142, minus 1, since H^+ was removed during ionization). In the case of FDCA, a prominent peak appeared at m/z of 155, which corresponds to the mass of FDCA minus one proton removed during ionization. The peak for FCA appeared at 139, which corresponds to the mass of FCA, 140, minus 1, as 1 H^+ was removed during ionization. The electropositive mode was best to ionize HMF. The peak for HMF appeared at 127, corresponding to the mass of HMF plus 1 H^+ added during ionization.

Results and Discussion

Base-free HMF oxidation over Pt

Previous work indicated that the use of Pt/ZrO_2 as catalyst for the oxidation of HMF at relatively higher temperatures (373 K) resulted in high selectivity to the diacid product FDCA (98%) without added base (23). The conditions of Lilga et al. were replicated in our reactor system using a physical mixture of Pt/C and ZrO_2. Indeed, similar product distributions were obtained (Table 5.1). Moreover, a separate reaction was performed under the same reaction conditions, but using only Pt/C. The results are seen in Table 5.1. It was discovered that the ZrO_2 support was not vital to the production of FDCA over Pt.

Table 5.1. Product selectivity during base-free oxidation of HMF over Pt and ZrO_2 Catalysts[a]

Catalyst	Conversion[b]	S_{FDCA}[c]
Lilga's Pt/ZrO_2	100%	>98%
Physical mixture Pt/C and ZrO_2	100%	100%
Pt/C	100%	100%

[a]reaction conditions: 0.3 M HMF; 1034 kPa O_2; HMF:Pt = 30 mol:mol; HMF:ZrO_2 = 1:1 mass:mass
[b]HMF conversion after 24 h
[c]selectivity to FDCA

Mechanism of base-free HMF oxidation over commercial Pt/C

Although Lilga's work (23) indicated oxidation of HMF in absence of homogeneous base was possible, no description of the reaction path was indicated. Therefore, we explored the mechanism of Pt-catalyzed HMF oxidation utilizing isotopically labeled O_2 and H_2O. This study on the base-free oxidation complements our earlier mechanistic study on base-promoted HMF oxidation (33).

To confirm that the products of HMF oxidation did not exchange O appreciably with liquid water, unlabeled HFCA, FCA, and FDCA were dissolved separately in $H_2{}^{18}O$ in the presence of Pt/C and heated to reaction temperature for the duration of a reaction experiment. The same type of control experiment was conducted with HMF, though the duration was 4 h because 100% conversion of HMF is realized in 4 h during a reaction. All experiments were performed under N_2 rather than O_2 to minimize oxidation.

Significant conversion of HFCA, even an in inert environment, was observed in a control experiment utilizing unlabeled water (60% conversion of HFCA in 18 h, with 83% selectivity to

FCA and 17% selectivity to FDCA). The parent peaks of unlabeled HFCA and FCA (142 g mol^{-1} and 140 g $mole^{-1}$, respectively) are 2 mass units apart, which would cause a problem in the analysis if ^{18}O were incorporated. The mass to charge ratio is the same for HFCA containing no ^{18}O and FCA with one ^{18}O incorporated (m/z = 141); thus, it is impossible to distinguish between the two compounds directly injected into the mass spectrometer. As this is the expected outcome (exchange in the aldehyde group due to reversible hydration in water, but no exchange in the acid group), an exchange experiment utilizing HFCA would not yield useful results and was therefore not performed. The exchange experiment utilizing FCA resulted in some oxidation, even under inert atmosphere, but the only product was FDCA. The parent peaks of FDCA (m/z = 155) and FCA (m/z = 139) are separated by 16 mass units, so peak overlap was not a concern in the analysis. Likewise, HMF and its oxidation product, HFCA, are separated by 16 mass units. The FDCA control experiment did not result in any conversion of FDCA.

To confirm that the alcohol moiety does not exchange ^{18}O with water under our reaction conditions, ethanol was tested as substrate (0.3 M ethanol, 18 h and 348 K; pressure 1034 kPa to keep substrate in liquid phase). No scrambling of oxygen was observed between ethanol and $H_2{}^{18}O$; thus, exchange between the hydroxymethyl group of HFCA and $H_2{}^{18}O$ was not expected. An exchange experiment for the dialdehyde product, DFF, was not performed because of the known reactivity of aldehydes in water.

The mass spectrum of the mixture from the HMF exchange experiment in $H_2{}^{18}O$ displayed a prominent peak at m/z = 129, corresponding to HMF with incorporation of one ^{18}O. Thus, scrambling of one oxygen atom in HMF with water must be accounted for when analyzing the final product. The oxygen atom that was most likely exchanged with water was that of the highly reactive aldehyde group, presumably the result of reversible hydration.

The spectrum from the FCA control experiment showed a prominent peak at m/z = 141, indicating incorporation of one ^{18}O atom from $H_2{}^{18}O$ in FCA. An additional smaller peak was seen at m/z = 143, suggesting the exchange of two ^{18}O atoms. Thus, the scrambling of at least one oxygen atom, and possibly two, in FCA must be taken into account when analyzing the final product FDCA. Very little exchange of oxygen between FDCA and $H_2{}^{18}O$ was observed.

Although some oxygen scrambling with $H_2{}^{18}O$ was observed with molecules that have an aldehyde group, some details about the oxidation mechanism can still be gleaned. If oxygen insertion occurred through dioxygen, HMF oxidation under $^{18}O_2$ in unlabeled water would be expected to produce FDCA containing two ^{18}O atoms (incorporated during the oxidation of the aldehydes to acids). If no label is found in the product, then oxygen addition utilized H_2O as an oxygen source.

The mass spectra of the FDCA products from HMF oxidations under $^{18}O_2$ in unlabeled water and under unlabeled dioxygen in $H_2{}^{18}O$ can be seen in Figure 6.

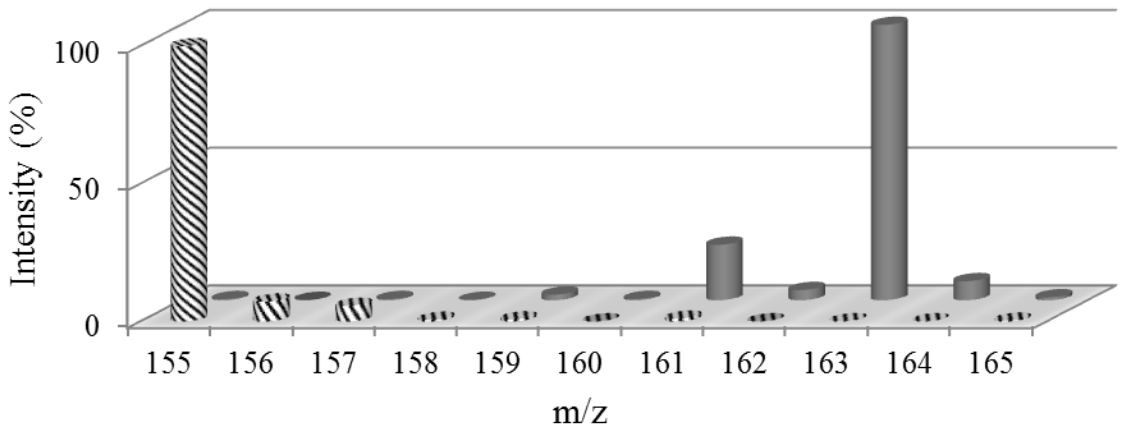

Figure 5.1. Mass spectra (electrospray negative mode) of major product, FDCA, from base-free HMF oxidation over Pt/C catalyst. Striped bars indicate experiments conducted in $^{18}O_2$ and $H_2{}^{16}O$; solid bars indicate experiments conducted in $^{16}O_2$ and $H_2{}^{18}O$. m/z of unlabeled FDCA = 155. Reaction conditions: T = 348 K, P = 345 kPa O_2; HMF:Pt = 100; 0.15 M HMF. HMF conversion = 100%.

As shown in Figure 5.1, the reaction performed under $^{18}O_2$ did not incorporate ^{18}O into the diacid product FDCA (m/z 155), whereas the reaction conducted in $H_2{}^{18}O$ incorporated four ^{18}O atoms into FDCA (m/z 163). Incorporation of four labeled ^{18}O atoms cannot be explained by oxygen scrambling between reaction intermediates and labeled water. Thus, the oxidation of HMF likely proceeds through H_2O to FDCA, analogous to the mechanism of HMF oxidation at high pH proposed previously (33).

We propose that the oxidation of HMF in base-free solution proceeds, like the high pH case, via geminal diol formation due to reversible hydration of aldehyde in water (accounting for two of the ^{18}O atoms incorporated into FDCA). Oxidation of the geminal diol to carboxylic acid likely occurs on the catalyst surface, depositing two electrons on the metal surface. Subsequent

activation of the alcohol moiety, on the catalyst surface, to form an aldehyde deposits two more electrons on the metal surface. The next step is the reversible of hydration of aldehyde to geminal diol in solution, accounting for the other two ^{18}O atoms found in the product acid. Finally, the geminal diol is oxidized on the metal surface, depositing a two more electrons on the metal surface. Consistent with earlier work, we propose that the role of dioxygen in HMF oxidation in base-free solution is to scavenge electrons from the metal surface, being reduced to peroxide and other species, thus closing the catalytic cycle in the process.

Stoichiometric consumption of hydrotalcite during HMF oxidation

As discussed previously, highly basic catalyst supports have been proposed to replace the inorganic base often added during aqueous-phase alcohol oxidation (24, 63). For example, the Ebitani research group developed highly active and selective Au and Pt catalysts with hydrotalcite as a support for base-free glycerol and HMF oxidation (24, 62, 64).

To explore the role solid bases in the oxidation reaction, we performed HMF oxidation with Au/TiO_2 with added hydrotalcite in the reaction medium. Because the oxidation activity of Au/TiO_2 has been studied previously, any differences in the observed activity or selectivity by adding hydrotalcite would most likely be attributed to a modification of the solution phase since Au is not in contact with the HT. The experimental conditions of Gupta *et al.* were matched as closely as possible in our reactor setup (1 mmol HMF in 6 cm^3 H_2O, T = 363 K, P = 340 kPa, HMF:Au = 150 mol:mol, mass HT = 0.13 g) (24). After 20 h, the product mixture was filtered, and the resulting mixture was analyzed via HPLC. The reaction was >99% selective to FDCA with 100% conversion of HMF and the carbon balance closing to 95%, which is similar to the results of Gupta *et al.*(24).

The liquid was recovered and analyzed via ICP (Galbraith Labs, Knoxville, TN) for Mg and Al content. Magnesium was present in a concentration of 0.16 M, indicating significant leaching of Mg into solution. Interestingly, the concentration of FDCA in this solution is also 0.16 M. The equimolar amounts of FDCA and Mg in solution suggest stoichiometric dissolution of the divalent magnesium. The Mg in solution (0.16 M) accounts for 70% of the Mg in the HT added to the reactor. Although this is a high percentage of Mg to leach into solution, a significant pH drop, from 9 to 6, was noted during the course of the reaction. The instability of HT at low values of pH ($5.0 < pH < 9.0$) has been documented in the literature, and results in preferential dissolution of Mg^{+2} (62). It is likely that the high conversion of HMF to diacid lowered the pH of the solution significantly, thus causing instability and dissolution of Mg^{+2} from the HT catalyst. It should be noted that the Al content of the product was <0.2 mM, which confirmed that Mg was preferentially leached from the HT by the product acid. This incongruent leaching of Mg, but not Al, from the HT catalyst in an acidic environment is also documented in the literature (62).

In an attempt to slow the rate of Mg dissolution, the amount of HT added to the reactor was increased by a factor of 3.75 to help maintain a higher pH throughout the reaction. The initial pH of the reaction medium was 9 but it decreased to 7 at the end of the reaction. Analysis of the solution from this run also showed preferential leaching of Mg to give a concentration of 0.13 M, which corresponded to 15% of the available Mg in the reactor. The concentration of FDCA at the end of the run was 0.12 M, which is quite similar to the amount of leached Mg, again suggesting stoichiometric dissolution of the Mg from hydrotalcite. Recently, a report on Ru/HT catalysts for the oxidation of HMF also indicated stoichiometric leaching (26).

Evidently, the addition of HT to the reactor served as a stoichiometric reagent rather than a heterogeneous catalyst for HMF conversion. Based on the mechanistic studies with labeled compounds and the observed leaching of Mg from HT, we conclude that solid base supports are most likely to react with the product acid and either deactivate by strong adsorption or dissolve by formation of soluble salts of the product acids.

Conclusions

The base-free aqueous oxidation of HMF to FDCA can be achieved over a Pt/C catalyst at 348 K. The mechanism of Pt-catalyzed base-free HMF oxidation in water was found to be the same as that at high pH, wherein the oxidation proceeds through active participation of H_2O and the role of O_2 is to scavenge electrons from the catalyst surface, thereby closing the catalytic cycle.

Since solid bases are attractive alternatives to the use of liquid bases that need to be neutralized at the end of the reaction, hydrotalcite was evaluated as an additive to Au-catalyzed oxidation of HMF in liquid water. Although the product diacid FDCA was formed with high selectivity, elemental analysis of the product solution revealed extensive dissolution of magnesium from the hydrotalcite. Thus, HT acted as stoichiometric replacement for added homogeneous base and not a true catalytic material.

Acknowledgements

Support from the National Science Foundation (Grant Nos. OISE 0730277 and EEC-0813570) is gratefully acknowledged.

Chapter 6

The influence of carbon support on the selective oxidation of HMF over Pt and Au nanoparticles

The work in this chapter was the basis for portions of the publication, Davis, S.E., Sanchez, A., Gosselink, R.W., Bitter, J.H., de Jong, K.J., Datye, A.K., and Davis, R.J. "The influence of carbon support and reaction conditions on the selective oxidation of 5-hydroxymethylfurfural over Pt and Au nanoparticles," in preparation.

Introduction

The diffusion of relatively large, biomass-derived molecules into the micropores of some catalyst supports may be transport limited, influencing measured reaction rates. Although carbon has been widely used as a catalyst support, the microporosity of activated carbon may hinder internal mass transfer (65). Reproducibility issues also plague the synthesis of activated carbon, which is detrimental to applications in catalysis (65). To ameliorate some of the transport problems, non-microporous supports, such as carbon nanofibers (CNF), may be beneficial.

Carbon nanofiber synthesis methods are highly reproducible and provide a uniform product. These materials can be functionalized with various surface groups, forming both acidic and basic sites, and can be used alone or as supports for metal nanoparticles. The acidic sites on oxy-functionalized CNF (CNF-ox) prepared by an oxidative treatment in acid have been studied in detail, as has their influence on the synthesis of supported Pt and Ni nanoparticles (66-68). Nitrogen-containing CNFs (CNF-N) are reported to be solid base catalysts (69-72). For example, Van Dommele et al. demonstrated the effectiveness of nitrogen-containing carbon nanotubes as solid base catalysts for the Knoevenagel condensation (70). Likewise, Gong et al. studied the

electrocatalytic activity of nitrogen-containing carbon nanotubes for oxygen reduction reactions for fuel cell applications (71). Moreover, CNF-N have been investigated recently as catalyst supports for several metals. Liu et al. highlighted the high dispersion and stability of Pd nanoparticles supported on CNF-N in the hydrodechlorination of chlorobenzene (72). The lone electron pair of pyridine species on the functionalized nanofibers is thought to interact with Pd, enabling a high dispersion of metal nanoparticles and preventing their aggregation. Similarly, Villa et al. report on Pd and Au-Pd catalysts supported on CNF and CNF-N (73). The metals supported on nitrogen-functionalized CNFs had smaller metal particle sizes and therefore higher overall catalytic activity for liquid-phase alcohol oxidation.

Although the body of literature investigating various applications of CNFs as catalyst supports is growing, their use in HMF oxidation has not yet been probed. This work seeks to understand the role of surface functional groups on CNF materials in the oxidation of HMF and HFCA.

Experimental Methods

Catalyst Preparation

The carbon nanofibers (CNF) used in this work were grown over a Ni/SiO_2 catalyst. First, a Ni/SiO_2 (5-wt% Ni) was prepared via homogeneous deposition-precipitation using SiO_2 (Degussa, Aerosil 200), $Ni(II)NO_3 \bullet 6H_2O$ (Acros, 99% purity), and urea (Acros) (74). The resulting catalyst was used to grow fibers by flowing $CO/H_2/N_2$ at 823 K as previously described (74). The material containing both CNF and Ni/SiO_2 catalyst was subsequently refluxed three times in 1.0 M KOH solution for 1 h each time to remove SiO_2, and then washed with deionized H_2O until the effluent was pH neutral. Next, the material was refluxed twice in 65% HNO_3 for 1 h each time to remove Ni and introduce oxygen into the CNF. The material was washed again with deionized H_2O until the effluent was pH neutral and dried in air at room temperature overnight. This material is referred to as CNF-ox.

Some of the CNF-ox material was further treated in NH_3 to replace oxygen-containing groups with nitrogen-containing groups (72). The CNF-ox sample was heated to 1123 K under flowing NH_3 (60 cm^3 STP min^{-1}), held under these conditions for 100 minutes, and cooled under flowing NH_3. The resulting materials are referred to as CNF-N.

The CNF materials were subsequently used to support Pt and Au nanoparticles. The Pt catalysts were prepared using an impregnation method (75). In brief, 0.16 g $H_2PtCl_6 \cdot 6(H_2O)$ was dissolved in 30 cm^3 distilled, deionized H_2O, to which 2.0 g of CNF-ox or CNF-N was added. The mixture was stirred at room temperature for 18 h. The catalysts were filtered from solution, washed several times with H_2O, and dried overnight in air at 403 K. The resulting catalysts were reduced in 100 cm^3 min^{-1} flowing H_2 (UHP, Messer gases) at 673 K, cooled in H_2, exposed to air and stored in a refrigerator. The supported Pt catalysts were used without further pretreatment.

The Au catalysts were synthesized using a sol method (47). First, a Au sol was prepared by dissolving 0.04 g $HAuCl_4 \bullet 3(H_2O)$ (Aldrich) in 1000 cm^3 deionized H_2O along with a 2 wt% polyvinyl alcohol (Acros) solution in a ratio of Au:PVA = 1:1 w:w. The colloid was reduced by adding 0.1 M aqueous solution of $NaBH_4$ (Aldrich) dropwise in 3:1 molar ratio of $NaBH_4$:Au. Following reduction, the sol was ruby red in color. The CNF support was added to the sol and the mixture was acidified to pH = 2 with H_2SO_4. The Au sol-CNF mixture was stirred for 4 h to allow the Au to deposit on CNF. The Au/CNF sample was recovered by filtration and washed with several liters of H_2O. The filtrate was clear in color, confirming the Au sol had deposited on the support. The catalyst was dried in air at 333 K overnight and subsequently treated in N_2 and H_2 (9:1 ratio) flowing at 150 cm^3 min^{-1} for 4 h at 573 K. The resulting Au catalyst was exposed to air and stored in a refrigerator. As with the Pt catalysts, the Au samples were used without any additional pretreatment. Metal weight loading (Au or Pt) was determined by ICP analysis performed by Galbraith Laboratories, Knoxville, TN.

Catalyst Characterization

Chemisorption of H_2

The dispersion of Pt was determined using a Micromeritics ASAP 2020 automated adsorption system. The Pt catalysts were heated to 473 K at 4 K min^{-1} under flowing H_2 (UHP, Messer Gas) and reduced for 1.5 h. The samples were evacuated for 2 h at 473 K and then cooled to 308 K for analysis. No H_2 uptake was observed on the bare CNF-ox or CNF-N materials.

Physisorption of N_2

The surface area of CNF-ox was also determined using a Micromeritics ASAP 2020 automated adsorption system. The CNF-ox material was heated to 473 K and held under vacuum for 16 h. The material was cooled to 77 K for N_2 adsorption.

Titration

The amount of acid and base sites on the carbon materials, with and without metals, was determined by titration with NaOH and HCl using a Titralab TIM 845 system (68, 70). To evaluate the acid site density, a solution of 0.01 M NaOH and 0.1 M KCl was used as titrant. The solid material (0.05 g) was dispersed in 60 cm^3 of 0.1 M KCl and titrated to pH 5 and pH 7.5, corresponding to the amount of strongly acidic groups and the total amount of acidic groups, respectively. To quantify the base site density, a solution of 2.0 mM HCl was used as titrant. To 50 cm^3 of 0.1 M KCl, 0.1 g of the solid material was added, and the mixture was titrated to pH 7.

Electron Microscopy

High-angle annular dark field (HAADF) imaging was performed using a JEOL 2010F FASTEM field emission gun scanning transmission electron microscope operated at 200kV. The catalyst samples were suspended in ethanol by grinding in an agate mortar and pestle, and deposited on a holey carbon support film on Cu TEM grids. The images were recorded and analyzed using Digital Micrograph software.

Oxidation reactions

The aqueous phase oxidation of HMF (Acros, ≥98% purity) or HFCA (ChemBridge, 95% purity) was carried out in a 50 cm^3 Parr Instrument Company 4592 batch reactor equipped with a glass liner. In all reactions, 7.0 cm^3 of the reactant solution was added to the reactor along with the appropriate amount of catalyst. The reactor was purged with flowing O_2 (UHP, Messer Gas) and then pressurized to the desired value. A constant pressure was maintained by a continuous O_2 feed. Samples of the product solution were acquired by removing the top of the reactor, taking the sample, flushing the reactor with O_2 and repressurizing. The maximum O_2 transport rate from the gas to the liquid was determined by oxidation of sodium sulfite (48), and the reactant oxidation rate was kept significantly below this limit when quantitative rates were measured. The samples from the oxidation reactions were filtered using PTFE 0.2 μm filters and diluted with deionized H_2O in a 1:3 sample:water ratio. The analysis was conducted using a Waters e2695 high performance liquid chromatograph (HPLC) at 303 K equipped with refractive index and UV/vis detectors. The HPLC utilized a Bio-Rad Aminex HPX-87H column and 5mM H_2SO_4 flowing at 0.5 cm^3 min^{-1} to perform the separation. The retention times and calibrations for observed products were determined by injecting known concentrations.

Results and Discussion

Carbon nanofibers as supports for Pt and Au nanoparticles

The oxidation of HMF was investigated over Pt and Au supported on carbon nanofibers that were functionalized with either oxygen- or nitrogen-containing groups. Table 6.1 summarizes the physical and chemical properties of the freshly prepared (reduced) materials.

The BET surface area for the CNF-ox support materials was found to be 170 m^2, in agreement with other reports (180-200 m^2 g^{-1}) (66, 67).

Table 6.1. Results from characterization of CNF materials

Catalyst	Weight loading metal (%)[a]	Metal Dispersion (%)	Metal Avg Diameter (nm)[b]	Metal Surface Avg Diameter (nm)[c]	Strong acid sites (mmol kg^{-1})[d]	Total acid sites (mmol kg^{-1})[d]	Total base sites (mmol kg^{-1})[e]
Pt/CNF-N	2.3	100[f]	0.7	0.9	-	-	26.0
Pt/CNF-ox	0.42	83[f]	1.6	2.2	0.0	45	-
Au/CNF-N	0.71	19[g]	3.7	5.4	-	-	20.7
Au/CNF-ox	0.60	18[g]	4.4	5.7	59	134	-
CNF-N	0	-	-	-	-	-	8.9
CNF-ox	0	-	-	-	164	333	-

[a]determined via ICP analysis
[b]determined via TEM analysis
[c]$\Sigma d^3/d^2$
[d]determined by dispersing 0.05 g of material in 50 cm^3 0.1 M KCl solution and titrating with 0.01 M NaOH and 0.1 M KCl solution. Strong acid sites determined by titration to pH = 5; total acid sites determined by titration to pH = 7.5
[e]determined by dispersing 0.1 g of material in 50 cm^3 0.1 M KCl solution and titrating with 2.0 mM HCl solution
[f]determined via H_2 chemisorption
[g]calculated as inverse of surface average diameter

The final metal loading of the Pt/CNF-ox catalyst was much lower than that of Pt/CNF-N (0.42 wt% and 2.3 wt %, respectively), although the synthesis procedures were identical and the intended loading was 3 wt% Pt for both. Expectedly, the presence of acidic or basic surface groups on the support material affected the uptake of H_2PtCl_6(aq) onto CNF. In the case of Au on CNF, the metal weight loadings were similar between the two catalysts (0.71 wt% Au/CNF-N and 0.60 wt % Au/CNF-ox) but both were less than the nominal 1 wt% that was targeted. The

acidic and basic surface functionalization did not have a substantial influence on the uptake of Au onto CNF materials, presumably because the synthesis procedure involved the adsorption of a pre-reduced Au sol onto the fibers instead of impregnation of unreduced metal precursors as was the case with Pt.

Results from titration of the acid and base sites are presented in Table 6.1. The initial pH of a 0.1 M KCl solution after adding CNF-ox was between 4 and 5, indicating that CNF-ox possessed acid sites. The materials were titrated to two endpoints, pH 5 and pH 7.5, to count sites of various acid strength. Strong acid groups, or those titrated to pH 5, are generally attributed to carboxylic acids (76). The acid sites titrated between pH 5 and pH 7.5 are considered to be fairly weak. From the titration of the CNF-ox support material, approximately half of the acid groups present on the surface are attributed to carboxylic acid groups (333 mmol kg^{-1} total acid groups with 164 mmol kg^{-1} strong acid groups). The addition of either Pt or Au to CNF-ox decreased the total concentration of acid groups as well as the concentration of strong acid groups. The Au/CNF-ox sample exposed 134 mmol kg^{-1} total acid groups with 59 mmol kg^{-1} attributed to strong acid groups, while Pt/CNF-ox contained 45 mmol kg^{-1} total acid groups with no strong acid groups. Although the loading of Pt (0.42 wt%) was slightly lower than the loading of Au on CNF-ox supports (0.60 wt % Au), the addition of Pt consumed the acid groups substantially more than the addition of Au. This result may be related to the much higher dispersion of Pt on CNF-ox (83%) compared to Au (18%).

The loss of acidic sites that occurred during synthesis of Pt and Au catalysts supported on CNF-ox may result from the deposition of metal and its reduction at elevated temperatures. The same trend was noted by Plomp et al. during Pt/CNF-ox synthesis via a homogeneous deposition-precipitation method. Dihydrogen dissociated on metal nanoparticles might migrate to

the support during the reduction of Pt (70, 75). Dihydrogen may also assist in the decomposition of oxygen-containing groups (75). Acidic sites may also anchor metal particles to the carbon surface, as noted in other works involving Pt/CNF-ox (66, 67).

The low uptake of Pt by CNF-ox during impregnation may be because of the lack of basic sites. Basic sites on carbon are reportedly the strongest anchoring sites for the H_2PtCl_6(aq) utilized in this synthesis method and are responsible for strong adsorption of $PtCl_6^{2-}$(aq) on C (75, 77). Basic sites incorporated in the CNF-N material via ammonia treatment were added at the expense of acidic sites, which is consistent with the results in Table 6.1 (72). The basic Pt/CNF-N material therefore had a higher loading of Pt than the acidic Pt/CNF-ox (2.3 wt% and 0.42 wt%, respectively), likely because of the greater concentration of strong anchoring sites for $PtCl_6^{2-}$(aq).

The basic nanofibers, CNF-N, were titrated with 2 mM HCl to determine the number of exposed basic sites. The initial pH of the material suspended in solution was between pH 8.5 and 9.1, confirming that they were overall basic. As seen in Table 6.1, the number of basic sites was higher on the supported catalysts (20.7 mmol kg^{-1} on Au/CNF-N and 26.0 mmol kg^{-1} on Pt/CNF-N) than on bare CNF-N (8.9 mmol kg^{-1}). The higher number of basic sites on the supported catalysts does not indicate that the metal nanoparticles are basic, but rather that the material likely has acidic and basic sites. This method of titrating acidic and basic sites measures a net acidity or basicity; i.e., CNF-N materials have more exposed basic sites than acidic sites. The higher number of basic sites on the supported catalysts may be attributed to the removal of residual acid groups during reduction of the catalysts by H_2 as described above, or could possibly indicate some anchoring of metal particles on residual acidic sites.

Electron microscopy of all supported metal catalysts revealed small, well-dispersed metal particles. Images of the support materials and all catalysts are seen in Figure 6.1. In particular,

the Pt catalysts had very small particles (average diameters 0.7 nm for Pt/CNF-N and 1.6 nm for Pt/CNF-ox). The Au catalysts contained metal particles of the same size (average diameters 3.7 nm for Au/CNF-N and 4.4 nm for Au/CNF-ox). Evidently, the nature of the surface groups did have a large influence on loading but not on the final metal particle size of supported Pt and Au catalysts.

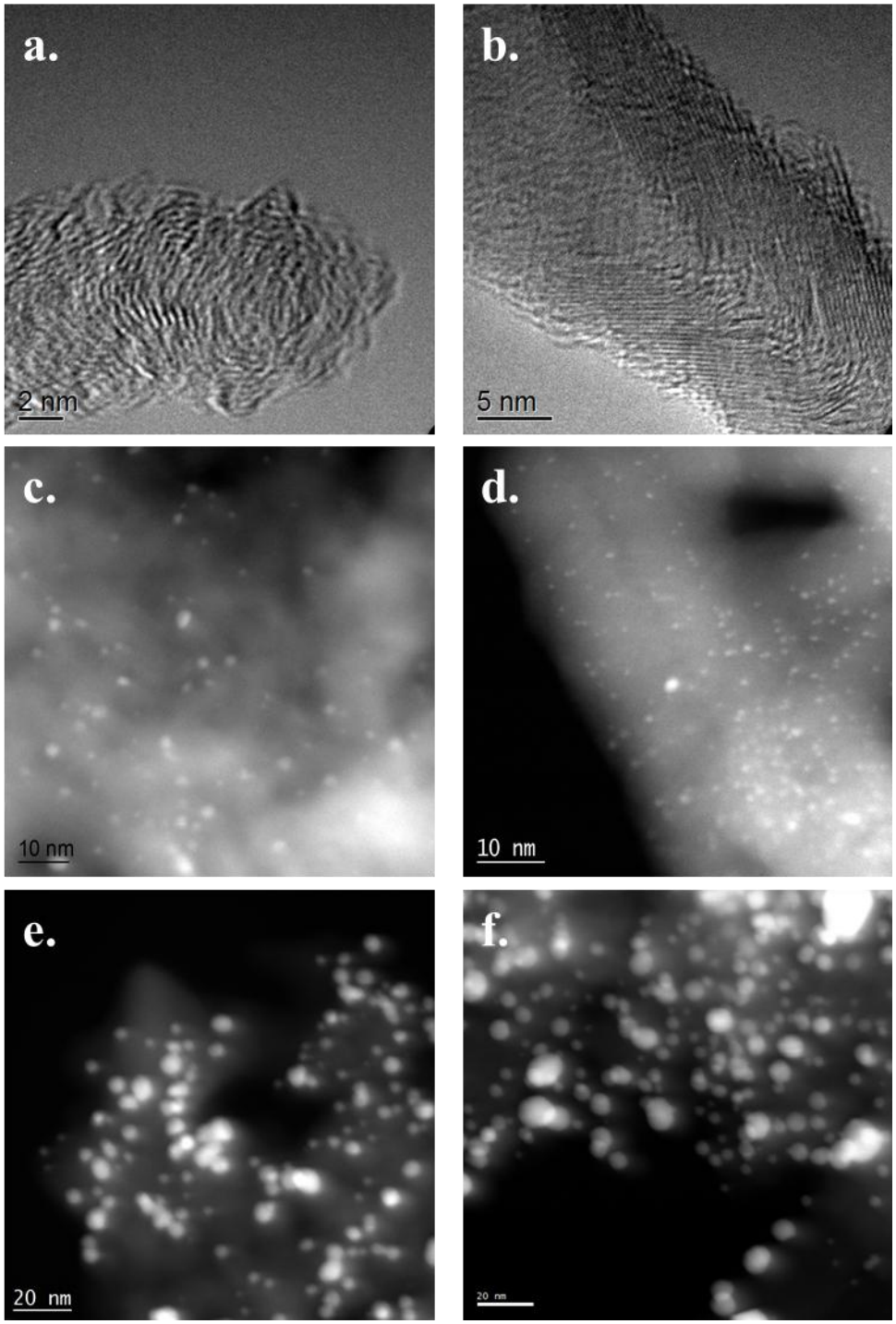

Figure 6.1 TEM images of [a] CNF-ox support, [b] CNF-N support, [c] Pt/CNF-ox, [d] Pt/CNF-N, [e] Au/CNF-ox, and [f] Au/CNF-N

Catalytic Activity of CNF-supported catalysts

Platinum and gold supported on CNF were tested as catalysts in the oxidation of HMF and the rates were compared to rates reported over other Pt/C and Au/C catalysts. As discussed earlier, the loading of catalyst was adjusted to keep the rate of conversion of substrate below the external (gas-to-liquid O_2) mass transfer limit. The turnover frequency (TOF) at a particular loading of each catalyst is reported in Table 6.2. It should be noted that, in control experiments, the bare support materials CNF-N and CNF-ox did not exhibit catalytic activity for HMF oxidation.

Table 6.2 Reaction rates over metal catalysts supported on CNF materials[a]

Catalyst	**HMF:Metal$_{surf}$**	**TOF(s^{-1})[b]**
Pt/CNF-ox	325	0.04
Pt/CNF-N	800	0.07
Au/CNF-ox	30000	3.6
Au/CNF-N	13900	2.0

[a]All reactions: 0.15 M HMF, 0.30 M NaOH, 690 kPa O_2, 295 K
[b]TOF calculated at 0.5 h based on consumption of HMF per mole of surface metal.

The TOFs obtained over the Pt catalysts were fairly similar, 0.04 s^{-1} for the CNF-ox-supported catalyst and 0.07 s^{-1} for the CNF-N-supported catalyst. Apparently, the presence of acidic or basic surface groups on CNF-supported Pt catalysts did not significantly influence the rate of HMF oxidation. In our previous work, the rate of HMF oxidation over a commercial 3 wt% Pt/C (Aldrich) catalyst under the same reaction conditions was 0.08 s^{-1} (18).

The CNF-supported Au catalysts exhibited much higher TOFs than the Pt catalysts, (2.0 s^{-1} over Au/CNF-N and 3.6 s^{-1} over Au/CNF-ox), which is typical for HMF oxidation over Au compared to Pt (18). The presence of surface groups on the CNF supports did not seem to significantly influence the rate of HMF oxidation over Au. The TOFs obtained over the CNF-supported catalysts were similar to those seen in our previous work for Au catalysts at the same reaction conditions (2.3 s^{-1} over a 0.77 wt% Au/C synthesized via a sol method, 5.0 s^{-1} over a 1 wt% Au/C catalyst obtained from the World Gold Council, and 1.6 s^{-1} over a 1.6 wt% Au/TiO_2 also obtained from the World Gold Council) (18).

The product distribution is compared in Table 6.3. Both Pt catalysts produced mostly HFCA near 50% conversion of HMF, with the Pt/CNF-ox demonstrating slightly lower HFCA selectivity (62%) than the Pt/CNF-N catalyst (76%). The Pt/CNF-ox catalyst was slightly more selective to the intermediate FCA (33%) than the Pt/CNF-N catalyst (16%), and both catalysts had less than 10% selectivity to the final product FDCA. Although there was some influence on selectivity to the intermediate products FCA and HFCA, it does not appear that the acidic or basic properties of Pt/CNF-N and Pt/CNF-ox had a significant effect on the selectivity to the diacid.

Table 6.3 Product selectivity during HMF oxidation over CNF-supported metal catalysts[a]

Catalyst	Conversion (%)	S_{HFCA}	S_{FCA}	S_{FDCA}
Pt/CNF-ox	53	62	33	5
Pt/CNF-N	48	76	16	8
Au/CNF-ox	50	100	0	0
Au/CNF-N	50	100	0	0

[a]Reaction conditions: HMF:Pt_{surf} = 325; CNF-N: HMF:Au_{surf} = 13,900; CNF-ox: HMF:Au_{surf} = 30,000; 0.15 M HMF in 0.3 M NaOH, 690 kPa O_2, 295 K

At low catalyst loadings (HMF:Au = 13,900 for Au/CNF-N and HMF:Au = 30,000 for Au/CNF-ox), selectivity to the intermediate HFCA was 100% over supported Au at all levels of conversion, for reactions utilizing 2:1 NaOH:HMF. Increasing the catalyst loading to a ratio of HMF:Au = 1400 increased the selectivity to the diacid FDCA significantly over the Au/CNF-N catalyst, though the same behavior was not observed over the Au/CNF-ox catalyst. The product distributions at different catalyst loadings are compared in Figure 6.2.

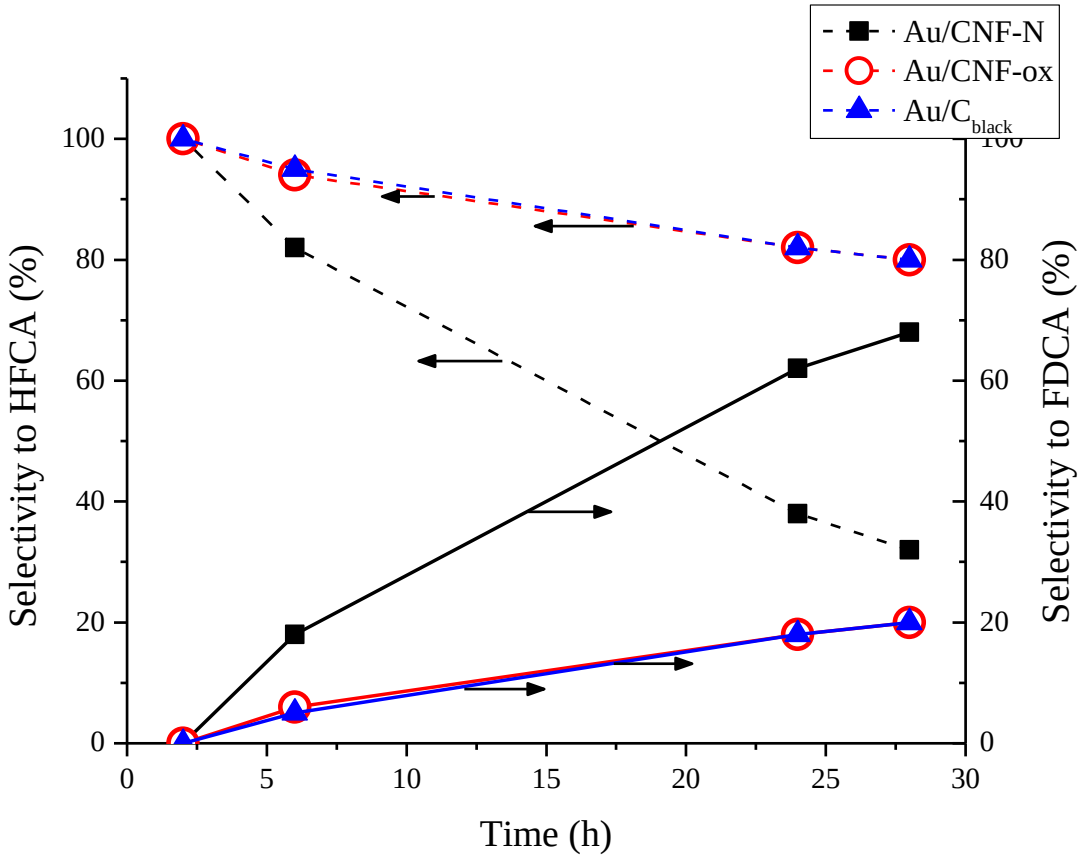

Figure 6.2. Selectivity to monoacid HFCA and diacid FDCA during HMF oxidation over Au catalysts. Reaction conditions: 0.15 M HMF, 0.30 M NaOH, 295 K, 690 kPa, HMF:Au_{surf} = 1400.

After 24 h and 100% conversion of HMF, the selectivity to FDCA was 62% over the Au/CNF-N catalyst, whereas under the same conditions the selectivity to FDCA was just 18% over Au/CNF-ox. For comparison, the product distribution over a previously described 0.77 wt% Au/C_{black} catalyst(18) was investigated for the same time period. The selectivity to FDCA was only 18% after 24 h and 100% conversion of HMF. Previous work confirmed that HMF oxidation over Au catalysts at similar conditions resulted in the formation of HFCA as a majority product; Au catalysts in the absence of a high concentration of NaOH were unable to activate the

alcohol moiety of HMF (18, 28). To produce substantial amounts of diacid over Au catalysts, either the NaOH:HMF ratio or the reaction temperature, or both, needed to be greatly increased (20, 21). In this work, however, the Au/CNF-N catalyst produced diacid with just 2:1 NaOH:HMF at 295 K, whereas the Au/CNF-ox and Au/C_{black} catalysts produced diacid at low levels at the same conditions.

To probe this difference in behavior further, an experiment was conducted using the monoacid HFCA as the substrate and Au/CNF-N as catalyst (0.15 M HFCA, 0.3 M NaOH, $HMF:Au_{total}$ = 420, 690 kPa O_2, 295 K). As expected, 82% conversion of HFCA in 24 h with 100% selectivity to the diacid FDCA was observed. An experiment under the same conditions but utilizing Au/C_{black} produced less than 5% conversion of HFCA in 24 h, demonstrating the enhanced activity of Au/CNF-N for producing the diacid FDCA via oxidation of an alcohol group. Finally, a physical mixture of Au/C_{black} and bare CNF-N was used in HFCA oxidation (0.15 M HFCA, 0.3 M NaOH, $HMF:Au_{total}$ = 420, 0.071 g CNF-N, 690 kPa O_2, 295 K) and results were about the same as those when Au/C_{black} was used alone (7% conversion in 24 h). This experiment confirmed that CNF-N was not influencing the reactivity results through the solution phase. Apparently, the Au nanoparticles must be supported CNF-N to improve HFCA oxidation activity. At this point, we cannot explain definitively the observed synergy of Au on CNF-N for diacid formation but will continue to explore its origins.

Previous studies of Pd catalysts supported on CNF-N for hydrodechlorination reactions suggested that the lone pairs of electrons on nitrogen atoms incorporated in CNF-N attract HCl molecules, removing HCl from the metal surface rapidly and preventing product inhibition (72). In our case, perhaps the pyridinic nitrogen species assists in the activation of the alcohol moiety of HMF and HFCA, a reaction that Au is seemingly unable to catalyze unless in presence of high

concentrations of base (20:1 NaOH:HMF)(21) and/or at elevated temperature (4:1 NaOH:HMF and 338 K) (20).

Conclusions

The investigation of HMF oxidation over Pt and Au supported on non-microporous carbon nanofibers produced turnover frequencies that were similar to those measured on microporous catalysts at the same conditions. Acidic or basic surface groups on the carbon nanofibers did not significantly influence the size of Pt or Au metal particles supported on them, although they affected the adsorption of H_2PtCl_6. The acidic CNF-ox material had a much lower uptake (0.42 wt%) of Pt than did the basic CNF-N material (2.3 wt%), despite identical synthesis procedures with and intended weight loading of 3 wt%. Presumably, the N-groups present on CNF-N materials have stronger anchoring sites for the negatively-charged platinum precursor. Since Au particles were synthesized in solution via a sol method, there was no need for the Au precursor to interact with the functional groups of CNF, and therefore there was no influence of functional groups on the size or loading of the gold particles. Regardless of CNF surface functionalization, particle sizes were the same within the same metal type (approximately 5 nm for Au and 1-2 nm for Pt). The rates of HMF oxidation were not influenced by the presence of acidic or basic sites in either the Pt or Au case. Interestingly, increasing the amount Au/CNF-N (to HMF:Au_{surf} = 1400) greatly increased the selectivity to diacid FDCA. Previous work showed that, under these conditions (2:1 NaOH:HMF, 295 K), Au catalysts produced the monoacid HFCA in a majority amount; oxidation of the hydroxymethyl group of HFCA only occurred over Au with much higher NaOH concentrations and/or temperature. This work demonstrated a

synergistic effect between Au and CNF-N in close contact that produced a FDCA in a majority amount at mild conditions.

Acknowledgements

Support from the National Science Foundation (Grant Nos. OISE 0730277 and EEC-0813570) is gratefully acknowledged. Microscopy and particle size analysis were helpfully provided by Angelica Sanchez, under the advisement of Abhaya Datye, at the University of New Mexico. The carbon nanofiber support was synthesized at Utrecht University, with the help and guidance of Robert W. Gosselink, Dr. Krijn P. de Jong, and Dr. Johannes (Harry) Bitter.

Chapter 7

Conclusions

The oxidation of 5-hydroxymethylfurfural is a complex reaction that is highly dependent on reaction conditions such as temperature, concentration of homogenous base, and choice of metal catalyst. In water at ambient temperature, the oxidation does not proceed in absence of homogeneous base over Pt or Au catalysts. The addition of NaOH to raise the pH and facilitate reaction is common, though the degradation of HMF at high pH via the Cannizzaro reaction is rapid. Selection of reaction conditions that enhance oxidation rate while limiting degradation is crucial.

Our work showed the rate of HMF oxidation was an order of magnitude higher over Au catalysts than over Pt catalysts under the same mild conditions, namely 2:1 NaOH:HMF mol:mol and 295 K. The rate of oxidation of HMF was measured as the rate of disappearance of HMF; typically, this is indicative of oxidation of the aldehyde moiety to acid.

Although the reaction rate of HMF was slower over Pt, the desired diacid product, FDCA, was obtained in majority under these conditions. The intermediate monoacid – alcohol product, HFCA, was obtained in a majority over the Au catalysts under the same conditions. Evidently, the activation of the alcohol moiety to aldehyde is not facile over Au at these conditions. However, by increasing the NaOH:HMF ratio to 20:1, a majority of the diacid product was realized. The activation of alcohol groups over Au is facilitated by OH^-.

The work discussed above provided three distinct scenarios for HMF oxidation: oxidation to diacid over Pt, oxidation to monoacid over Au at “low” base concentrations (2:1 NaOH:HMF), and oxidation to diacid over Au at “high” base concentrations (20:1 NaOH:HMF).

Whether these three scenarios proceeded via the same mechanism was investigated though the use of istopically-labeled $H_2{}^{18}O$ and $^{18}O_2$. The same mechanism was proposed for all three scenarios: first, the rapid, reversible hydration of the aldehyde moiety, followed by hydrogen transfer to form one acid group. Next, the activation of the alcohol moiety to an aldehyde, facilitated by hydroxide ions, was proposed. The oxidation of this aldehyde proceeds in the same manner as the first. The origin of inserted O was shown to be water, and the presence of peroxide in solution suggested the reduction of O_2. Thus, the role of O_2 was proposed to be scavenging electrons from the metal surface, closing the catalytic cycle and allowing the reaction to proceed, analogous to the mechanism of glycerol oxidation (54).

Although the oxidation of HMF over Pt at our typical loading at ambient temperature requires addition of base, raising the temperature to 348 K allows for high yield of FDCA even at neutral pH. The same result is not observed over Au catalysts. The mechanism of base-free HMF oxidation over Pt catalysts was likewise studied using isotopically-labeled $H_2{}^{18}O$ and $^{18}O_2$, and the same mechanism for O insertion as in the high pH case was proposed.

While the reaction mechanism is an important piece in understanding HMF oxidation, understanding the kinetics of the reaction is equally significant. The effects of substrate and therefore NaOH concentrations, O_2 pressure, and temperature on reaction rate were previously unknown, and have been studied over a commercially-available Pt/C catalyst for both HMF and HFCA oxidation. The reaction rates, as previously discussed, were determined by disappearance of substrate. As the typical first oxidation product of HMF is HFCA, the rate of HMF oxidation represents aldehyde oxidation. The oxidation of HFCA represents oxidation of alcohol.

In both cases, the reactions were found to be zero order in substrate concentration, indicating that the Pt surface was highly covered in substrate. Interestingly, the reaction rate of

HMF was first order in NaOH concentration, but the rate of HFCA oxidation was zero order above a threshold of 2:1 NaOH:HFCA. Apparently, the oxidation rate of aldehyde is more influenced by NaOH concentration than is the oxidation rate of alcohol. Consistent with the proposed mechanism, the reaction rate with respect to O_2 pressure was also found to be zero order. Surprisingly, Arrhenius-type plots revealed nearly identical overall activation energies for HMF and HFCA, possibly because of the prevalence of OH^- in solution and the large role played by solution phase chemistry (reversible hydration of aldehydes, deprotonation of alcohols) in these reactions.

The previous sections have discussed in detail the positive effect of homogeneous base on HMF oxidation rate. The addition of homogeneous base, however, is undesirable from an environmental and economic standpoint. Thus, there is interest in finding alternative catalysts or reaction conditions to remove the need for homogeneous base.

A logical area of exploration is the use of solid bases as supports for metal catalysts. However, the acid products of the oxidation will likely adsorb strongly on the solid bases, or worse, react with the support, thereby leaching it into solution. If solid bases are to be used for catalyst supports, the interaction between them and the organic acid products would need to be quite weak, which likely precludes their use in aqueous media where acids are formed.

There are a number of reports in the literature investigating the use of hydrotalcite materials as catalyst supports in alcohol oxidation reactions (26, 78-82). Typically, these investigations were conducted in nonpolar solvents (i.e. toluene or xylene), which presented no problem because aldehydes were the final products. Leaching of hydrotalcite supports in aqueous solutions, however, can be significant, as acid products can react with the solid base. This was shown in this work in the case of Au supported on HT for HMF oxidation. Even if the supported

transition metal does not leach from the catalyst, it is possible for the hydrotalcite support to be dissolved by the product acid. Therefore, careful analysis of leaching of the basic support is imperative when aqueous solutions are involved.

Another important issue to consider in the transformation of relatively large, biomass-derived molecules is the potential for internal diffusion limitations when metal nanoparticle catalysts are supported on microporous materials. The application of nonmicroporous carbon nanofibers (CNF) as catalyst supports in the synthesis of Pt and Au catalysts was used to evaluate this effect in our own work. The turnover frequencies measured over CNF-supported Pt and Au catalysts were similar to those found over Pt and Au supported on microporous materials; thus, internal mass diffusion was not expected to affect the rates observed in this work.

The functionalization of CNF materials with acid and base groups was carried out by treatment in acid or ammonia, respectively, and the presence of these groups did not influence observed reaction rates for HMF oxidation. Basic groups on CNFs proved to be better anchoring sites for H_2PtCl_4 than did the acid sites; thus, adsorption of Pt was greater on basic CNF materials than on acidic CNF materials. The metal dispersion of Pt, however, was not affected by the surface functional groups, and was high in both cases. Presence of acid or base sites on CNF did not influence adsorption or dispersion of Au in the prepared catalysts.

Using a relatively high loading of Au supported on basic CNF (Au/CNF-N) in the oxidation of HMF yielded an interesting result. A high selectivity to the diacid product FDCA was observed in the presence of just 2:1 NaOH:HMF. The use of a Au/C_{black} catalyst, under the same conditions, produced a majority of the monoacid HFCA intermediate product. A physical mixture of the Au/C_{black} catalyst and bare CNF-N materials behaved as the Au/C_{black} alone, producing a majority of HFCA. Finally, a reaction using monoacid HFCA as substrate and

Au/CNF-N as catalyst resulted in a majority of the diacid product FDCA. Apparently, a synergy exists between Au and CNF-N which allows for the activation of the alcohol moiety of HFCA even in relatively low concentrations of base (2:1 NaOH:HMF).

Future recommendations

Exploring the interesting synergy between gold and basic carbon nanofibers

During the investigation of carbon nanofibers as catalyst supports, a synergy was noted between Au and the basic CNF-N material, wherein the oxidation of the alcohol moiety of HFCA was observed even in low concentrations of base (2:1 NaOH:HMF). The origin of the enhanced activity has not been explored and further investigations are advised. An understanding of the interaction between Au and CNF-N may help guide future catalyst synthesis. Additionally, the application of Au/CNF-N to other reactions influenced by NaOH concentration, such as glycerol oxidation, is recommended for study.

Varying the solvent system

As discussed previously, interest in eliminating homogeneous base from HMF oxidation is currently appearing in the literature. However, the solubility of the acid products is very low in neutral water (22, 23). Few reports in the literature have investigated HMF oxidation in methanol solvent, producing esters which are readily soluble in methanol (28, 31). One of these reports utilizes a homogeneous base and Au/TiO_2; the other is in absence of homogeneous base over Au/CeO_2. If the shift toward base-free oxidation of HMF is to continue, it is recommended that a

different solvent system (methanol as an example) is chosen to minimize precipitation of product acids.

Use of a flow reactor system

To our knowledge, Lilga et al. have provided the only report on HMF oxidation in a flow system (23). The use of a flow system may provide a practical means for producing diacid FDCA in neutral water. The solubility of FDCA in neutral water increases with temperature. A flow system could potentially perform HMF oxidation at temperatures sufficiently high to maintain adequate FDCA solubility, thus limiting product precipitation and inhibition. Downstream separation of product FDCA would be simple because as the product mixture cooled, the acid would precipitate. Although Lilga et al. have done some preliminary investigations of HMF oxidation in a flow reactor, their work was limited to Pt catalysts on a limited number of supports.

References

[1] T. L. Donaldson and O. L. Culberson. An industrial model of commodity chemicals from renewable resources. Energy 9 (1984) 693-707.

[2] J. N. Chheda, G. W. Huber and J. A. Dumesic. Liquid-phase catalytic processing of biomass-derived oxygenated hydrocarbons to fuels and chemicals. Angew.Chem.Int.Ed. 46 (2007) 7164-7183.

[3] J. J. Bozell and G. R. Petersen. Technology development for the production of biobased products from biorefinery carbohydrates - the US department of energy's top 10 revisited. Green Chem. 12 (2010) 539-554.

[4] T. Werpy and G. R. Petersen. Top value added chemicals from biomass. Department of Energy, Office of Scientific and Technical Information No. DOE/GO-102004-1992 (2004)

[5] A. Gandini, A. J. D. Silvestre, C. Pascoal Neto, A. F. Sousa and M. Gomes. The furan counterpart of poly(ethylene terephthalate): An alternative material based on renewable resources. J. Polym. Sci., Part A: Polym. Chem. 47 (2008) 295-298.

[6] http://avantium.com/yxy/markets-partnerships/commercialization.html. Accessed 9/14/14 Sept 2012.

[7] J. Ma, X. Yu and Y. Pang. Synthesis and crystallinity of poly(butylene 2,5-furandicarboxylate). Polymer 53 (2012) 4145-4151.

[8] D. Mercadier, L. Rigal, J. P. Gaset and J. P. Gorrichon. Synthesis of 5-hydroxymethyl-2-furancarboxaldehyde catalyzed by cationic exchange resins. J. Chem. Technol. Biotechnol. 31 (1981) 489-496.

[9] C. Moreau, R. Durand, S. Raziglade, et al. Dehydration of fructose to 5-hydroxymethylfurfural over H-mordenites. Appl. Catal., A 145 (1996) 211-224.

[10] J. N. Chheda, Y. Roman-Leshkov and J. A. Dumesic. Production of 5-hydroxymethylfurfural by dehydration of biomass-derived mono- and poly-saccharides. Green Chem. 9 (2007) 342-350.

[11] Maria J. Climent, Avelino Corma and Sara Iborra. Converting carbohydrates to bulk chemicals and fine chemicals over heterogeneous catalysts. Green Chem. 3 (2011) 520-540.

[12] Y. Roman-Leshkov, J. N. Chheda and J. A. Dumesic. Phase modifiers promote efficient production of hydroxymethylfurfural from fructose. Science 312 (2006) 1933-1937.

[13] A. A. Rosatella, S. P. Simeonov, R. F. M. Frade and C. A. M. Afonso. 5-hydroxymethylfurfural (HMF) as a building block platform: Biological properties, synthesis, and synthetic applications. Green Chem. 13 (2010) 754-793.

[14] H. B. Zhao, J. E. Holladay, H. Brown and Z. C. Zhang. Metal chlorides in ionic liquid solvents convert sugars to 5-hydroxymethylfurfural. Science 316 (2007) 1597-1600.

[15] C. Carlini, P. Patrono, A. M. R. Galletti, G. Sbrana and V. Zima. Selective oxidation of 5-hydroxymethyl-2-furaldehyde to furan-2,5-dicarboxaldehyde by catalytic systems based on vanadyl phosphate. Appl.Catal.A-Gen. 289 (2005) 197-204.

[16] M. L. Ribeiro and U. Schuchardt. Cooperative effect of cobalt acetylacetonate and silica in the catalytic cyclization and oxidation of fructose to 2,5-furandicarboxylic acid. Catal.Comm. 4 (2003) 83-86.

[17] M. Kroger, U. Prusse and K. D. Vorlop. A new approach for the production of 2,5-furandicarboxylic acid by in situ oxidation of 5-hydroxymethylfurfural starting from fructose. Top. Catal. 13 (2000) 237-242.

[18] S. E. Davis, L. R. Houk, E. C. Tamargo, A. K. Datye and R. J. Davis. Oxidation of 5-hydroxymethylfurfural over supported pt, pd and au catalysts. Catal. Today 160 (2011) 55-60.

[19] T. Pasini, M. Piccinini, M. Blosi, et al. Selective oxidation of 5-hydroxymethyl-2-furfural using supported gold-copper nanoparticles. Green Chem. 13 (2011) 2091-2099.

[20] O. Casanova, S. Iborra and A. Corma. Biomass into chemicals: Aerobic oxidation of 5-hydroxymethyl-2-furfural into 2,5-furandicarboxylic acid with gold nanoparticle catalysts. ChemSusChem 2 (2009) 1138-1144.

[21] Y. Y. Gorbanev, S. K. Klitgaard, J. M. Woodley, C. H. Christensen and A. Riisager. Gold-catalyzed aerobic oxidation of 5-hydroxymethylfurfural in water at ambient temperature. ChemSusChem 2 (2009) 672-675.

[22] S. M. Payne and F. M. Kerton. Solubility of bio-sourced feedstocks in 'green' solvents. Green Chem. 12 (2010) 1648-1653.

[23] M. A. Lilga, R. T. Hallen and M. Gray. Production of oxidized derivatives of 5-hydroxymethylfurfural (HMF). Top. Catal. 53 (2010) 1264-1269.

[24] N. K. Gupta, S. Nishimura, A. Takagaki and K. Ebitani. Hydrotalcite supported gold-nanoparticle-catalyzed highly efficient base-free aqueous oxidation of 5-hydroxymethylfurfural into 2,5-furandicarboxylic acid under atmospheric oxygen pressure. Green Chem. 13 (2011) 824-827.

[25] B. N. Zope, S. E. Davis and R. J. Davis. Influence of reaction conditions on diacid formation during au-catalyzed oxidation of glycerol and hydroxymethylfurfural. Top.Catal. 55 (2012) 24-32.

[26] Y. Y. Gorbanev, S. Kegnaes and A. Riisager. Selective aerobic oxidation of 5-hydroxymethylfurfural in water over solid ruthenium hydroxide catalysts with magnesium-based supports. Catal.Lett. 141 (2011) 1752-1760.

[27] P. Verdeguer, N. Merat and A. Gaset. Catalytic oxidation of HMF to 2,5-furandicarboxylic acid. J. Mol. Catal. 85 (1993) 327-344.

[28] E. Taarning, I. S. Nielsen, K. Egeblad, R. Madsen and C. H. Christensen. Chemicals from renewables: Aerobic oxidation of furfural and hydroxymethylfurfural over gold catalysts. ChemSusChem 1 (2008) 75-78.

[29] Davide Ferri and Alfons Baiker. Advances in infrared spectroscopy of catalytic solid liquid interfaces: The case of selective alcohol oxidation. Topics in Catalysis 52 (2009) 1323-1333.

[30] M. J. Beier, T. W. Hansen and J. D. Grunwaldt. Selective liquid-phase oxidation of alcohols catalyzed by a silver-based catalyst promoted by the presence of ceria. J.Catal. 266 (2009) 320-330.

[31] O. Casanova, S. Iborra and A. Corma. Biomass into chemicals: One pot-base free oxidative esterification of 5-hydroxymethyl-2-furfural into 2,5-dimethylfuroate with gold on nanoparticulated ceria. J.Catal. 265 (2009) 109-116.

[32] A. Abad, P. Concepcion, A. Corma and H. Garcia. A collaborative effect between gold and a support induces the selective oxidation of alcohols. Angew.Chem.Int.Ed. 44 (2005) 4066-4069.

[33] S. E. Davis, B. N. Zope and R. J. Davis. On the mechanism of of selective oxidation of 5-hydroxymethylfurfural to 2,5-furandicarboxylic acid over supported pt and au catalysts. Green Chem. 14 (2012) 143-147.

[34] B. Saha, S. Dutta and M. M. Abu-Omar. Aerobic oxidation of 5-hydroxymethyfurfural with homogeneous and nanoparticulate catalysts. Catal.Sci.Technol. 2 (2012) 79-81.

[35] P. Vinke, H. E. van Dam and H. van Bekkum. Platinum catalyzed oxidation of 5-hydroxymethylfurfural. New Developments in Selective Oxidation 55 (1990) 147-157.

[36] K. Yamaguchi and N. Mizuno. Supported ruthenium catalyst for the heterogeneous oxidation of alcohols with molecular oxygen. Angew.Chem.Int.Ed. 41 (2002) 4538-4541.

[37] K. Mori, T. Hara, T. Mizugaki, K. Ebitani and K. Kaneda. Hydroxyapaptite-supported palladium nanoclusters: A highly active heterogeneous catalyst for selective oxidation of alcohols by use of molecular oxygen. J.Am.Chem. 126 (2004) 10657-10666.

[38] X. Yang, X. Wang, J. and Qui. Aerobic oxidation of alcohols over carbon nanotube-supported ru catalysts assembled at the interfaces of emulsion droplets. Appl.Catal.A-Gen. 382 (2010) 131-137.

[39] P. Fristrup, L. B. Johansen and C. H. Christensen. Mechanistic investigation of the gold-catalyzed aerobic oxidation of alcohols. Catal.Lett. 120 (2008) 184-190.

[40] M. Kotani, T. Koike, K. Yamaguchi and N. Mizuno. Ruthenium hydroxide on magnetite as a magnetically separable heterogeneous catalyst for liquid-phase oxidation and reduction. Green Chem. 8 (2006) 735-741.

[41] J. Chen, Q. Zhang, Y. Wang and H. Wan. Size-dependent catalytic activity of supported palladium nanoparticles for aerobic oxidation of alcohols. Adv.Synth.Catal. 350 (2008) 453-464.

[42] K. Yamaguchi, K. Mori, T. Mizugaki, K. Ebitani and K. Kaneda. Creation of a monomeric ru species on the surface of hydroxyapatite as an efficient heterogeneous catalyst for aerobic alcohol oxidation. J.Am.Chem.Soc. 122 (2000) 7144-7145.

[43] S. Mori, M. Takubo, K. Makida, et al. A simple and efficient oxidation of alcohols with rutheium on carbon. ChemComm 34 (2009) 5159-5161.

[44] K. Yamaguchi and N. Mizuno. Scope, kinetics, and mechanistic aspects of aerobic oxidations catalyzed by ruthenium supported on alumina. Chem.Eur.J. 9 (2003) 4353-4361.

[45] K. B. Sharpless, K. Akashi and K. Oshima. Ruthenium catalyzed oxidation of alcohols to aldehydes and ketones by amine-N-oxides. Tetrahedron Lett. 17 (1976) 2503-2506.

[46] F. A. Carey. Organic chemistry. 1 (2003) 712-717.

[47] L. Prati and G. Martra. New gold catalysts for liquid phase oxidation. Gold Bull. 32 (1999) 96-101.

[48] B. Maier, C. Dietrich and J. Büchs. Correct application of the sulphite oxidation methodology of measuring the volumetric mass transfer coefficient kLa under non-pressurized and pressurized conditions. Food Bioprod. Process. 79 (2001) 107-113.

[49] J. E. Benson, H. S. Hwang and M. Boudart. Hydrogen-oxygen titration method for the measurement of supported palladium surface area. J. Catal. 30 (1973) 146-153.

[50] M. Boudart and G. Djega-Mariadassou. Kinetics of heterogeneous catalytic reactions. (1984) 222.

[51] W. C. Ketchie, M. Murayama and R. J. Davis. Promotional effect of hydroxyl on the aqueous phase oxidation of carbon monoxide and glycerol over supported au catalysts. Top. Catal. 44 (2007) 307-317.

[52] L. Prati, A. Villa, C. Campione and P. Spontoni. Effect of gold addition on pt and pd catalysts in liquid phse oxidation. Top.Catal. 44 (2007) 319-324.

[53] W. C. Ketchie, M. Murayama and R. J. Davis. Selective oxidation of glycerol over carbon-supported AuPd catalysts. J. Catal. 250 (2007) 264-273.

[54] B. N. Zope, D. D. Hibbitts, M. Neurock and R. J. Davis. Reactivity of the gold/water interface during selective oxidation catalysis. Science 330 (2010) 74-78.

[55] B. N. Zope, D. D. Hibbitts, M. Neurock and R. J. Davis. Reactivity of the gold/water interface during selective oxidation catalysis. Science 330 (2010) 74-78.

[56] C. N. Satterfield and A. H. Bonnell. Anal. Chem. 27 (1955) 1174.

[57] B. N. Zope and R. J. Davis. Influence of reactor configuration on the selective oxidation of glycerol over Au/TiO2. Top. Catal. 52 (2009)

[58] K. Heyns, C. Rudiger and H. Paulsen. Chem. Ber. 106 (1973) 623.

[59] T. Mallat and A. Baiker. Oxidation of alcohols with molecular oxygen on solid catalysts. Chem. Rev. 104 (2004) 3037-3058.

[60] A. A. Gewirth and M. S. Thorum. Electroreduction of dioxygen for fuel-cell applications: Materials and challenges. Inorg. Chem. 49 (2010) 3557-3566.

[61] M. A. Lilga, R. T. Hallen, J. Hu, J. White and M. Gray. Hydroxymethylfurfural oxdiation methods.

[62] M. Jobbagy and A. Regazzoni. Dissolution of nano-size mg-al-cl hydrotalcite in aqueous media. Appl. 51 (2011) 366-369.

[63] Alberto Villa, Gabriel M. Veith and Laura Prati. Selective oxidation of glycerol under acidic conditions using gold catalysts. Angewandte Chemie 49 (2010) 4499-4502.

[64] A. Takagaki, M. Takahashi, S. Nishimura and K. Ebitani. One-pot synthesis of 2,5-diformylfuran from carbohydrate derivatives by sulfonated resin and hydrotalcite-supported ruthenium catalysts. ACS Catal. 1 (2011) 1562-1565.

[65] Krijn P. De Jong and John W. Geus. Carbon nanofibers: Catalytic synthesis and applications. Catalysis Reviews 42 (2000) 481-510.

[66] M. L. Toebes, M. K. van der Lee, L. M. Tang, et al. Preparation of carbon nanofiber supported platinum and ruthenium catalysts: Comparison of ion adsorption and homogeneous deposition precipitation. J. Phys. Chem. B 108 (2004) 11611-11619.

[67] M. L. Toebes, J. M. P. van Heeswijk, J. H. Bitter, A. J. van Dillen and K. P. de Jong. The influence of oxidation on the texture and the number of oxygen-containing surface groups of carbon nanofibers. Carbon 42 (2004) 307-315.

[68] A. J. Plomp, D. S. Su, K. P. de Jong and J. H. Bitter. On the nature of oxygen-containing surface groups on carbon nanofibers and their role for platinum deposition- an XPS and titration study. J. Phys. Chem. C 113 (2009) 9865-9869.

[69] R. Arrigo, M. Havecker, R. Schlogl and D. S. Su. Dynamic surface rearrangement and thermal stability of nitrogen functional groups on carbon nanotubes. Chem. Commun. 2008 (2008) 4891-4893.

[70] S. van Dommele, K. P. de Jong and J. H. Bitter. Nitrogen-containing carbon nanotubes as solid base catalysts. Chem. Commun. (2006) 4859-4861.

[71] K. Gong, F. Du, Z. Xia, M. Durstock and L. Dai. Nitrogen-doped carbon nanotube arrays with high electrocatalytic activity for oxygen reduction. Science 323 (2009) 760-764.

[72] Q. Liu, Z. Cui, Z. Ma, S. Bian and W. Song. Highly active and stable material for catalytic hydrodechlorination using ammonia-treated carbon nanofibers as pd supports. J. Phys. Chem. C 112 (2008) 1199-1203.

[73] A. Villa, D. Wang, P. Spontoni, R. Arrigo, D. Su and L. Prati. Nitrogen functionalized carbon nanostructures supported pd and au-pd NPs as catalyst for alcohols oxidation. J. Phys. Chem. C 157 (2010) 89-93.

[74] M. L. Toebes, J. H. Bitter, A. J. van Dillen and K. P. de Jong. Impact of the structure and reactivity of nickel particles on the catalytic growth of carbon nanofibers. Catal. Today 46 (2002) 33-42.

[75] M. A. Fraga, E. Jordao, M. J. Mendes, M. M. A. Freitas, J. L. Faria and J. L. Figueiredo. Properties of carbon-supported platinum catalysts: Role of carbon surface sites. J. Catal. 209 (2002) 355-364.

[76] M. K. van der Lee, A. J. van Dillen, J. H. Bitter and K. P. de Jong. Deposition precipitation for the preparation of carbon nanofiber supported nickel catalsyts. J. Am. Chem. Soc. 127 (2005) 13573-13582.

[77] X. Hao, S. Barnes and J. R. Regalbuto. A fundamental study of pt impregnation of carbon: Adsorption equilibrium and particle synthesis. J. Catal. 279 (2011) 48-65.

[78] W. Fang, J. Chen, Q. Zhang, W. Deng and Y. Wang. Hydrotalcite-supported gold catalyst for the oxidant-free dehydrogenation of benzyl alcohol: Studies on support and gold size effects. Chem.Eur.J. 17 (2011) 1247-1256.

[79] T. Mitsudome, Y. Mikami, H. Funai, T. Mizugaki, K. Jitsukawa and K. Kaneda. Oxidant-free alcohol dehydrogenation using a reusable hydrotalcite-supported silver nanoparticle catalyst. Angew. Chem. Int. Ed. 47 (2008) 138-141.

[80] T. Mitsudome, A. Noujima, T. Mizugaki, K. Jitsukawa and K. Kaneda. Efficient aerobic oxidation of alcohols using a hydrotalcite-supported gold nanoparticle catalyst. Adv.Synth.Catal. 351 (2009) 1890-1896.

[81] K. Ebitani, K. Motokura, T. Mizugaki and K. Kaneda. Heterotrimetallic RuMnMn species on a hydrotalcite surface as highly efficient heterogenous catalysts for liquid-phase oxidation of alcohols with molecular oxygen. Angew.Chem.Int.Ed. 44 (2005) 3423-3426.

[82] T. Matsushita, K. Ebitani and K. Kaneda. Highly efficient oxidation of alcohols and aromatic compounds catalysed by the ru-co-al hydrotalcite in the presence of molecular oxygen. Chem.Commun. 3 (1999) 265-266.

[83] C. van Katz. Anisotropic model compounds. PhD Dissertation Utrecht University (2008)

[84] A. B. Davila-Ibanez, M. A. Correa-Duarte and V. Salgueirino. Magnetic recoverable catalysts: Assessment on CTAB-stabilized gold nanostructures. J. Mater. Chem. 20 (2009) 326-330.

[85] X. Zhang, H. Wang and B. Q. Xu. Remarkable nanosize effect of zirconia in Au/ZrO_2 catalyst for CO oxidation. J. Phys. Chem. B 109 (2005) 9678-9683.

[86] A. Al Baradii, B. B. Kokoh, H. Huse, C. Lamy, and J.-M. Leger. Selective electrocatalyic oxidation of 2,5-dihydroxymethylfruan in aqueous medium: a chromatographic analysis of the reaction products. Electrochimica Acta 44 (1999) 2779-2787.

[87] G. Grabowski, J. Lewkowski, and R. Skowronski. The electrochemical oxidation of 5-hydroxymethylfurfural with the nickel oxide/hydroxide electrode. Electrochimica Acta 36 (1991) 1995.

Appendix A.

Alternative Au/CNF-ox synthesis methods

Several other methods for the synthesis of Au/CNF-ox catalysts were attempted during my stay at Utrecht University, Utrecht, The Netherlands. Namely, a variety of different stabilizers were studied for the generation of a Au sol to be supported on CNF-ox materials. The wavelength corresponding to maximum absorbance is indicative of the size of Au nanoparticles in a colloidal solution, thus the sols were characterized by UV-Vis spectroscopy. The supported catalysts were characterized by X-Ray diffraction (XRD) and TEM.

Citrate Stabilized Au Nanoparticles

Citrate is both a stabilizing and reducing agent for the generation of Au sols (73).

Synthesis method

A 2.4 mM $HAuCl_4$ solution was prepared and heated to either 323, 338, or 368 K while being stirred. Once the desired temperature was reached, a 0.3 M citrate solution was added in 50:1 w:w Citrate:Au. After 3 h, a sample of the colloid solution was taken for UV-Vis analysis. To the solution, 1.0 g CNF-ox was added and stirred overnight. The fibers were filtered and washed with 2.0 L of DI H_2O before being dried in air at 393 K overnight.

Characterization of sols and supported metals

Table A.1 Characterization results of Au sols and supported catalysts generated using citrate

Temperature of colloid generation	Aging time of colloids (h)	Color of colloids	Maximum absorbance wavelength (colloids) (nm)	Au particle size estimated by XRD (supported catalysts) (nm)	Au particle mean diameter estimated by TEM (supported catalysts) (nm)	Au particle surface avg diameter estimated by TEM (supported catalysts) (nm)
323 K	3	Purple	537	10.7	21.4	24.5
323 K	28	Dark pink	529	16.8	23.0	26.8
338 K	3	Red	526	10.2	20.1	21.6
353 K	3	Red	526	N/A	N/A	N/A

Reaction results

None of the Au/CNF-ox catalysts synthesized using citrate was active for HMF oxidation.

CTAB Stabilized Au Nanoparticles

The stabilizer CTAB was used in conjunction with reducing agent $NaBH_4$ to generate a gold sol (83, 84).

Synthesis method

A 5 mM $HAuCl_4$ solution was added along with either a 0.1 or 0.2 M CTAB solution to round bottom flask. A 0.01 M $NaBH_4$ solution was added dropwise and the mixture was stirred

for 0.5 h, after which the CNF-ox support was added and the slurry was stirred overnight. The catalyst was washed with many liters of water until the filtrate was no longer soapy. The catalyst was dried in air at 120˚C overnight.

Characterization of sols and supported metal catalysts

Table A.2 Characterization results of Au sols and supported catalysts generated using CTAB

CTAB concentration (M)	**Maximum absorbance wavelength (colloids) (nm)[a]**	**Particle size estimated by XRD (supported catalysts) (nm)**
0.2 M	N/A	16.4
0.1M	N/A	24.2

[a]The absorbance of CTAB was much too high to gain insight into the size of Au nanoparticles generated. Moreover, the colloids generated using CTAB were highly unstable.

Reaction results

None of the Au/CNF-ox catalysts prepared using CTAB stabilizer was active for HMF oxidation.

PVA Stabilized Au Nanoparticles

Polyvinyl alcohol is used as a stabilizing agent, together with $NaBH_4$ as a reducing agent, in the synthesis of gold colloids.

Synthesis Method

A 5 mM $HAuCl_4$ solution was heated to the desired temperature on a hotplate. A 2 wt% polyvinyl alcohol solution (PVA) was added (PVA:Au 0.62:1 w:w), followed by a 0.1 M $NaBH_4$ ($NaBH_4$:Au 4:1 mol:mol). Within a few minutes of colloid generation, CNF, suspended in 100 cm^3 of ultrapure water and acidified to pH 2 with HCl, were added to the flask and stirred for 1 h. The catalyst was filtered and washed with several liters of water.

Characterization of sols and supported metal catalysts

Table A.3 Characterization results of Au sols and supported catalysts generated using PVA

Temperature of colloid generation	**Color of colloids**	**Maximum absorbance wavelength (colloids) (nm)**
273 K	Brown	n/a
295 K	Red	515
323 K	Red	519

Reaction results

None of the Au/CNF-ox catalysts prepared **at Utrecht University** using PVA stabilizer was active for HMF oxidation.

Appendix B.

Au/ZrO_2 catalyst synthesis

Synthesis procedure

Commercially available ZrO2 (Sigma Aldrich, 99% purity) was dispersed in a 0.1 wt % $HAuCl_4$ solution at ambient temperature (85). The slurry was stirred for 6 h and then the solution pH was adjusted to 9 by adding 0.2 M NH_4OH. The solution was aged for 2 h at the altered pH. The catalyst was filtered and washed with several liters of DI H2O before being dried in air at 333 K overnight. Calcination in air at 100 cm^3 min^{-1} for 5 h was followed by cooling in flowing air. The catalyst was stored in a vial and used without pretreatment.

Reactivity Testing

The activity of Au/ZrO_2 for HMF oxidation was tested in both high pH conditions (0.15 M HMF, 0.30 M NaOH, 295 K, 690 kPa O_2) and neutral pH conditions (0.15 M HMF, 0.30 M NaOH, 348 K, 690 kPa O_2).

In the high pH case, 100% conversion of HMF was realized in 3 h with 96% selectivity to diacid FDCA. In the neutral pH conditions, no HMF oxidation products were detected after 18 h.

Appendix C.

Au/TiO_2 catalyst synthesis

An Au/TiO_2 catalyst was synthesized via an ion exchange method. Briefly, 10 g of Degussa Aeroxide TiO_2 P25 (Lot #4168012498), and 0.32 g $HAuCl_4$ $3H_2O$ was dispersed in 1.6 L DI H_2O and heated to 343 K while stirring. Once at 343 K, the slurry was maintained at this temperature under stirring for 1 h. A 4 M NH_4OH solution (0.1 L) was added and the mixture was again stirred for 1 h. The catalyst was filtered off and washed with 6 L DI H_2O and subsequently dried in air at 333 K. Calcination was performed in air flowing at 100 cm3 min-1 at 573 K for 4 h. The sample was cooled in flowing air, stored in a refrigerator and used without further pretreatment.

ICP-OES analysis (Galbraith Laboratories) indicated the sample was 1.5 wt% Au. TEM analysis (Angelica Sanchez and Abhaya Datye, University of New Mexico) indicates a mean particle diameter of 3.6 nm.

The sample was active for HMF oxidation.

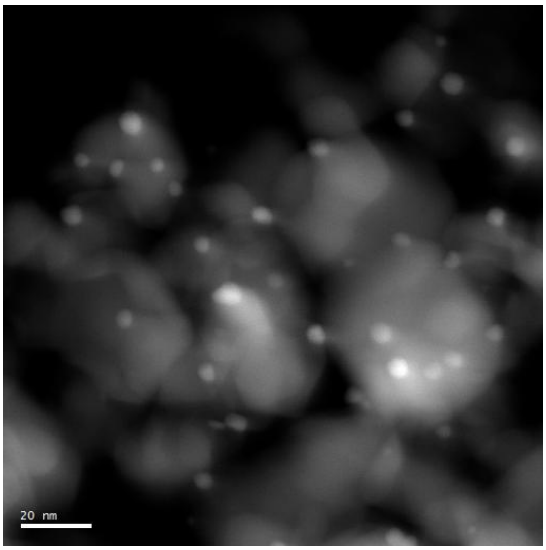

Figure A.1. TEM image of Au/TiO_2 catalyst. (courtesy A. Sanchez, UNM)

Appendix C.

Titration of supported catalysts

The titration of additional (non-CNF) catalysts followed the same procedure as Chapter 6. The results are reported below.

Table A.4 Results of supported catalyst titration

Catalyst	Initial pH	Titrated Strong Acid Sites (mmol kg^{-1})	Titrated Total Acid Sites (mmol kg^{-1})	Titrated Base Sites (mmol kg^{-1})
Pt/C	8.6	-	-	143
Au/TiO_2	6.2	-	22	-

Attempted titration of Au/C_{black} was unsuccessful due to hydrophobicity of the sample.

Additional notes on titration using the Titralab system:

- The solution of KCl should be degassed prior to use to remove dissolved CO_2.
- Bubbling N_2 through the solution being titrated prevents dissolution of CO_2.
- Prior to titration, the background titration of KCl solution (a volume of solution equal to the amount used to suspend the solid sample) should be performed. This background volume should be taken into account when calculating the value of titrated sites on the solid sample.
- It is advised that the equilibration time be set to 10 seconds.

Appendix D.

Results of selected base-free or O_2-free experiments

Various reaction conditions have been tested for HMF oxidation, many with little success. The results of selected experiments that may be useful to future researchers are included in this appendix.

Electrocatalysis has been applied to oxidation of HMF and of 2,5-bis-hydroxymethylfuran. This information can be found in References [86] and [87].

Table A.5 Results of selected base-free or O_2-free experiments

Catalyst	**NaOH:HMF**	**T (K)**	**P (gas) (kPa)**	**t (h)**	**Conversion**	**S_{HFCA}**	**S_{FCA}**	**S_{FDCA}**
Au/TiO_2	0	358	1035 (O_2)	18	71	91	6	3
Au/TiO_2[a]	2	295	690 (N_2)	6	90	67 (yield)		
Au/TiO_2[b]	0	363	690 (O_2)	18	25			100
Au/TiO_2 + ZrO_2	0	363	345 (O_2)	15	38	89		11
Au/TiO_2[c]	20	295	690 (He)	22	100	85 (yield)		
Pt/C[c]	2	295	690 (N_2)	6	65	16 (yield)		
Pt/C[b]	0	348	345 (N_2)	18	50			100

[a]Carbon balance is 150%; other known product is dialcohol BHMF

[b]Substrate was acid-aldehyde intermediate FCA

[c]Balance of products unidentified

Appendix E.

Treatment of CNF with NH_3

The CNF-ox materials were packed in a quartz tube as seen in Figure A.1. Nitrogen was flown through the tube at 60 cm^3 min^{-1} while the tube was heated to 1073 K over 250 min. When the desired temperature was reached, the flow was switched to NH_3 for 2 h. After 2 h, the flow was maintained but the furnace turned off. Once cool, the CNF-N materials were stored in a glass vial.

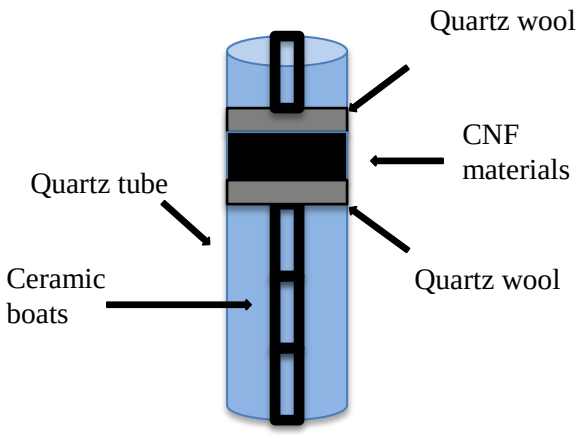

Figure A.2 Schematic of quartz tube for ammonia treatment of CNF-ox

Appendix F.

Dissolution of silica at high pH

The dissolution of silica from glass is possible at high pH conditions like those used for HMF oxidation. To test the potential effect dissolution of silica may have on HMF oxidation rate or product distribution, we compared the results obtained using a glass liner with those obtained using a Teflon liner in the reactor. No significant effect was noted on oxidation rate or product distribution.

Table A.6 Comparison of HMF oxidation in reactor liners[a]

	Glass Liner	**Teflon Liner**
TOF (s^{-1})[b]	0.062	0.057
Conversion @ 2h	62	61
S_{HFCA} @ 2h	56	57
S_{FCA} @ 2h	27	29
S_{FDCA} @ 2h	16	14

[a]reaction conditions: 0.15 M HMF, 0.3.0 M NaOH, 0.010 g 3 wt% Pt/C (Aldrich), 295 K, 690 kPa O_2

[b]TOF based on moles of HMF consumed in 30 minutes per mole of surface Pt

Appendix G.

Sample chromatograms

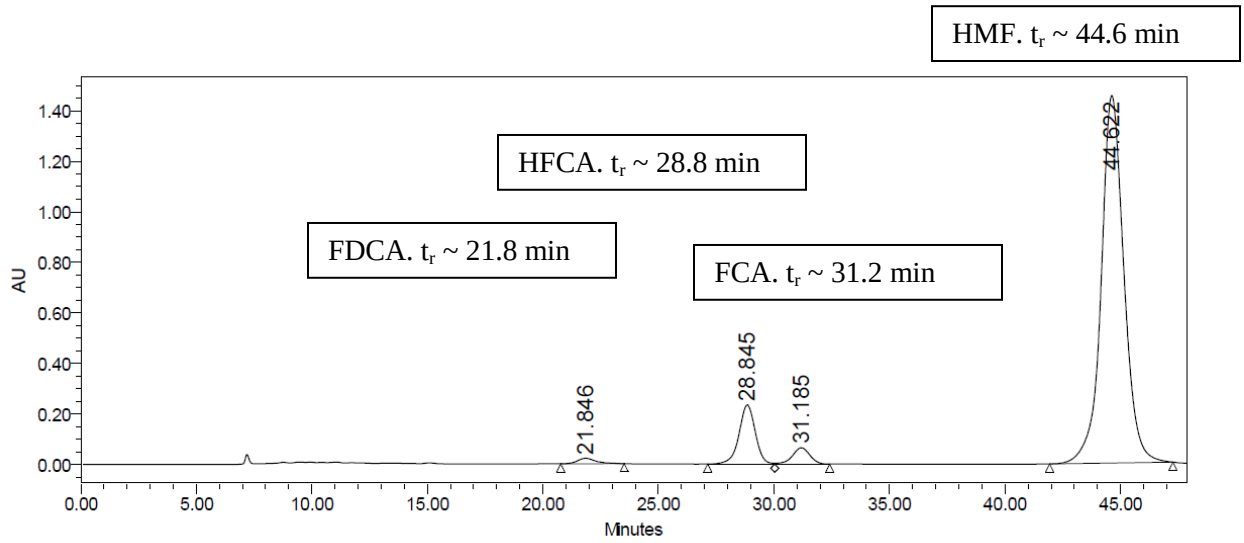

Figure A.3. Sample chromatogram, HMF and oxidation products using Bio-Rad Aminex column. UV detector at wavelength 230 nm (HPLC conditions: 5 mM H_2SO_4 mobile phase flowing at 0.5 mL min^{-1}; column temperature 303 K)

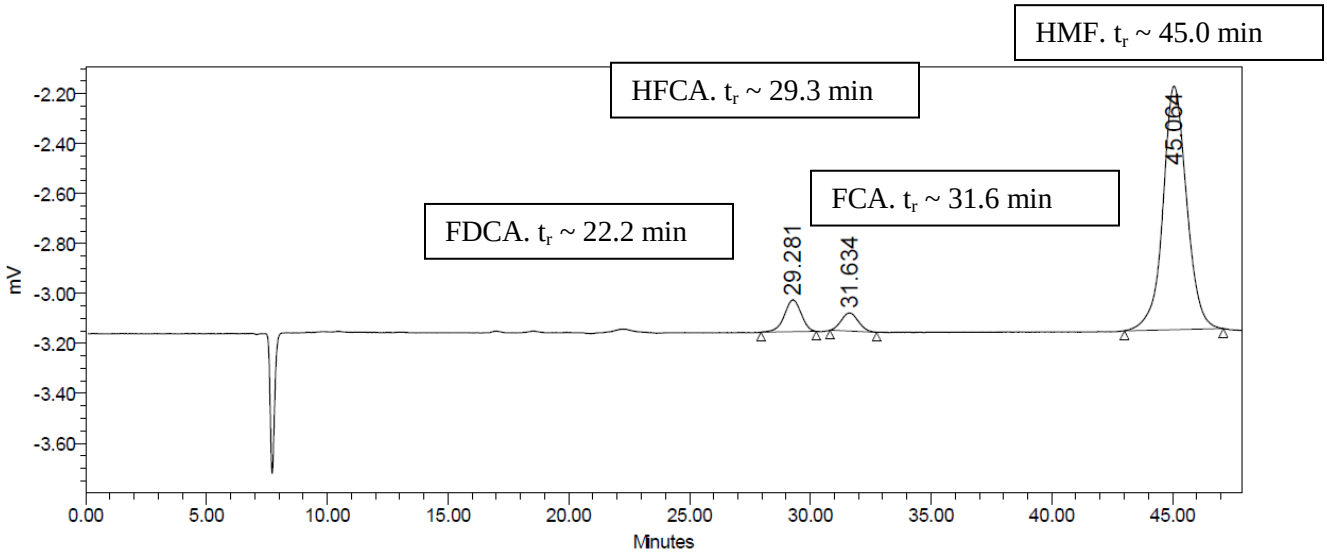

Figure A.4. Sample chromatogram, HMF and oxidation products using Bio-Rad Aminex column. RI detector (detector temperature 303 K). (HPLC conditions: 5 mM H_2SO_4 mobile phase flowing at 0.5 mL min^{-1}; column temperature 303 K)

Appendix H.

H_2 chemisorption on bare CNFs

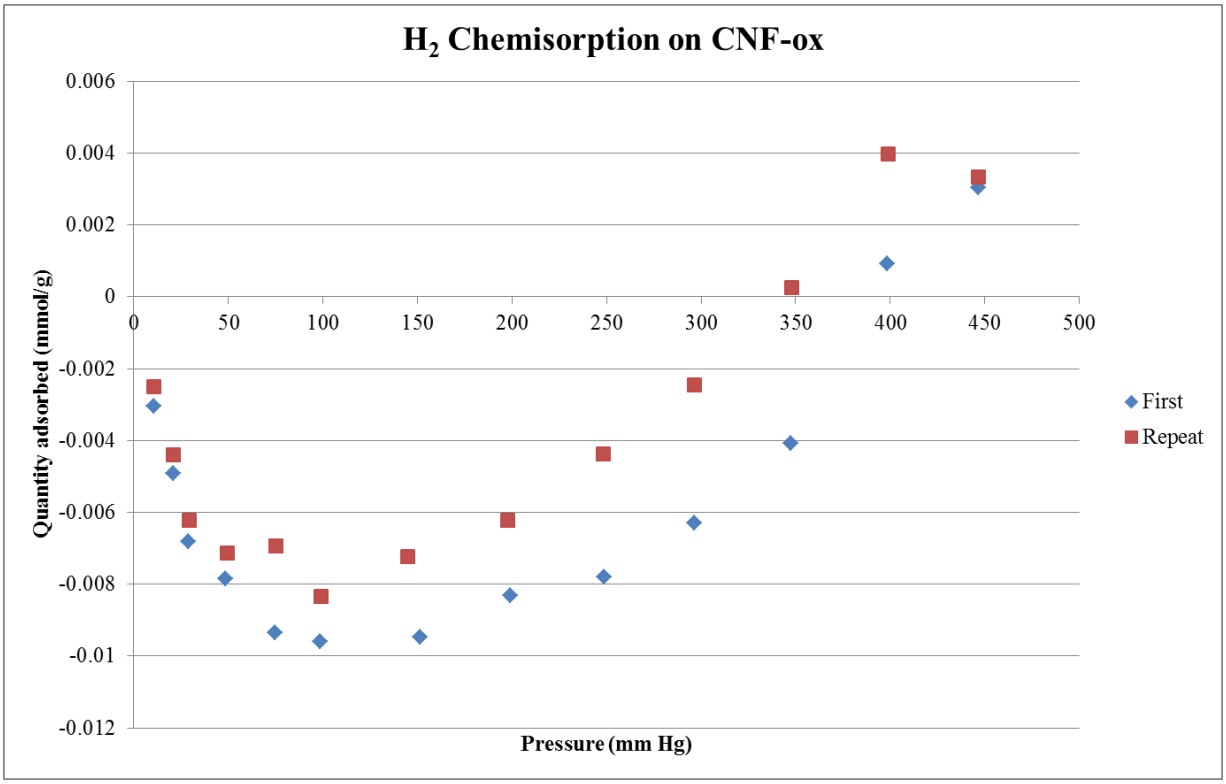

Figure A.5 H_2 chemisorption isotherm for bare CNF-ox material

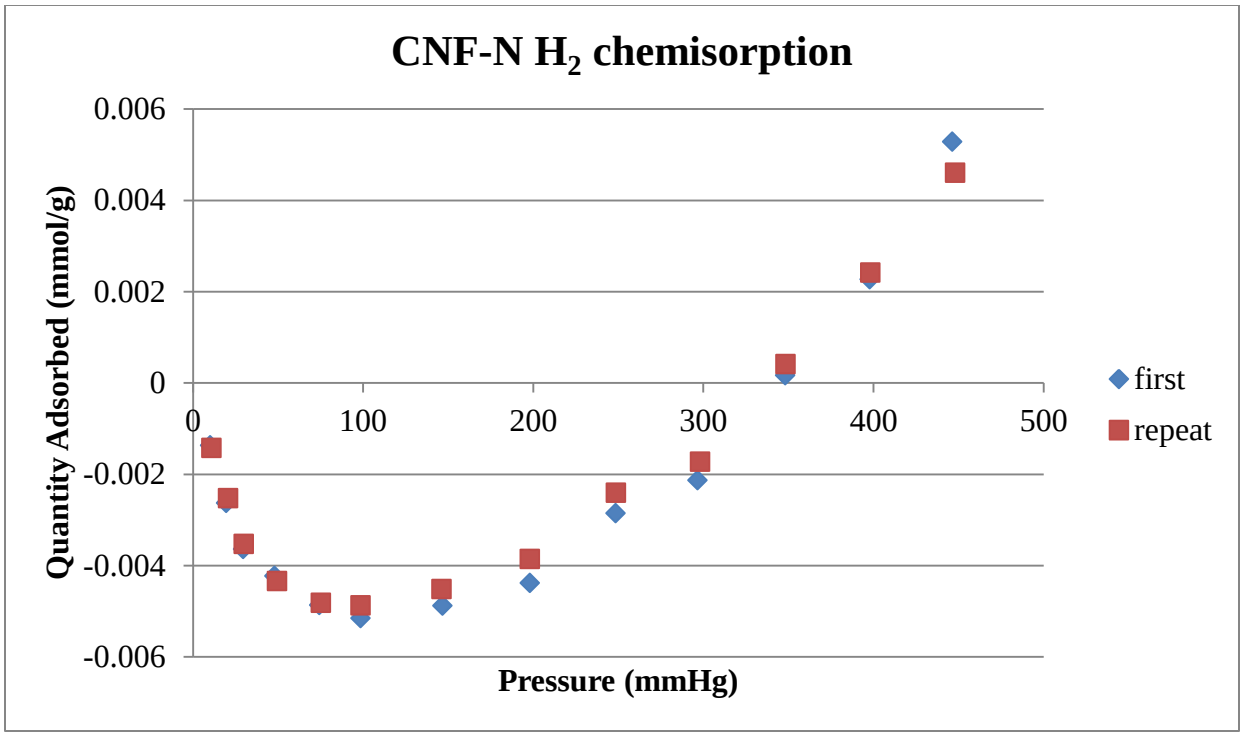

Figure A.6. H_2 chemisorption isotherm for bare CNF-N material

Appendix I.

Oxidation of HMF under transport-limited conditions

A **rough** investigation of the effect of an external mass transport limitation on HMF oxidation rate was performed by using air as oxidant at a relatively low pressure (138 kPa). This pressure value was chosen based on the following:

Typical results of HMF oxidation over Pt/C at standard conditions (295 K, 0.15 M HMF, 0.3 M NaOH, 0.01 g 3 wt% Pt/C, 690 kPa O_2) demonstrate 13-16% conversion of HMF in 0.25 h, which is 1.37 x 10^{-4} moles HMF converted (mostly to HFCA, aldehyde oxidation). Based on our proposed mechanism (see Chapter 3), the deposition of electrons on the metal catalyst surface occurs:

$$1.37\ x\ 10^{-4} moles\ HMF\ consumed * \frac{2\ moles\ electrons\ deposited}{1\ mole\ HMF\ consumed} = 2.73\ x\ 10^{-4}\ moles\ electrons\ deposited$$

One O_2 removes one electron, therefore 2.73 x 10^{-4} moles of O_2 are consumed in 0.25 h to scavenge electrons from the metal surface, a flux of 3.03 x 10^{-7} moles O_2 s^{-1}.

The flux of O_2 at 690 kPa O_2 (gauge) and 295 K in the reactor used for this work, determined via sodium sulfite oxidation, is 9.8 x 10^{-7} moles O_2 s^{-1}. In order for transport limited conditions to be achieved, this flux would need to be below 3.03 x 10^{-7}.

Switching to pressurized air rather than pure O_2, and assuming air is 21 mol% O_2, at 690 kPa (gauge) the flux of O_2 can be estimated near 2.06 x 10^{-7} moles O_2 s^{-1}. At lower pressure, the flux of O_2 would be lower. Therefore, the lowest pressure that could reasonably be maintained

using our equipment was chosen to limit transport of O_2 from the gas to liquid phase. This pressure is 138 kPa (gauge).

To examine the influence of O_2 pressure on HMF oxidation rate, an experiment was conducted using 138 kPa (gauge) air and the standard reaction conditions (0.15 M HMF, 0.3 M NaOH, 295 K, 0.01 g 3 wt% Pt/C). The turnover frequency was measured at 0.25 h based on consumption of HMF, and found to be 0.067 s^{-1}, which is 33% lower than that measured under non-mass transport limited conditions. In contrast, an experiment using the same conditions but 138 kPa (gauge) O_2 instead of air demonstrated TOF of 0.11 s^{-1}.

It should be noted that these experiments are for informational purposes only. The data collected for the low pressure air runs was obtained at very low conversion (~8%) and may be significantly influenced by the accuracy of the HPLC. In other words, I believe the trend that the HMF oxidation rate is limited by the flux of O_2 clearing excess charge from the metal surface, but I do not have complete confidence in the TOF values.

Appendix J.

Notes on Precision and Accuracy of Measured Rates

The carbon balance based on HPLC analysis was >90% for all data reported in this work.

Several runs were completed for each reported data point. An example is given in Table A.7, for the influence of initial HFCA concentration on the HFCA oxidation rate. The initial concentration of HFCA is given, as is the time and conversion of HFCA at which TOF was calculated. The average TOF for all runs of the same initial HFCA concentration and the standard deviation of the data points is also given.

As a measure of accuracy of the data, the TOF was also calculated based on appearance of products and then divided by the TOF calculated based on consumption of substrate. Ideally, the ratio is 1. These values are given in the last column of Table A.7 and are typical of all data points in the kinetics study.

Table A.7. Influence of Initial HFCA Concentration on TOF

[HFCA] (M)	time (min)	Conversion (%)	TOF[a] (s^{-1})	Average TOF (s^{-1})	Std Dev of TOF	$TOF_{products}$/ $TOF_{reactant}$
0.15 M	60	16	0.016	0.015	0.0012	1.02
0.15 M	60	15	0.014			1.18
0.15 M	60	17	0.016			0.99
0.10 M	60	19	0.013	0.011	0.0021	1.02
0.10 M	60	16	0.01			1.25
0.05 M	30	24	0.015	0.013	0.0024	0.84
0.05 M	30	15	0.01			0.98
0.05 M	30	23	0.015			0.91
0.05 M	30	20	0.013			0.93

[a]TOF calculated as moles of HFCA converted in given time per mole of surface metal in reactor.